November / December 2023
Volume 52, Number 6

AppliedRadiology®

YEARS

The Journal of Practical Medical Imaging and Management

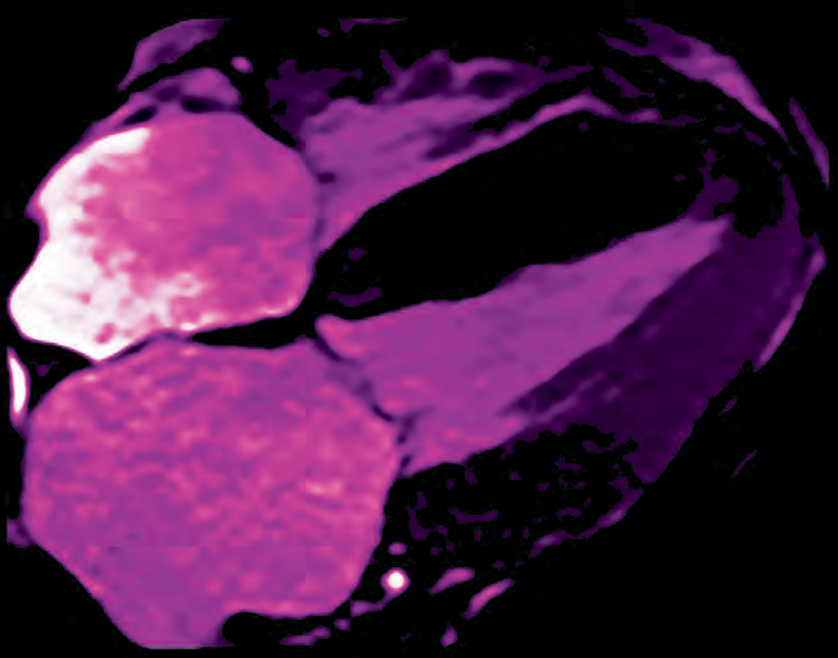

CME Radiological Detection of Cardiac Amyloid: MRI with Pathological Correlation

Imaging Testicular Torsion

MRI Safety: Prepare for New Guidance

Playing with Fire: Burnout Among Radiologists a Growing Concern

Shoulder Effusion as Ultrasound Mimic of Axillary Lymphadenopathy

www.appliedradiology.com

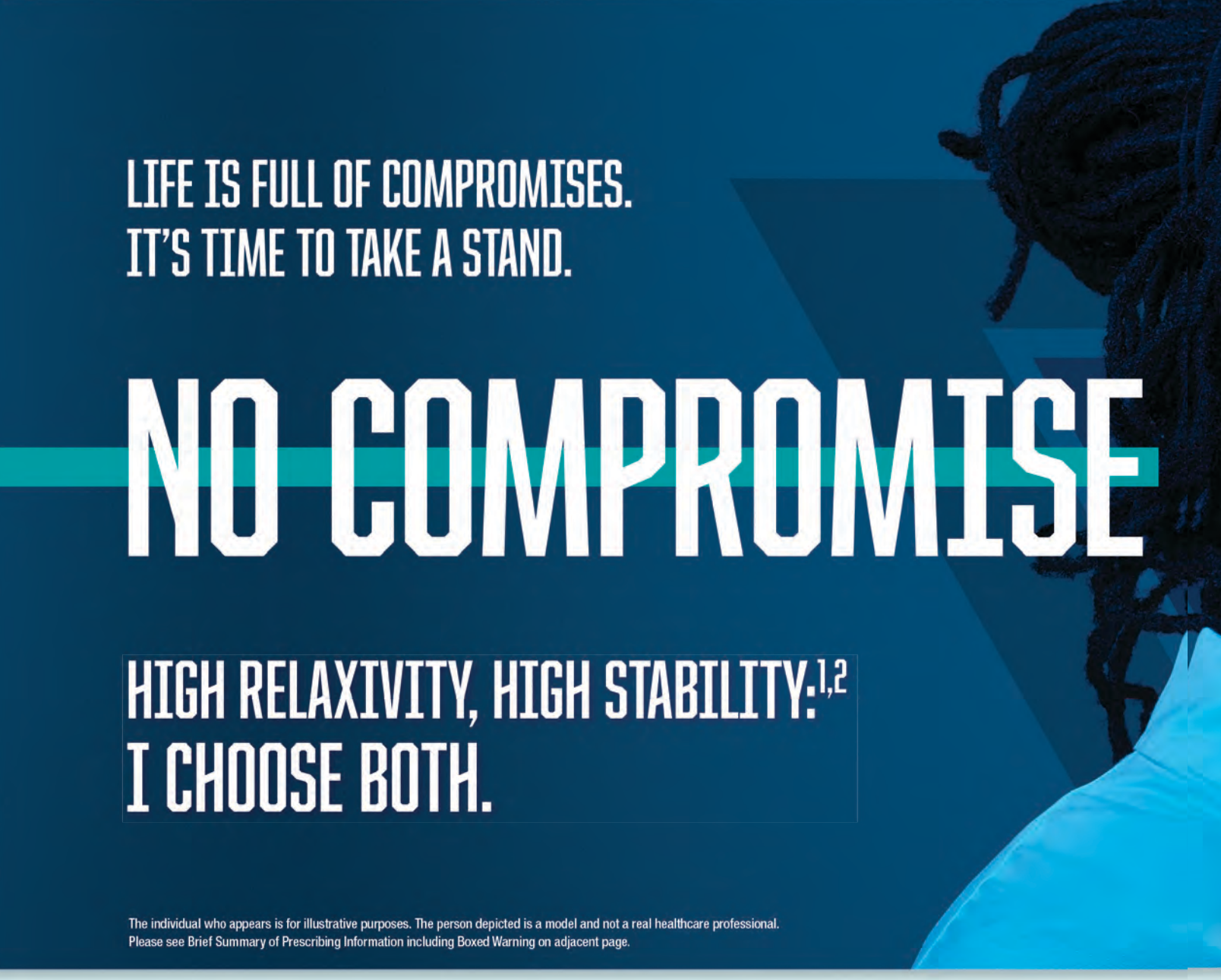

LIFE IS FULL OF COMPROMISES. IT'S TIME TO TAKE A STAND.

NO COMPROMISE

HIGH RELAXIVITY, HIGH STABILITY:[1,2] I CHOOSE BOTH.

The individual who appears is for illustrative purposes. The person depicted is a model and not a real healthcare professional.
Please see Brief Summary of Prescribing Information including Boxed Warning on adjacent page.

VUEWAY™ (gadopiclenol) solution for injection

Indications
VUEWAY injection is indicated in adults and children aged 2 years and older for use with magnetic resonance imaging (MRI) to detect and visualize lesions with abnormal vascularity in:

- the central nervous system (brain, spine and surrounding tissues),
- the body (head and neck, thorax, abdomen, pelvis, and musculoskeletal system).

IMPORTANT SAFETY INFORMATION

WARNING: NEPHROGENIC SYSTEMIC FIBROSIS (NSF)

Gadolinium-based contrast agents (GBCAs) increase the risk for NSF among patients with impaired elimination of the drugs. Avoid use of GBCAs in these patients unless the diagnostic information is essential and not available with non-contrasted MRI or other modalities. NSF may result in fatal or debilitating fibrosis affecting the skin, muscle and internal organs.

- **The risk for NSF appears highest among patients with:**
  - **Chronic, severe kidney disease (GFR <30 mL/min/1.73 m^2), or**
  - **Acute kidney injury.**
- **Screen patients for acute kidney injury and other conditions that may reduce renal function. For patients at risk for chronically reduced renal function (e.g. age >60 years, hypertension, diabetes), estimate the glomerular filtration rate (GFR) through laboratory testing.**
- **For patients at highest risk for NSF, do not exceed the recommended VUEWAY dose and allow a sufficient period of time for elimination of the drug from the body prior to any re-administration.**

Contraindications
VUEWAY injection is contraindicated in patients with history of hypersensitivity reactions to VUEWAY.

Warnings
Risk of **nephrogenic systemic fibrosis** is increased in patients using GBCA agents that have impaired elimination of the drugs, with the highest risk in patients chronic, severe kidney disease as well as patients with acute kidney injury. Avoid use of GBCAs among these patients unless the diagnostic information is essential and not available with non-contrast MRI or other modalities.

Hypersensitivity reactions, including serious hypersensitivity reactions, could occur during use or shortly following VUEWAY administration. Assess all patients for any history of a reaction to contrast media, bronchial asthma and/or allergic disorders, administer VUEWAY only in situations where trained personnel and therapies are promptly available for the treatment of hypersensitivity reactions, and observe patients for signs and symptoms of hypersensitivity reactions after administration.

INTRODUCING

Vueway™
(gadopiclenol) injection
485.1 mg/mL

HALF THE GADOLINIUM DOSE COMPARED TO OTHER MACROCYCLIC GBCAS IN APPROVED INDICATIONS.[1,3-6] FROM BRACCO, YOUR TRUSTED PARTNER IN MRI.

BRACCO
LIFE FROM INSIDE

Gadolinium retention can be for months or years in several organs after administration. The highest concentrations (nanomoles per gram of tissue) have been identified in the bone, followed by other organs (brain, skin, kidney, liver and spleen). Minimize repetitive GBCA imaging studies, particularly closely spaced studies, when possible.

Acute kidney injury requiring dialysis has occurred with the use of GBCAs in patients with chronically reduced renal function. The risk of acute kidney injury may increase with increasing dose of the contrast agent.

Ensure catheter and venous patency before injecting as **extravasation** may occur, and cause tissue irritation.

VUEWAY may **impair the visualization of lesions** seen on non-contrast MRI. Therefore, caution should be exercised when Vueway MRI scans are interpreted without a companion non-contrast MRI scan.

The most common adverse reactions (incidence ≥ 0.5%) are injection site pain (0.7%), and headache (0.7%).

You are encouraged to report negative side effects of prescription drugs to the FDA. Visit www.fda.gov/medwatch or call 1-800-FDA-1088.

Please see BRIEF SUMMARY of Prescribing Information for VUEWAY, including BOXED WARNING on Nephrogenic Systemic Fibrosis.

Manufactured for Bracco Diagnostics Inc. by Liebel-Flarsheim Company LLC - Raleigh, NC, USA 27616.

VUEWAY is a trademark of Bracco Imaging S.p.A.

References: 1. Vueway™ (gadopiclenol) Injection Full Prescribing Information. Monroe Twp., NJ: Bracco Diagnostics Inc.; September 2022. **2.** Robic C, Port M, Rousseaux O, et al. Physicochemical and Pharmacokinetic Profiles of Gadopiclenol: A New Macrocyclic Gadolinium Chelate With High T1 Relaxivity. *Invest Radiol.* 2019 Aug;54: 475–484. **3.** GADAVIST® (gadobutrol) Injection. Full Prescribing Information. Bayer HealthCare Pharmaceuticals Inc. Whippany, NJ; April 2022. **4.** DOTAREM® (gadoterate meglumine) Injection. Full Prescribing Information. Guerbet LLC. Princeton, NJ; April 2022. **5.** CLARISCAN™ (gadoterate meglumine) injection for intravenous use. Full Prescribing Information. GE Healthcare. Marlborough, MA; February 2020. **6.** ProHance® (Gadoteridol) Injection. Full Prescribing Information and Patient Medication Guide. Monroe Twp., NJ: Bracco Diagnostics Inc.; December 2020.

VISIT VUEWAY.COM FOR MORE INFORMATION

Bracco Diagnostics Inc.
259 Prospect Plains Road, Building H
Monroe Township, NJ 08831 USA
Phone: 609-514-2200
Toll Free: 1-877-272-2269 (U.S. only)
Fax: 609-514-2446

Bracco Diagnostics Inc.

Vueway™

(gadopiclenol) injection, for intravenous use

BRIEF SUMMARY: Please see package insert of full prescribing information.

WARNING: NEPHROGENIC SYSTEMIC FIBROSIS (NSF)

Gadolinium-based contrast agents (GBCAs) increase the risk for NSF among patients with impaired elimination of the drugs. Avoid use of GBCAs in these patients unless the diagnostic information is essential and not available with non-contrasted MRI or other modalities. NSF may result in fatal or debilitating fibrosis affecting the skin, muscle and internal organs.

- **The risk for NSF appears highest among patients with:**
  - **Chronic, severe kidney disease (GFR <30 mL/min/1.73 m²), or**
  - **Acute kidney injury.**
- **Screen patients for acute kidney injury and other conditions that may reduce renal function. For patients at risk for chronically reduced renal function (e.g. age >60 years, hypertension, diabetes), estimate the glomerular filtration rate (GFR) through laboratory testing.**
- **For patients at highest risk for NSF, do not exceed the recommended Vueway dose and allow a sufficient period of time for elimination of the drug from the body prior to any re-administration *[see Warnings and Precautions (5.1) in the full Prescribing Information]*.**

INDICATIONS AND USAGE

Vueway™ (gadopiclenol) is a gadolinium-based contrast agent indicated in adult and pediatric patients aged 2 years and older for use with magnetic resonance imaging (MRI) to detect and visualize lesions with abnormal vascularity in:

- the central nervous system (brain, spine, and associated tissues),
- the body (head and neck, thorax, abdomen, pelvis, and musculoskeletal system).

CONTRAINDICATIONS

Vueway is contraindicated in patients with history of hypersensitivity reactions to gadopiclenol.

WARNINGS AND PRECAUTIONS

Nephrogenic Systemic Fibrosis Gadolinium-based contrast agents (GBCAs) increase the risk for nephrogenic systemic fibrosis (NSF) among patients with impaired elimination of the drugs. Avoid use of GBCAs among these patients unless the diagnostic information is essential and not available with non-contrast MRI or other modalities. The GBCA-associated NSF risk appears highest for patients with chronic, severe kidney disease (GFR <30 mL/min/1.73 m²) as well as patients with acute kidney injury. The risk appears lower for patients with chronic, moderate kidney disease (GFR 30-59 mL/min/1.73 m²) and little, if any, for patients with chronic, mild kidney disease (GFR 60-89 mL/min/1.73 m²). NSF may result in fatal or debilitating fibrosis affecting the skin, muscle, and internal organs. Report any diagnosis of NSF following Vueway administration to Bracco Diagnostics Inc. (1-800-257-5181) or FDA (1-800-FDA-1088 or www.fda.gov/medwatch).

Screen patients for acute kidney injury and other conditions that may reduce renal function. Features of acute kidney injury consist of rapid (over hours to days) and usually reversible decrease in kidney function, commonly in the setting of surgery, severe infection, injury or drug-induced kidney toxicity. Serum creatinine levels and estimated GFR may not reliably assess renal function in the setting of acute kidney injury. For patients at risk for chronically reduced renal function (e.g., age >60 years, diabetes mellitus or chronic hypertension), estimate the GFR through laboratory testing.

Among the factors that may increase the risk for NSF are repeated or higher than recommended doses of a GBCA and the degree of renal impairment at the time of exposure. Record the specific GBCA and the dose administered to a patient. For patients at highest risk for NSF, do not exceed the recommended Vueway dose and allow a sufficient period of time for elimination of the drug prior to re-administration. For patients receiving hemodialysis, physicians may consider the prompt initiation of hemodialysis following the administration of a GBCA in order to enhance the contrast agent's elimination *[see Use in Specific Populations (8.6) and Clinical Pharmacology (12.3) in the full Prescribing Information]*. The usefulness of hemodialysis in the prevention of NSF is unknown.

Hypersensitivity Reactions With GBCAs, serious hypersensitivity reactions have occurred. In most cases, initial symptoms occurred within minutes of GBCA administration and resolved with prompt emergency treatment.

- Before Vueway administration, assess all patients for any history of a reaction to contrast media, bronchial asthma and/or allergic disorders. These patients may have an increased risk for a hypersensitivity reaction to Vueway.
- Vueway is contraindicated in patients with history of hypersensitivity reactions to Vueway *[see Contraindications (4) in the full Prescribing Information]*.
- Administer Vueway only in situations where trained personnel and therapies are promptly available for the treatment of hypersensitivity reactions, including personnel trained in resuscitation.
- During and following Vueway administration, observe patients for signs and symptoms of hypersensitivity reactions.

Gadolinium Retention Gadolinium is retained for months or years in several organs. The highest concentrations (nanomoles per gram of tissue) have been identified in the bone, followed by other organs (e.g. brain, skin, kidney, liver, and spleen). The duration of retention also varies by tissue and is longest in bone. Linear GBCAs cause more retention than macrocyclic GBCAs. At equivalent doses, gadolinium retention varies among the linear agents with gadodiamide causing greater retention than other linear agents such as gadoxetate disodium, and gadobenate dimeglumine. Retention is lowest and similar among the macrocyclic GBCAs such as gadoterate meglumine, gadobutrol, gadoteridol, and gadopiclenol.

Consequences of gadolinium retention in the brain have not been established. Pathologic and clinical consequences of GBCA administration and retention in skin and other organs have been established in patients with impaired renal function *[see Warnings and Precautions (5.1) in the full Prescribing Information]*. There are rare reports of pathologic skin changes in patients with normal renal function. Adverse events involving multiple organ systems have been reported in patients with normal renal function without an established causal link to gadolinium.

While clinical consequences of gadolinium retention have not been established in patients with normal renal function, certain patients might be at higher risk. These include patients requiring multiple lifetime doses, pregnant and pediatric patients, and patients with inflammatory conditions. Consider the retention characteristics of the agent when choosing a GBCA for these patients. Minimize repetitive GBCA imaging studies, particularly closely spaced studies, when possible.

Acute Kidney Injury In patients with chronically reduced renal function, acute kidney injury requiring dialysis has occurred with the use of GBCAs. The risk of acute kidney injury may increase with increasing dose of the contrast agent. Do not exceed the recommended dose.

Extravasation and Injection Site Reactions Injection site reactions such as injection site pain have been reported in the clinical studies with Vueway *[see Adverse Reactions (6.1) in the full Prescribing Information]*. Extravasation during Vueway administration may result in tissue irritation *[see Nonclinical Toxicology (13.2) in the full Prescribing Information]*. Ensure catheter and venous patency before the injection of Vueway.

Interference with Visualization of Lesions Visible with Non-Contrast MRI As with any GBCA, Vueway may impair the visualization of lesions seen on non-contrast MRI. Therefore, caution should be exercised when Vueway MRI scans are interpreted without a companion non-contrast MRI scan.

ADVERSE REACTIONS

The following serious adverse reactions are discussed elsewhere in labeling:

- Nephrogenic Systemic Fibrosis *[see Warnings and Precautions (5.1) in the full Prescribing Information]*
- Hypersensitivity Reactions *[see Contraindications (4) and Warnings and Precautions (5.2) in the full Prescribing Information]*

Clinical Trials Experience Because clinical trials are conducted under widely varying conditions, adverse reaction rates observed in the clinical trials of a drug cannot be directly compared to rates in the clinical trials of another drug and may not reflect the rates observed in clinical practice.

The safety of Vueway was evaluated in 1,047 patients who received Vueway at doses ranging from 0.025 mmol/kg (one half the recommended dose) to 0.3 mmol/kg (six times the recommended dose). A total of 708 patients received the recommended dose of 0.05 mmol/kg. Among patients who received the recommended dose, the average age was 51 years (range 2 years to 88 years) and 56% were female. The ethnic distribution was 79% White, 10% Asian, 7% American Indian or Alaska native, 2% Black, and 2% patients of other or unspecified ethnic groups.

Overall, approximately 4.7% of subjects receiving the labeled dose reported one or more adverse reactions.

Table 1 lists adverse reactions that occurred in >0.2% of patients who received 0.05 mmol/kg Vueway.

TABLE 1. ADVERSE REACTIONS REPORTED IN >0.2% OF PATIENTS RECEIVING VUEWAY IN CLINICAL TRIALS

Adverse Reaction	Vueway 0.05 mmol/kg (n=708) (%)
Injection site pain	0.7
Headache	0.7
Nausea	0.4
Injection site warmth	0.4
Injection site coldness	0.3
Dizziness	0.3
Local swelling	0.3

Adverse reactions that occurred with a frequency ≤ 0.2% in patients who received 0.05 mmol/kg Vueway included: maculopapular rash, vomiting, worsened renal impairment, feeling hot, pyrexia, oral paresthesia, dysgeusia, diarrhea, pruritus, allergic dermatitis, erythema, injection site paresthesia, Cystatin C increase, and blood creatinine increase.

Adverse Reactions in Pediatric Patients

One study with a single dose of Vueway (0.05 mmol/kg) was conducted in 80 pediatric patients aged 2 years to 17 years, including 60 patients who underwent a central nervous system (CNS) MRI and 20 patients who underwent a body MRI. One adverse reaction (maculopapular rash of moderate severity) in one patient (1.3%) was reported in the CNS cohort.

USE IN SPECIFIC POPULATIONS

Pregnancy Risk Summary There are no available data on Vueway use in pregnant women to evaluate for a drug-associated risk of major birth defects, miscarriage or other adverse maternal or fetal outcomes. GBCAs cross the human placenta and result in fetal exposure and gadolinium retention. The available human data on GBCA exposure during pregnancy and adverse fetal outcomes are limited and inconclusive *(see Data)*. In animal reproduction studies, there were no adverse developmental effects observed in rats or rabbits with intravenous administration of Vueway during organogenesis *(see Data)*. Because of the potential risks of gadolinium to the fetus, use Vueway only if imaging is essential during pregnancy and cannot be delayed. The estimated background risk of major birth defects and miscarriage for the indicated population(s) are unknown. All pregnancies have a background risk of birth defect, loss, or other adverse outcomes. In the U.S. general population, the estimated background risk of major birth defects and miscarriage in clinically recognized pregnancies is 2% to 4% and 15% to 20% respectively. Data *Human Data* Contrast enhancement is visualized in the placenta and fetal tissues after maternal GBCA administration. Cohort studies and case reports on exposure to GBCAs during pregnancy have not reported a clear association between GBCAs and adverse effects in the exposed neonates. However, a retrospective cohort study comparing pregnant women who had a GBCA MRI to pregnant women who did not have an MRI reported a higher occurrence of stillbirths and neonatal deaths in the group receiving GBCA MRI. Limitations of this study include a lack of comparison with non-contrast MRI and lack of information about the maternal indication for MRI. Overall, these data preclude a reliable evaluation of the potential risk of adverse fetal outcomes with the use of GBCAs in pregnancy.

Animal Data Gadolinium Retention: GBCAs administered to pregnant non-human primates (0.1 mmol/kg on gestational days 85 and 135) result in measurable gadolinium concentration in the offspring in bone, brain, skin, liver, kidney, and spleen for at least 7 months. GBCAs administered to pregnant mice (2 mmol/kg daily on gestational days 16 through 19) result in measurable gadolinium concentrations in the pups in bone, brain, kidney, liver, blood, muscle, and spleen at one-month postnatal age.

Reproductive Toxicology: Animal reproduction studies conducted with gadopiclenol showed some signs of maternal toxicity in rats at 10 mmol/kg and rabbits at 5 mmol/kg (corresponding to 52 times and 57 times the recommended human dose, respectively). This maternal toxicity was characterized in both species by swelling, decreased activity, and lower gestation weight gain and food consumption.

No effect on embryo-fetal development was observed in rats at 10 mmol/kg (corresponding to 52 times the recommended human dose). In rabbits, a lower mean fetal body weight was observed at 5 mmol/kg (corresponding to 57 times the recommended human dose) and this was attributed as a consequence of the lower gestation weight gain.

Lactation Risk Summary There are no data on the presence of gadopiclenol in human milk, the effects on the breastfed infant, or the effects on milk production. However, published lactation data on other GBCAs indicate that 0.01% to 0.04% of the maternal gadolinium dose is excreted in breast milk. Additionally, there is limited GBCA gastrointestinal absorption in the breast-fed infant. Gadopiclenol is present in rat milk. When a drug is present in animal milk, it is likely that the drug will be present in human milk *(see Data)*. The developmental and health benefits of breastfeeding should be considered along with the mother's clinical need for Vueway and any potential adverse effects on the breastfed infant from Vueway or from the underlying maternal condition. Data In lactating rats receiving single intravenous injection of [^{153}Gd]-gadopiclenol, 0.3% and 0.2% of the total administered radioactivity was transferred to the pups via maternal milk at 6 hours and 24 hours after administration, respectively. Furthermore, in nursing rat pups, oral absorption of gadopiclenol was 3.6%.

Pediatric Use The safety and effectiveness of Vueway for use with MRI to detect and visualize lesions with abnormal vascularity in the CNS (brain, spine, and associated tissues), and the body (head and neck, thorax, abdomen, pelvis, and musculoskeletal system) have been established in pediatric patients aged 2 years and older.

Use of Vueway in this age group is supported by evidence from adequate and well-controlled studies in adults with additional pharmacokinetic and safety data from an open-label, uncontrolled, multicenter, single dose study of Vueway (0.05 mmol/kg) in 80 pediatric patients aged 2 to 17 years. The 80 patients consisted of 60 patients who underwent a CNS MRI and 20 patients who underwent a body MRI *[see Adverse Reactions (6.1) and Clinical Pharmacology (12.3) in the full Prescribing Information]*.

The safety and effectiveness of Vueway have not been established in pediatric patients younger than 2 years of age.

Geriatric Use Of the total number of Vueway-treated patients in clinical studies, 270 (26%) patients were 65 years of age and over, while 62 (6%) patients were 75 years of age and over. No overall differences in safety or efficacy were observed between these subjects and younger subjects.

This drug is known to be substantially excreted by the kidney, and the risk of adverse reactions to this drug may be greater in patients with impaired renal function. Because elderly patients are more likely to have decreased renal function, it may be useful to monitor renal function.

Renal Impairment In patients with renal impairment, the exposure of gadopiclenol is increased compared to patients with normal renal function. This may increase the risk of adverse reactions such as nephrogenic systemic fibrosis (NSF). Avoid use of GBCAs among these patients unless the diagnostic information is essential and not available with non-contrast MRI or other modalities. No dose adjustment of Vueway is recommended for patients with renal impairment. Vueway can be removed from the body by hemodialysis *[see Warnings and Precautions (5.1, 5.3, 5.4) and Clinical Pharmacology (12.3) in the full Prescribing Information]*.

OVERDOSAGE

Among subjects who received a single 0.3 mmol/kg intravenous dose of gadopiclenol (6 times the recommended dose of Vueway), headache and nausea were the most frequently reported adverse reactions. Gadopiclenol can be removed from the body by hemodialysis *[see Clinical Pharmacology (12.3) in the full Prescribing Information]*.

PATIENT COUNSELING INFORMATION Advise the patient to read the FDA-approved patient labeling (Medication Guide).

Nephrogenic Systemic Fibrosis Inform the patient that Vueway may increase the risk for NSF among patients with impaired elimination of the drugs and that NSF may result in fatal or debilitating fibrosis affecting the skin, muscle and internal organs.

Instruct the patients to contact their physician if they develop signs or symptoms of NSF following Vueway administration, such as burning, itching, swelling, scaling, hardening and tightening of the skin; red or dark patches on the skin; stiffness in joints with trouble moving, bending or straightening the arms, hands, legs or feet; pain in the hip bones or ribs; or muscle weakness *[see Warnings and Precautions (5.1) in the full Prescribing Information]*.

Gadolinium Retention Advise patients that gadolinium is retained for months or years in brain, bone, skin, and other organs following Vueway administration even in patients with normal renal function. The clinical consequences of retention are unknown. Retention depends on multiple factors and is greater following administration of linear GBCAs than following administration of macrocyclic GBCAs *[see Warnings and Precautions (5.3) in the full Prescribing Information]*.

Injection Site Reactions Inform the patient that Vueway may cause reactions along the venous injection site, such as mild and transient burning or pain or feeling of warmth or coldness at the injection site *[see Warnings and Precautions (5.5) in the full Prescribing Information]*.

Pregnancy Advise pregnant women of the potential risk of fetal exposure to Vueway *[see Use in Specific Populations (8.1) in the full Prescribing Information]*.

Rx only

US Patent No. 10,973,934

Manufactured for Bracco Diagnostics Inc. by Liebel-Flarsheim Company LLC - Raleigh, NC, USA 27616.

Toll Free: 1-877-272-2269 (U.S. only)

Revised November 2022

US-VW-2200022 11/22

AppliedRadiology®

The Journal of Practical Medical Imaging and Management

Anderson Publishing, Ltd
180 Glenside Avenue,
Scotch Plains, NJ 07076
Tel: 908-301-1995
Fax: 908-301-1997
info@appliedradiology.com

Editorial Advisory Board

Applied Radiology®

The Journal of Practical Medical Imaging and Management

November / December 2023
Vol 52 No 6

Applied Radiology (ISSN 0160-9963, USPS 943180) is published in print 6 times a year, January, March, May, July, September, and November, by Anderson Publishing Ltd at 180 Glenside Ave., Scotch Plains NJ 07076. Periodicals postage paid at Scotch Plains, NJ and additional mailing offices. Free subscriptions for US-based qualified radiology professionals. Subscriptions for the US and its territories and possessions: $115 per year, $225 for two years. Foreign and Canadian subscriptions $215 for one year payable in US funds, international money orders, or by credit card only. Postmaster: Please send address changes to Applied Radiology, PO Box 317, Lincolnshire, IL 60069-0317 (847-564-5942) or email AppliedRadiology@0meda.com.

Full Circle Integration

Guerbet, a global leader in diagnostic imaging, continues to strengthen its informatics portfolio.

Dose&Care®
Patient X-ray dose management solution

Contrast&Care®
Injection data management solution

icobrain
Cloud-based AI solutions

Close the Loop
with smart connectivity

Explore Guerbet's AI Solutions at **RSNA Booth 1711**

Guerbet

digitalsolutions.guerbet.com

GU07220108

Dr Schwartz is the Editor-in-Chief of *Applied Radiology*. She is the chief of the Division of Neuroradiology and holds the Robert A. Zimmerman Chair in Pediatric Neuroradiology in the Department of Radiology at The Children's Hospital of Philadelphia. She is also a professor of radiology, Perelman School of Medicine, University of Pennsylvania. Dr Schwartz can be reached at erin@appliedradiology.com.

In Defense of Becoming Less Possessive

Erin Simon Schwartz, MD

Recently, several members of the *Applied Radiology* editorial advisory board and I had a—let's call it a discussion— about our policy requiring the use of the nonpossessive form of condition-specific eponyms (eg, Parkinson disease rather than Parkinson's disease).

First—and this may seem pedantic—using the possessive form of the person for whom the condition is named is grammatically incorrect. The condition is not their personal disorder but is one named after them. In addition, the American Medical Association's (AMA) Manual of Style, the US National Institutes of Health, and the World Health Organization all agree that condition-specific eponyms should not include the apostrophe "s."[1-3]

But even more importantly, as others have so aptly stated, "(B)efore groaning about diving into grammatical nuances in medicine, let us remember that how we speak about our patients often mirrors how we treat them."[4] I agree. If using the possessive risks offending or making those living with a given condition uncomfortable, as the National Down Syndrome Society and the Down Syndrome community have clearly expressed, stating that an "apostrophe 's' connotes ownership or possession[5]" then it is imperative for us in the medical community to respect that.

Of course, there will continue to be some exceptions. As has always been our practice in accordance with the AMA Manual of Style, we will never alter the titles of articles or journals cited either in the body or the references appearing at the end of our articles, even when they employ the possessive. Press releases issued by other organizations that we share through our social media channels and email lists will also remain unchanged. Similarly, we will continue to respect the legal names of organizations; eg, the Alzheimer's Association®.

Language and usage are constantly evolving; while some changes seem to win almost instant acceptance, others take more time. "Google" went from a proper noun to a verb almost instantaneously. On the other hand, many people bristle at the use of the word "they" as a singular pronoun; some say it is just another new-fangled attempt at political correctness. However, not only do most major style guides, including those of the AMA, American Psychological Association, and Associated Press, endorse it, the use of "they" as a singular pronoun dates as far back as 1375.[6]

Ultimately, word choice and usage matter, especially in medicine. Let's hope it doesn't take another 650 years for nonpossessive condition- and disease-specific eponyms to be accepted as our standard.

Bidding Farewell

Please join me in thanking **Melissa Davis, MD, MBA,** as she transitions off the editorial advisory board. Dr Davis was the associate editor for our Emergency Radiology section, and we wish her well. Those of you with expertise in this subspecialty are invited to email me to apply for this position.

References

1) Gregoline B. Eponyms. AMA Manual of Style: A Guide for Authors and Editors (11th ed.) Published: 03 February 2020. Accessed September 16, 2023.

2) Classification and nomenclature of malformation. *Lancet*. 1974 Apr;303(7861):798. doi: 10.1016/S0140-6736(74)92858-X

3) World Health Organization. WHO style guide [Internet] The Organization; 2004. http://www.ianphi.org/documents/pdfs/toolkit/who_style-guide.pdf.

4) Mason J, Johnson W, Swadron S. Possessive eponyms: removing the apostrophe from medical diagnoses. Emergency Medicine Residents' Association. October 10, 2022. https://www.emra.org/emresident/article/eponyms.

5) https://ndss.org/preferred-language. Accessed September 16, 2023.

6) https://www.oed.com/dictionary/they_pron?tab=meaning_and_use#18519607. Accessed September 16, 2023.

Radiological Detection of Cardiac Amyloid: MRI with Pathological Correlation

Description

Cardiac involvement in light chain and transthyretin amyloidosis is commonly encountered by radiologists. Cardiac MRI is the primary imaging modality for cardiac amyloid (CA) with high sensitivity and specificity. However, other cardiac conditions can mimic CA, potentially affecting the accuracy of diagnosis. Knowledge of these mimics will help improve diagnosis and management of CA.

This activity is designed to educate trainees and radiologists on the typical and atypical findings of cardiac amyloidosis on cardiac MRI and nuclear medicine. This will reduce positive and false negative interpretations and lead to improved diagnosis.

Learning Objectives

Upon completing this activity, the reader should be able to:

- Describe classic imaging findings of cardiac amyloidosis on cardiac magnetic resonance.
- Identify the mimics of cardiac amyloidosis on cardiac magnetic resonance imaging.
- Explain the role of nuclear medicine in the diagnosis of cardiac amyloidosis.

Target Audience

- Radiologists
- Related Imaging Professionals

Authors

Navpreet Kaur Khurana, MBBS; Saurabh Jha, MD.

Affiliations: University of Pennsylvania, Department of Radiology, Philadelphia, Pennsylvania (Dr Khurana);

Department of Radiology, Hospital of University of Pennsylvania, Philadelphia, Pennsylvania (Dr Jha)

Commercial Support

None

Accreditation/ Designation Statement

This activity has been planned and implemented in accordance with the accreditation requirements and policies of the Accreditation Council for Continuing Medical Education (ACCME) through the joint providership of IAME and Anderson Publishing.

IAME is accredited by the ACCME to provide continuing medical education for physicians. IAME designates this enduring material for a maximum of 1 AMA PRA Category 1 Credits™. Physicians should claim only the credit commensurate with the extent of their participation in the activity.

Instructions

This activity is designed to be completed within the designated time period. To successfully earn credit, participants must complete the activity during the valid credit period. To receive CME credit, you must:

1. Review this article in its entirety.
2. Visit *appliedradiology.org/SAM2*.
3. Log into your account or create an account (new users).
4. Complete the post-test and review the discussion and references.
5. Complete the evaluation.
6. Print your certificate.

Estimated time for completion: 1 hour

Date of release and review: November 1, 2023

Expiration date: October 31, 2024

Disclosures

Planner: Erin Simon Schwartz, MD, discloses no relevant financial relationships with any ineligible companies.

Authors: Navpreet Kaur Khurana, MBBS, discloses no relevant financial relationships with ineligible companies. Saurabh Jha, MD,, discloses no relevant financial relationships with ineligible companies.

IAME has assessed conflict of interest with its faculty, authors, editors, and any individuals who were in a position to control the content of this CME activity. Any identified relevant conflicts of interest have been mitigated. IAME's planners, content reviewers, and editorial staff disclose no relationships with ineligible entities.

Radiological Detection of Cardiac Amyloid: MRI with Pathological Correlation

Navpreet Kaur Khurana, MBBS; Saurabh Jha, MD

Approximately 50% of patients with light chain (AL) amyloidosis have cardiac amyloidosis (CA) and 30% of patients over 75 years with heart failure with preserved ejection fraction have transthyretin (ATTR) amyloidosis.[1] Cardiac MRI (cMRI) is the primary imaging modality for CA, with a high sensitivity and specificity for evaluating AL and ATTR. However, the diagnostic accuracy and clinical relevance of the MRI findings depend on the pretest probability of these conditions.[2] Although over 50 proteins cause amyloidosis, AL and ATTR are most commonly responsible for cardiac amyloidosis.[3]

The AL type includes multiple myeloma, monoclonal gammopathy of undetermined significance (MGUS), and Waldenstrom macroglobulinemia, while the ATTR type is typically age-related or results from a mutation in transthyretin. Various laboratory, imaging, and histopathological investigations (Table) are undertaken to detect and monitor systemic amyloidosis according to the type of protein involved.

Cardiac amyloidosis can cause a low-voltage electrocardiogram.

Table. Diagnosis of Cardiac Amyloidosis

Types	▪Light chain (AL)
	▪Transthyretin (ATTR)
Lab Investigations	▪B-type natriuretic peptide (BNP)
	▪Serum free light chains (kappa & lambda)
	▪Serum immunofixation electrophoresis
	▪Troponin I or Troponin T
	▪Prealbumin
	▪Renal function test
	▪Urinalysis
Imaging	▪Echocardiography
	▪Cardiac MR
	▪Technetium-99 pyrophosphate scan
Histopathology	▪Endomyocardial biopsy
	▪Abdominal fat pad biopsy
	▪Solid organ biopsy

Deposition of amyloid protein can increase myocardial and valve thickness and left ventricle (LV) mass, cause bi-atrial enlargement and pericardial/pleural effusions. The disease disproportionately affects the basal segments of the heart and often spares the apical segments. Pathognomonic findings of CA are rarely present. Mostly, findings of CA are nonspecific and can mimic those of other diseases. Cardiac findings often must be contextualized with extracardiac signs. For example, in the absence of a monoclonal protein in serum or urine, increased myocardial pyrophosphate (PYP) uptake has >99% specificity and positive predictive value for cardiac ATTR amyloidosis.[4]

Cardiac MRI

On cMRI, cardiac amyloidosis typically leads to diffuse subendocardial or transmural late gadolinium enhancement (LGE) and elevated native T1 and extracellular volume (ECV), dark blood pool on LGE images, inversion of time to myocardial and blood

Affiliations: Department of Radiology, University of Pennsylvania, Philadelphia, Pennsylvania (Dr Khurana) Department of Radiology, Hospital of University of Pennsylvania, Philadelphia, Pennsylvania (Dr Jha)
Keywords: Cardiac amyloid, CMR, Late gadolinium enhancement

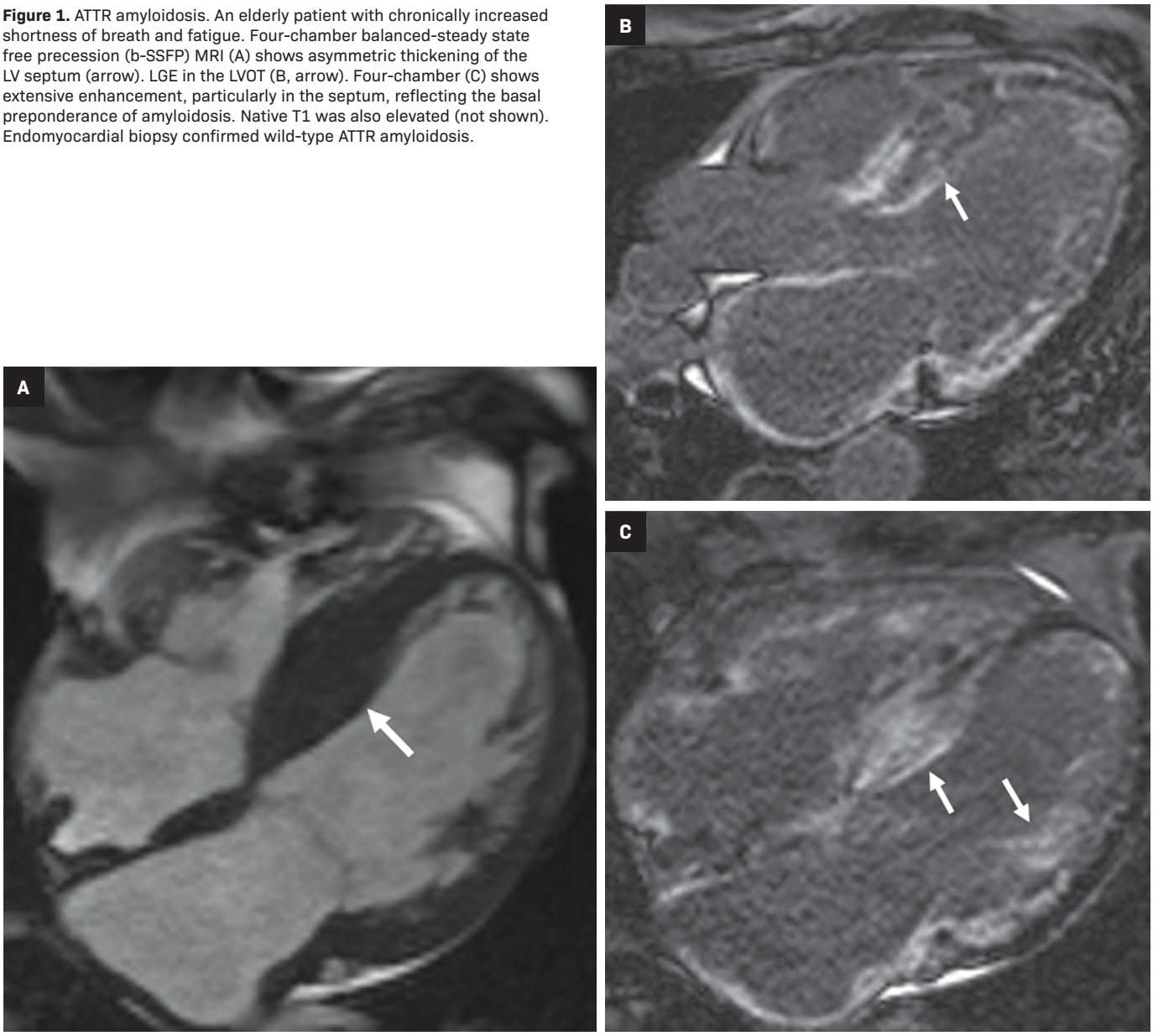

Figure 1. ATTR amyloidosis. An elderly patient with chronically increased shortness of breath and fatigue. Four-chamber balanced-steady state free precession (b-SSFP) MRI (A) shows asymmetric thickening of the LV septum (arrow). LGE in the LVOT (B, arrow). Four-chamber (C) shows extensive enhancement, particularly in the septum, reflecting the basal preponderance of amyloidosis. Native T1 was also elevated (not shown). Endomyocardial biopsy confirmed wild-type ATTR amyloidosis.

pool nulling, and difficulty nulling the myocardium on T1 scout.[5] LGE predominates in the basal segments of the myocardium (Figure 1) due to heterogeneous mechanical dysfunction, defined as a myocardial longitudinal strain impairment pattern. Progression from subendocardial (Figure 2) to diffuse transmural LGE (Figure 3) correlates with disease progression.

Atypical patterns of LGE (Figure 4) include focal patchy LGE, subepicardial LGE, and diffuse patchy LGE.[3] Extensive and transmural LGE and asymmetric septal thickening are more commonly associated with ATTR amyloidosis.[6] According to a recent meta-analysis, the sensitivity and specificity of CMR against endomyocardial biopsy reference was found to be 85.7% and 92.0%, respectively.[7]

Recent advancements in cardiac imaging techniques rely on quantitative myocardial assessment to detect cardiomyopathies. Native T1 mapping illustrates the absolute T1 relaxation times on a pixel-by-pixel basis. Unlike LGE, which is influenced by windowing and nulling, T1 mapping enables direct quantification of T1 values. This characteristic allows T1 mapping to potentially identify diffuse structural changes in the myocardium that may not be detectable through other noninvasive methods like LGE.

The primary factors contributing to increased native T1 values are edema (increased tissue water content seen in conditions like acute infarction or inflammation) and an expansion of the interstitial space

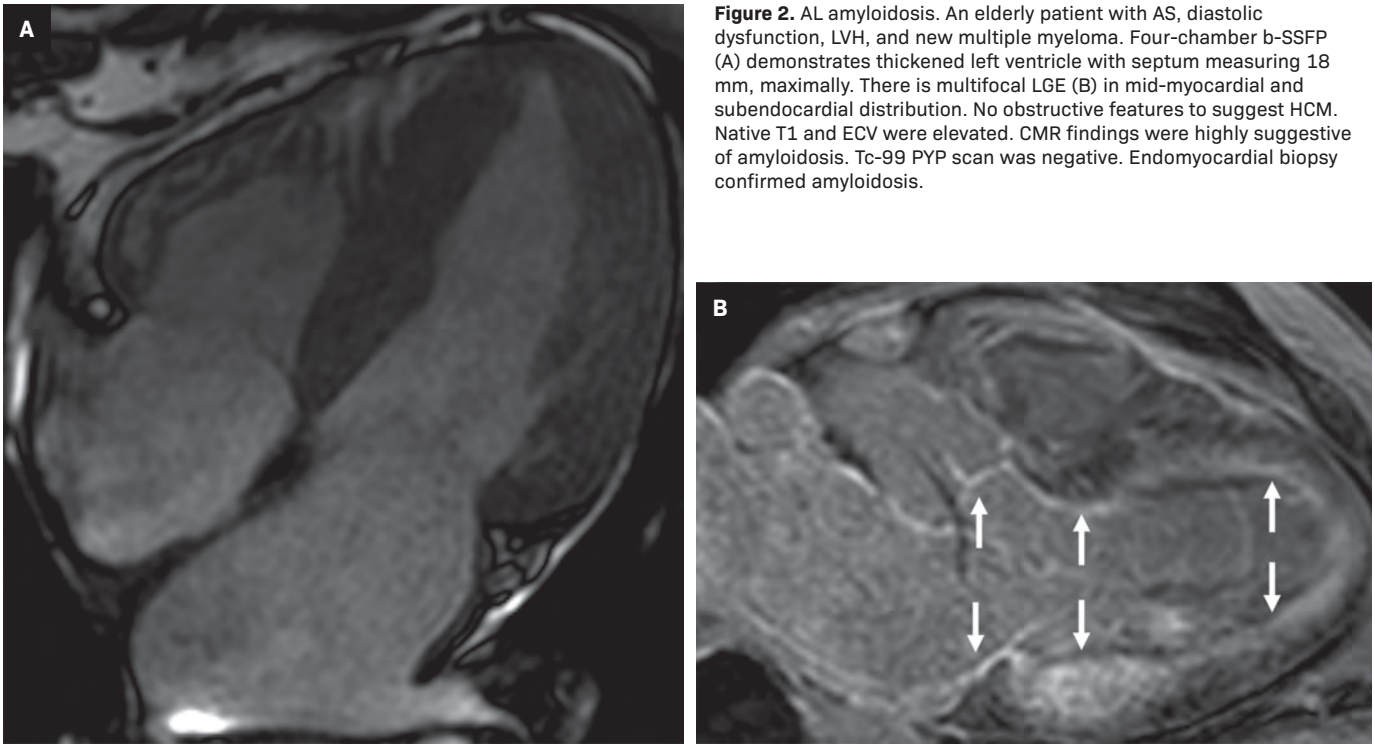

Figure 2. AL amyloidosis. An elderly patient with AS, diastolic dysfunction, LVH, and new multiple myeloma. Four-chamber b-SSFP (A) demonstrates thickened left ventricle with septum measuring 18 mm, maximally. There is multifocal LGE (B) in mid-myocardial and subendocardial distribution. No obstructive features to suggest HCM. Native T1 and ECV were elevated. CMR findings were highly suggestive of amyloidosis. Tc-99 PYP scan was negative. Endomyocardial biopsy confirmed amyloidosis.

Figure 3. Concomitant AL and ATTR amyloidosis. An elderly patient with CAD, atrial fibrillation and ventricular tachycardia. Four-chamber b-SSFP (A) shows bi-atrial enlargement and severe concentric hypertrophy. There is extensive LGE (B) with LV and RV involvement. Native T1 and ECV were elevated. There was grade 3 uptake on PYP scan (not shown). Endomyocardial biopsy demonstrated AL and wild-type ATTR amyloidosis.

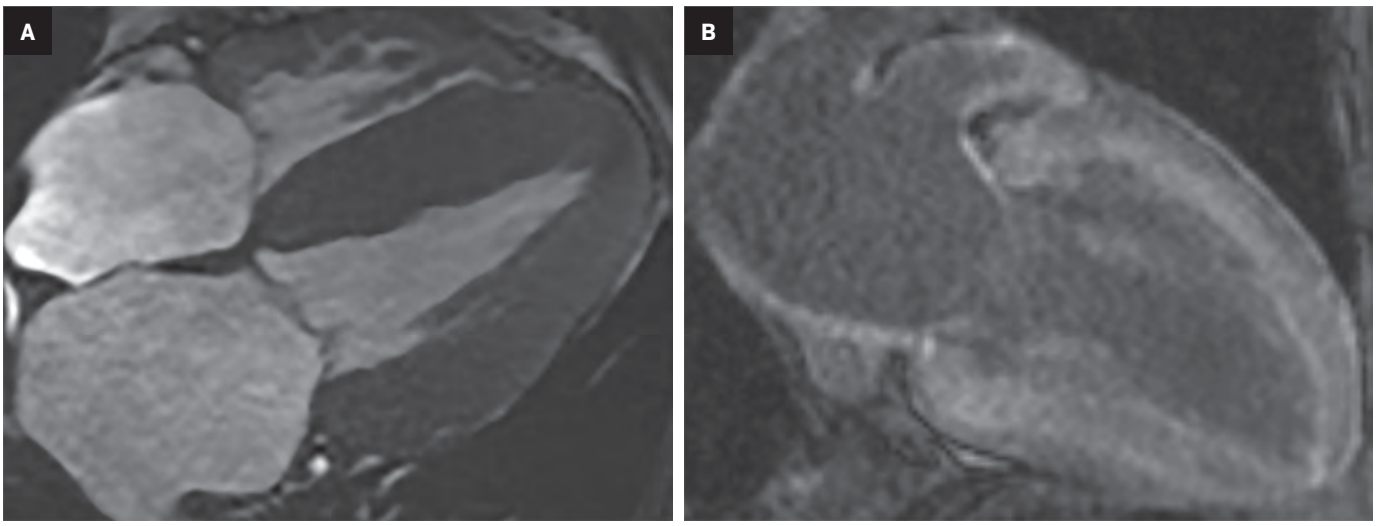

(such as fibrosis in infarction, cardiomyopathy, and amyloid deposition). On the other hand, low native T1 values are associated with lipid overload (eg, Anderson-Fabry disease, lipomatous metaplasia in chronic myocardial infarction) and iron overload. Native T1 values represent a combined signal from myocytes and ECV, which can sometimes lead to pseudonormalization of abnormal values. Notably, native T1 mapping can be performed even in patients with severe renal impairment, for whom the use of gadolinium-based contrast agents is not suitable.

Contrast-enhanced T1 mapping is primarily used in combination with native T1 mapping to determine the ECV fraction. Standard gadolinium-based contrast agents are distributed in the extracellular space, leading to a decrease in myocardial T1 relaxation times proportional to the local gadolinium concentration. Consequently, areas with fibrosis and scar tissue exhibit shorter T1 relaxation times,

Figure 4. AL amyloidosis. An adult with HTN, prediabetes, and atrial flutter presented with dyspnea. CMR revealed increased myocardial native T1 and difficulty in nulling the myocardium on T1 scout (not shown). Three-chamber (A) b-SSFP (B) shows concentric thickening of the LV. Patchy, mid-myocardial LGE is present (B). The patient was subsequently found to have subclinical lytic bone lesions and was diagnosed with multiple myeloma. Endomyocardial biopsy confirmed AL-type amyloidosis.

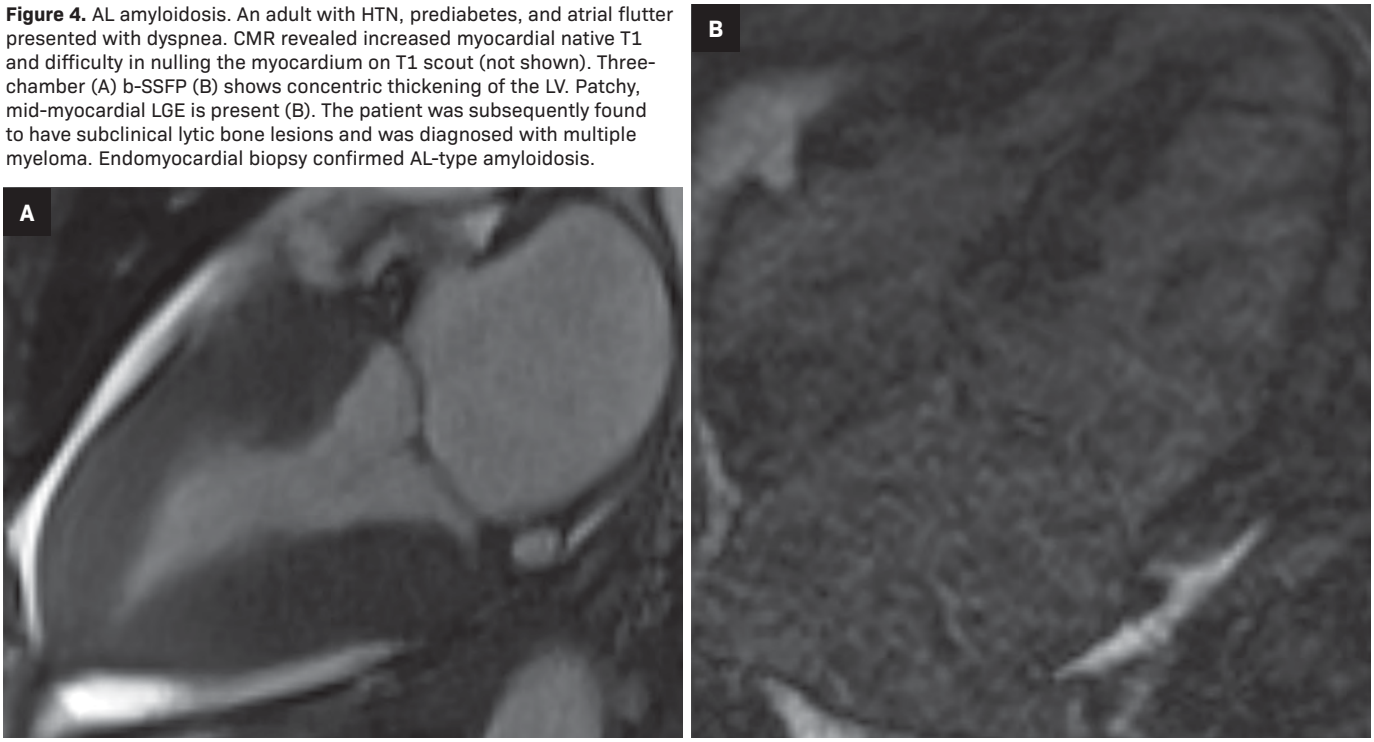

particularly after contrast administration. The hematocrit level reflects the cellular component of blood. Measuring the ECV, which encompasses the interstitium and extracellular matrix, involves obtaining T1 values of myocardial tissue and blood before and after administering contrast agents, along with the patient's hematocrit value. ECV serves as an indicator of myocardial tissue remodeling and provides a measurement unit that aligns with physiological understanding.

Normal ECV values of around 25.3% (at 1.5 T) have been observed in healthy individuals. Apart from amyloid deposition, an increased ECV is commonly associated with excessive collagen deposition, making it a more reliable measure of myocardial fibrosis. Conversely, low ECV values are found in cases of thrombus formation and fat/lipomatous metaplasia. ECV can be calculated for specific myocardial regions or visualized using ECV maps. Elevated native T1 is 89% sensitive and 80% specific, and increased ECV is 93% sensitive and 87% specific for CA.[8]

Mimics and Mimicry

Detecting cardiac amyloidosis on cMRI is challenging despite advancements in imaging techniques. Additionally, the histopathological evidence required to validate CMR interpretations remains limited. Nonischemic and ischemic cardiomyopathies may mimic cardiac amyloid on imaging.

False-Positive Interpretations

The imaging features of CA may overlap with ischemic heart disease, hypertrophic cardiomyopathy (HCM), hypertensive heart disease, acute myocarditis, and other infiltrative disorders like Anderson-Fabry disease and iron overload. In this section, we discuss specific examples of false-positive interpretations and challenges in accurate identification of CA.

Coronary artery disease (CAD) leads to fibrosis of cardiac tissue causing ischemic cardiomyopathy. In ischemic cardiomyopathy, there is subendocardial and transmural LGE, though the distribution is territorial rather than diffuse. In such instances, quantitative assessment becomes critical. Although native T1 may be increased, ECV is usually normal (Figure 5).

In HCM, asymmetric septal thickening is characteristically seen along with systolic anterior mitral valve movement, causing LV outflow tract (LVOT) obstruction and leading to a high-velocity jet in the LVOT tract. Variations in HCM presentation include apical thickening, symmetric hypertrophy, and absence of LVOT obstruction. The typical LGE pattern seen in HCM is intramyocardial confluent areas representing areas of fibrosis, myocardial disarray, necrosis, and scarring. LGE and T1 mapping play a role in prognostic evaluation.

Poor contrast between blood pool and myocardium, characteristically seen in CA, is nonspecific and can also be seen in HCM. Patients with HCM exhibit high native T1 values as compared to those with healthy hearts or hypertensive heart disease, although the elevation is significantly

Figure 5. CAD. An adult with chronic kidney disease and stroke history presented with acute decompensated heart failure and recurrent large pericardial effusion. Short-axis (A) half-Fourier acquisition, single-shot turbo spin echo (HASTE) shows myocardial thickening and pericardial effusion. There is multifocal mid-myocardial LGE (B, C) and a single apical segment of subendocardial delayed enhancement (C, arrowhead). Poor contrast between the blood pool and the myocardium raised the possibility of amyloidosis. Endomyocardial biopsy was positive for trichrome staining, demonstrating areas of fibrosis. No amyloid was seen on Congo red staining.

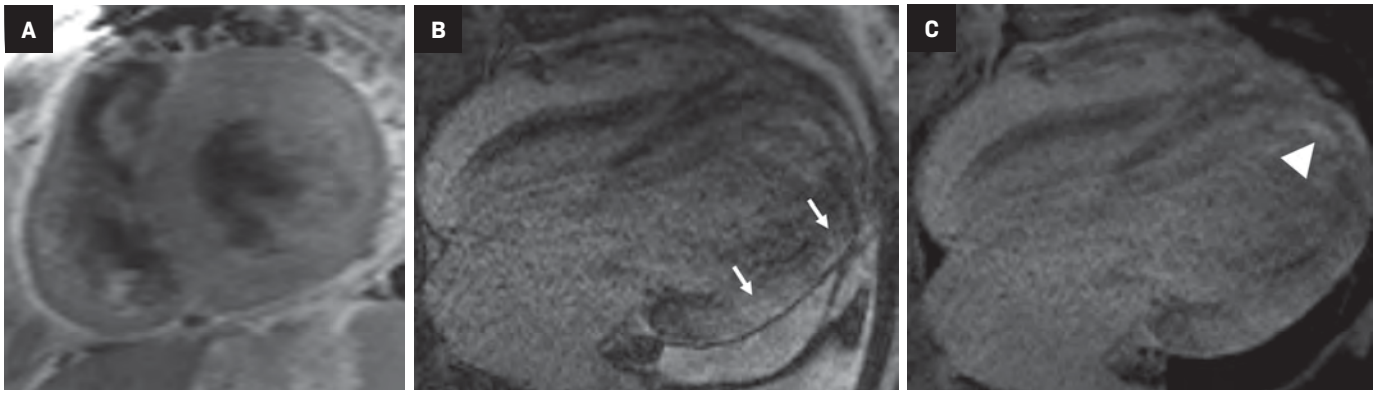

Figure 6. HCM. An elderly patient with HTN, CAD, AS, dyspnea, and AL amyloidosis. LVEF is hyperdynamic and LV is thickened, maximal 21 mm in septum (A, B). Intense mid-myocardial LGE in the basolateral wall (C) and weak confluent LGE across septal, inferior, and lateral walls at the base (D). The absence of LVOT obstruction and LGE basal preponderance pattern favored amyloid. However, the hyperdynamic EF, low LV end systolic volume, normal ECV, and good contrast between blood pool and myocardium favored severe LVH /HCM. Though replacement fibrosis can be seen in HCM, extensive LGE would depress LV EF. Endomyocardial biopsy was negative for amyloid. Scattered foci of cardiomyocyte hypertrophy and significant interstitial fibrosis favored HCM.

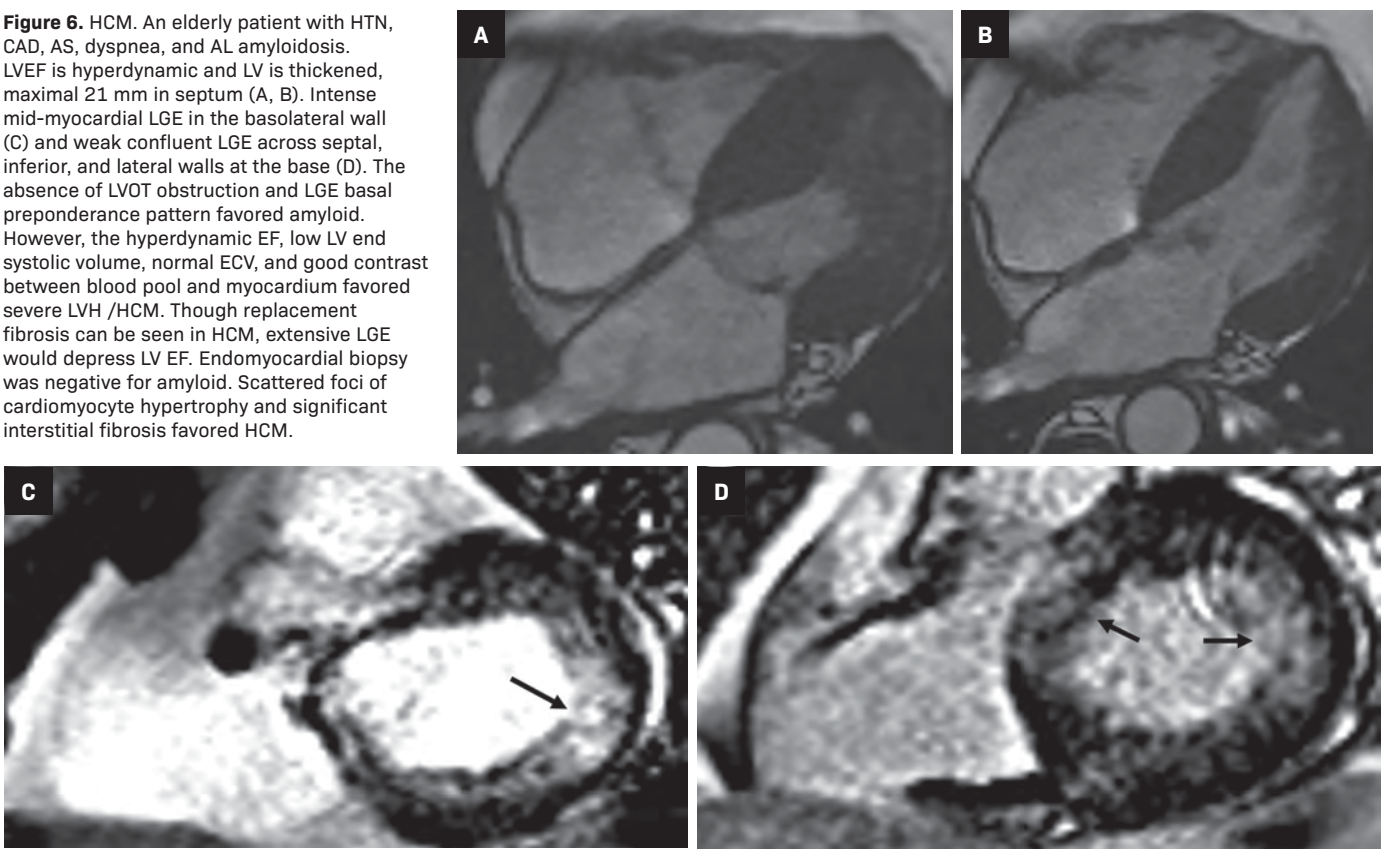

higher in patients with CA.[9,10,11] In HCM, native T1 and ECV are known to be elevated even in the absence of LGE.[12] If there is diffuse LGE, the ejection fraction will likely be depressed in a patient with HCM (Figure 6).

Hypertensive heart disease can resemble CA because it leads to wall thickening, elevated native T1, and LGE which can be variable in extent and distribution. Specifically, when there is left-ventricular wall thickening that cannot be accounted for by arterial hypertension (HTN), it is important to consider the possibility of ATTR amyloidosis, especially in older men.[13] Dilated cardiac chambers and reduced ejection fraction that often accompany severe hypertensive cardiomyopathy, as well as a normal myocardial nulling pattern, can provide essential clues to distinguish between the two (Figure 7).

Myocarditis can also mimic CA, although it typically presents acutely and in young persons. Endomyocardial biopsy remains the gold standard for the diagnosis of myocarditis, but

Figure 7. Hypertensive cardiomyopathy. An adult with HTN, mild decrease in functional capacity, and dilated cardiomyopathy with reduced LVEF. Four-chamber b-SSFP (A) demonstrates bi-atrial and LV enlargement. There is diffuse, near circumferential myocardial delayed enhancement (B, C, arrows). Native T1 and ECV are mildly elevated, EFs are low, and there is poor contrast between blood-pool and myocardium. Endomyocardial biopsy revealed severe subendocardial fibrosis, amyloid negative.

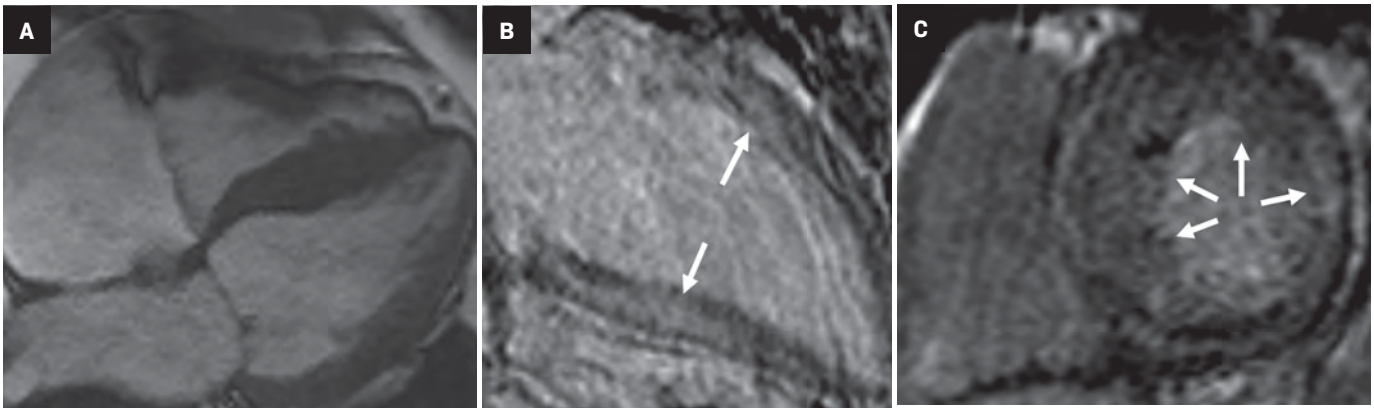

Figure 8. ATTR amyloidosis. An elderly patient with congestive heart failure (CHF) and severe AS. EF was low. Four-chamber b-SSFP (A) shows dilated LV with LVH. PSIR images (B) show patchy areas of mid-myocardial delayed enhancement. The findings were not characteristic of CA. PYP scan was negative for ATTR amyloid (C). Endomyocardial biopsy revealed diffuse fibrosis and Congo red staining. Typing revealed AANF-type and wild type transthyretin amyloidosis.

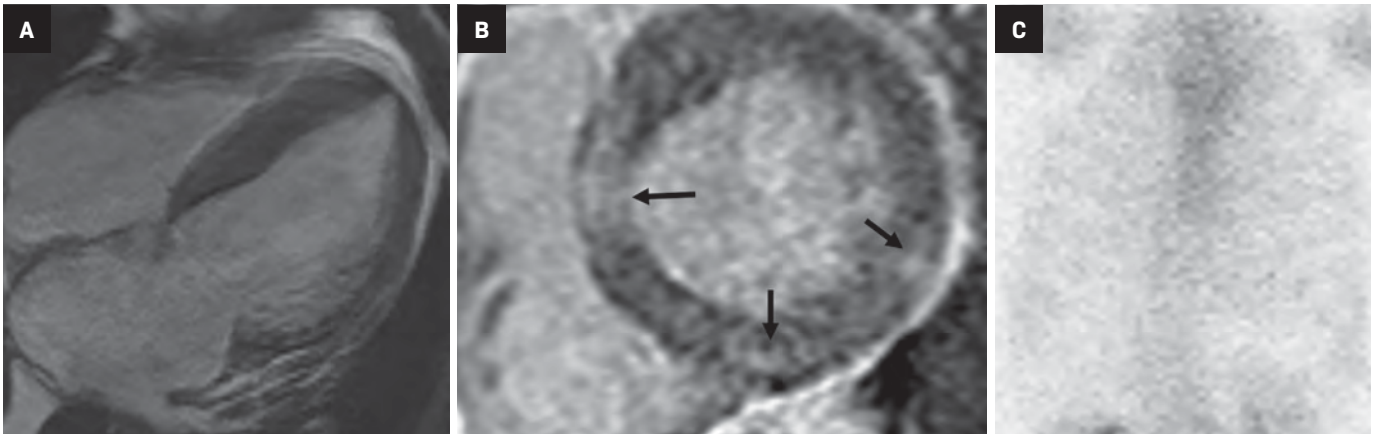

the patchy nature of inflammation causes a low rate of detection of ~ 35%.[14] CMR typically shows dilated cardiac chambers and a patchy, nonischemic LGE distribution from epicardium to mid-myocardium.[13]

Storage disorders like Anderson-Fabry disease and iron overload can also mimic CA. Fabry disease leads to a typical inferolateral mid-wall LGE pattern. Native T1 values are characteristically decreased and are shown to precede the development of left ventricular hypertrophy (LVH).[15]

False-Negative Interpretations

False-negative interpretations can result from the presence of concomitant cardiac pathologies and comorbidities, causing atypical imaging findings. The prevalence of calcific aortic stenosis (AS) and CA tends to rise with advancing age, and it is not uncommon for these conditions to coexist in elderly individuals. Identifying CA in patients with AS poses specific challenges owing to similar pathophysiological, clinical, and imaging features between the two conditions. Among individuals with calcifying AS, studies have reported the occurrence of ATTR amyloidosis in approximately 32% of men over age 74.[16] However, more recent research indicates a prevalence ranging from 12 to 16%.[17,18] Furthermore, patients with both calcifying AS and ATTR amyloidosis have notably poorer survival rates following valve replacement interventions or surgeries when compared to those without amyloidosis.[19]

Therefore, confirming the diagnosis of CA is crucial as it can guide the therapeutic management of AS and potentially involve the utilization of recently developed pharmacological treatments targeting ATTR amyloidosis. Certain features that point toward concomitant CA in patients with AS include a low-voltage ECG despite LVH, severe biventricular hypertrophy, severe LV longitudinal strain with apical sparing, myocardial granular speckling on echocardiography; and extensive LV LGE with elevated ECV on CMR.[20] (Figure 8)

Figure 9. ATTR amyloidosis. An elderly patient with primary familial cardiomyopathy, recurrent pulmonary embolism, HTN, and atrial fibrillation, with increased shortness of breath and fatigue. CMR demonstrates moderately dilated left and right atrium, relatively thick proximal interventricular septum. PSIR images show predominantly mesomyocardial, band-shaped, delayed enhancement in the inferolateral wall near the base of the heart (A, B, arrows). Good contrast between the blood pool and myocardium is seen. On inversion time cine scout images (not shown), normal myocardial nulling pattern was seen. Findings were not typical for CA. Endomyocardial biopsy revealed wild-type ATTR amyloidosis.

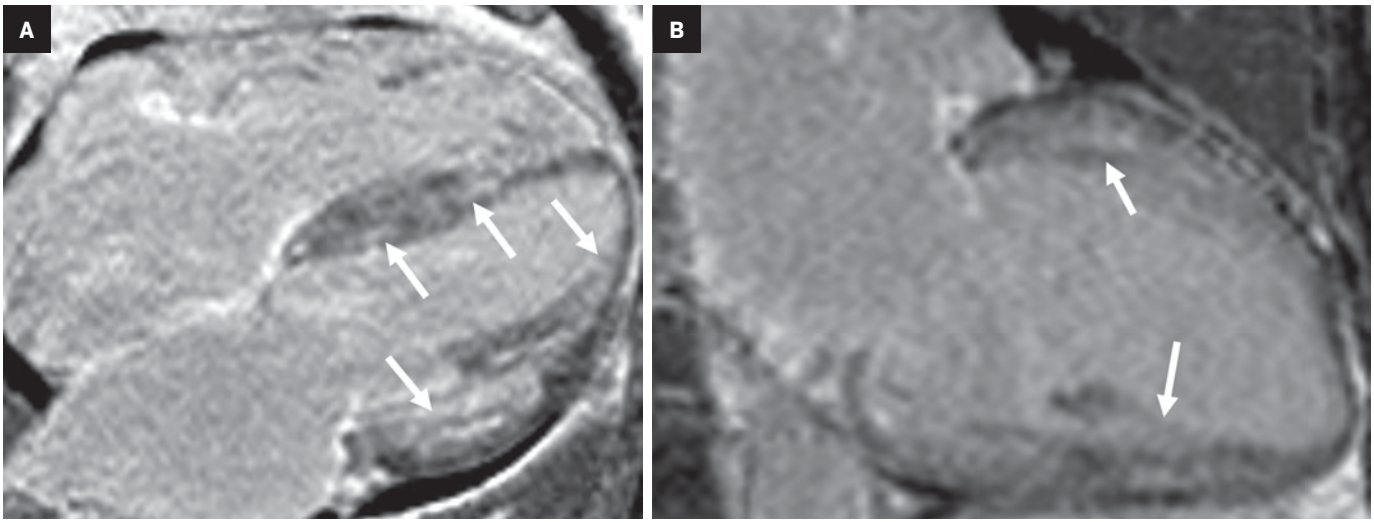

Figure 10. ATTR amyloidosis. An elderly patient with CHF, severe AS, and HTN with suspected sarcoidosis. Four-chamber b-SSFP (A) demonstrates cardiomegaly with dilation of the LA. There is predominant mid-myocardial LGE in the inferoseptum from the base to the mid-LV and the basal lateral/inferolateral wall, and focal LGE at the RV insertion points (B, arrows). Native T1 and ECV were elevated, Findings were thought to be consistent with cardiac sarcoidosis; however, PET was negative. Endomyocardial biopsy revealed ATTR-positive amyloidosis.

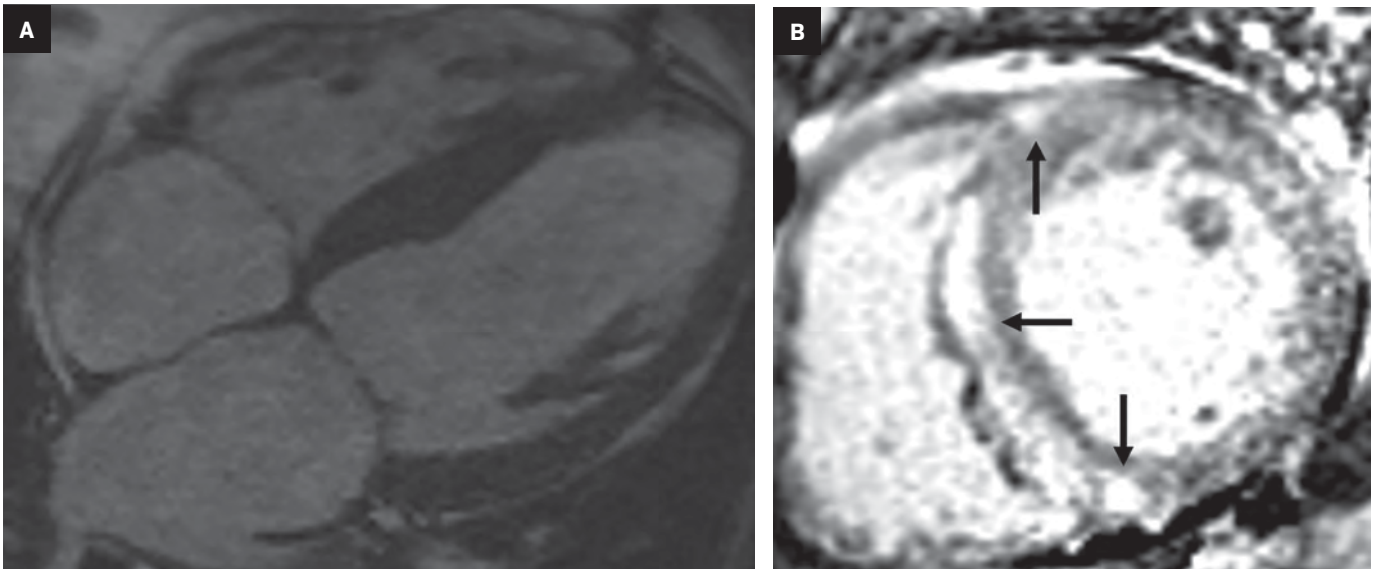

Idiosyncratic myocardial nulling and poor contrast between blood pool and myocardium on inversion recovery sequences are characteristically seen in CA. To an extent, the time chosen to perform LGE sequences is arbitrary, and this can lead to false negative interpretations. Furthermore, poor contrast between the blood pool and myocardium depends on contrast kinetics, making the procedure nonspecific (Figure 9). Phase-sensitive inversion-recovery (PSIR) sequences reduce the need for optimal null point determination. Cardiac sarcoidosis can resemble CA, as the former has a variety of appearances on CMR and can be transmural and multifocal (Figure 10). Cardiac involvement, associated with a significantly worse prognosis, is found in about 25% of patients with sarcoidosis at autopsy. Clinically, however, it is only diagnosed in 5% of patients with sarcoidosis.[21] Like CA, sarcoidosis leads to elevated native T1 and ECV.

Assessment of pretest probability of CA is essential to limit false-negative interpretations. The presence of known TTR gene mutations, together with nonspecific LGE characteristics,

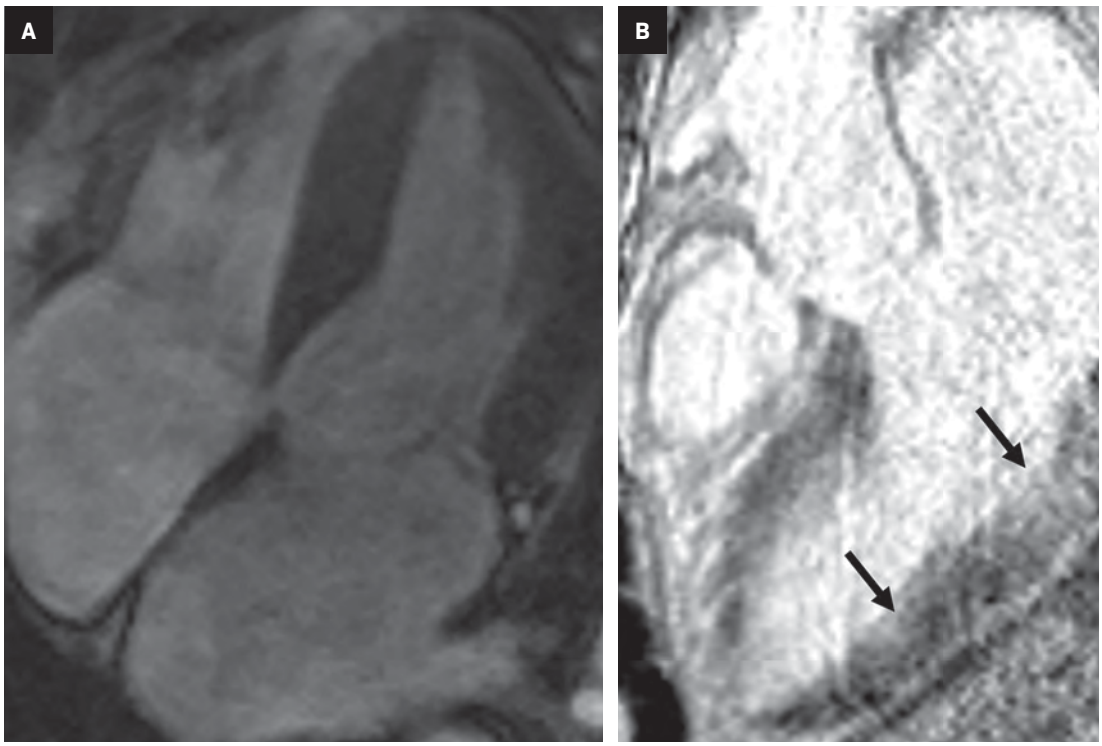

Figure 11. ATTR amyloidosis. An adult who underwent liver transplant with a known *Glu*61*Gly* (mutated transthyretin) gene variant presented with increased shortness of breath and fatigue. Transthoracic echocardiogram demonstrated LVEF of 45% and mild concentric LVH. Four-chamber b-SSFP (A) demonstrates normal LV size. Delayed enhancement PSIR image (B) shows diffuse, patchy myocardial delayed enhancement from the subendocardium to subepicardium, and mostly involving the lateral wall. Findings are nonspecific and not the typical amyloid pattern.Endomyocardial biopsy showed TTR amyloidosis with *Glu*61*Gly* gene variant confirming the deposition of transthyretin from the transplanted liver.

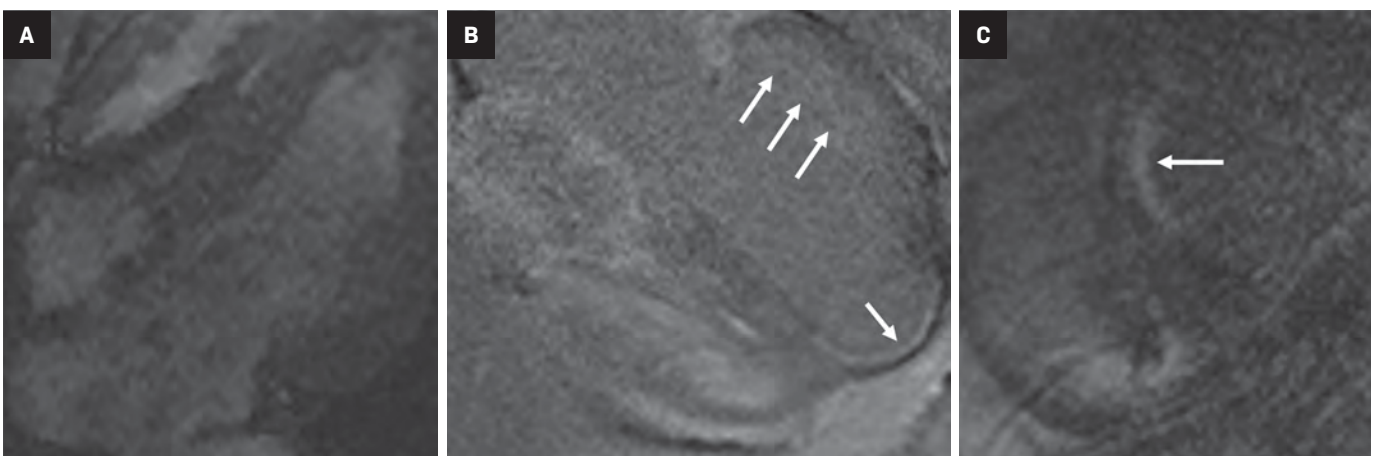

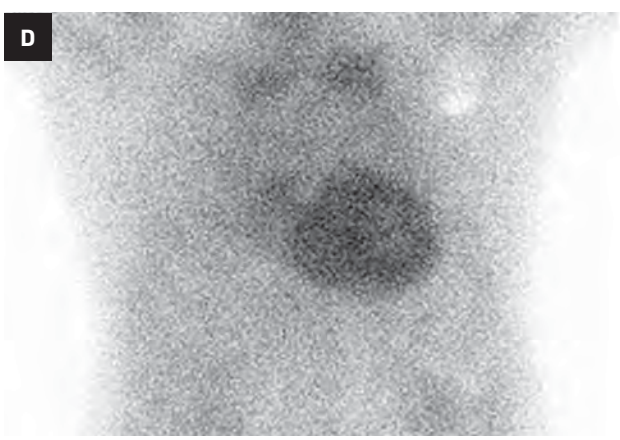

Figure 12. ATTR amyloidosis. An elderly patient with history of atrial fibrillation, ventricular tachycardia, HTN, and CAD presented with heart failure. Four-chamber b-SSFP (A) demonstrates LV thickening. There is LGE in the anterior and anterior septal walls that extends from base to apex; toward the base there is near transmural involvement, while toward the apex, the involvement is more subendocardial than it is transmural, (B, C, arrows). The morphology and distribution of LGE is ischemic. The patient developed chronic heart failure, and PYP scan after a year demonstrated Grade 3 PYP uptake (D), highly suggestive of ATTR amyloidosis. Endocardial biopsy confirmed wild type cardiac ATTR amyloidosis.

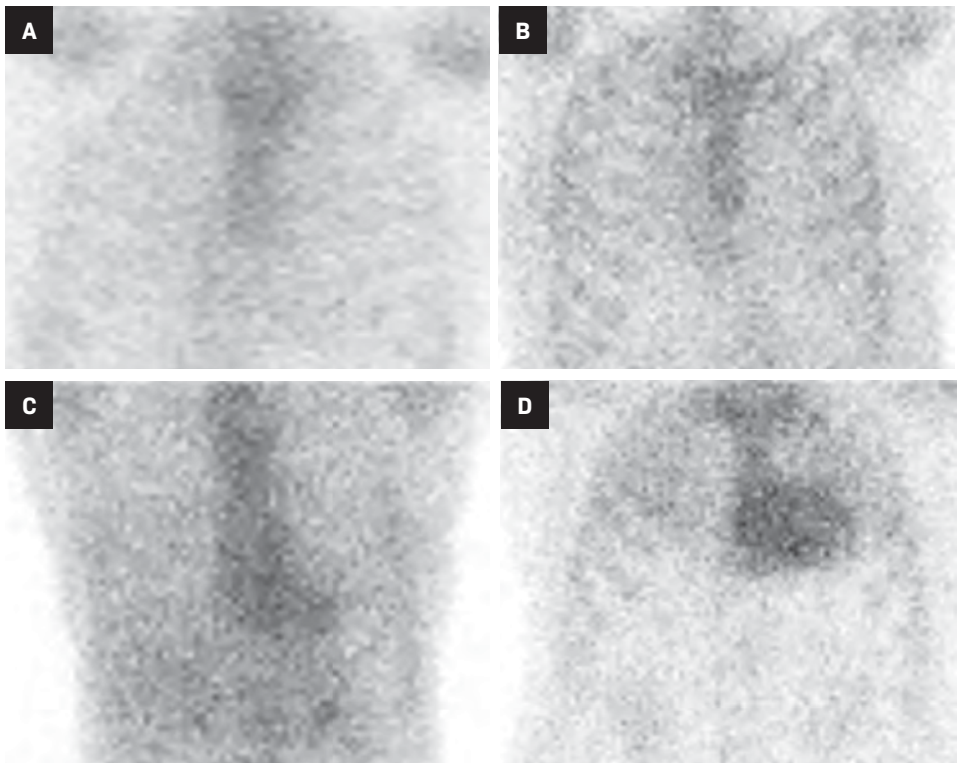

Figure 13. Visual grading system. Planar Tc99 PYP scan demonstrating the uptake of transthyretin amyloid relative to the rib uptake. A = Grade 0, B = Grade 1, C = Grade 2, D = Grade 3.

Figure 14. ATTR amyloidosis NM imaging. SPECT/CT Tc-99m PYP scan demonstrating Grade 3 uptake (greater than rib uptake with mild/absent rib uptake). H/CL = 2.62. There is no significant blood pool present.

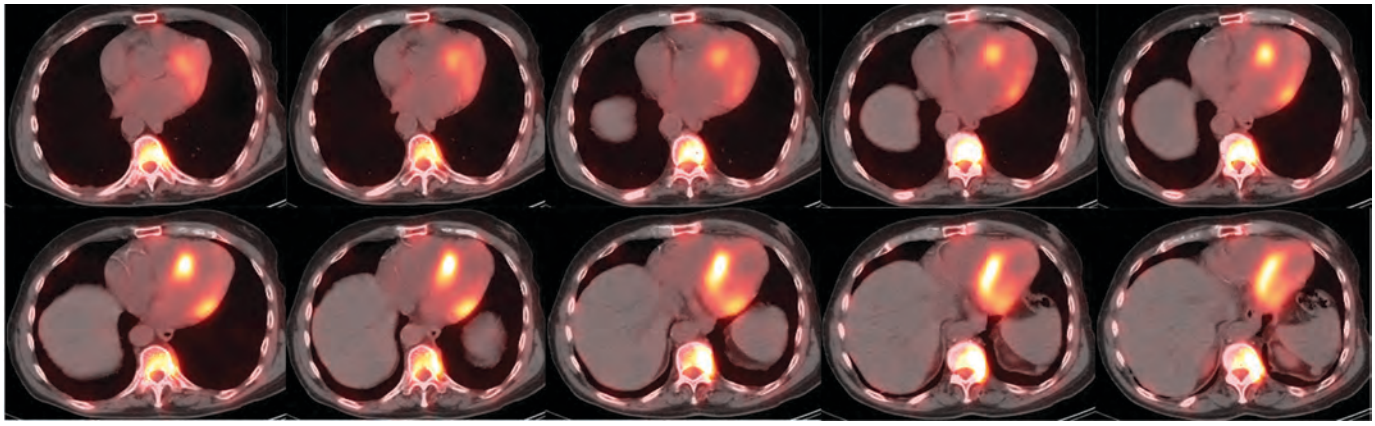

must raise suspicion for ATTR (Figure 11). The TTR gene has over 100 single nucleotide polymorphisms, with 80 confirmed pathogenic mutations. These variations result in variant TTR amyloidosis, which exhibits diverse clinical phenotypes and patterns of inheritance.

Certain mutations, such as V30M and V122I, are associated with cardiac involvement, with V122I being prevalent, and potentially contributing to the development of heart failure, in the US African American population.[22] As more treatments and preventive strategies emerge, the TTR genotype of patients can assist in guiding family screening. A streamlined approach to assessing pretest genetic risk could provide patients and clinicians with valuable guidance when considering genetic testing.

Early CA may cause territorial LGE distribution that mimics ischemic cardiac disease (Figure 12). Quantitative T1 assessment and bone scintigraphy are useful in such situations to screen patients with nonspecific CMR findings.

Role of Nuclear Imaging

Nuclear imaging plays a significant role in detecting ATTR amyloidosis. The modality offers high specificity (88.6-97.1%) and sensitivity (90.9 - 91.5%)[4] for distinguishing between ATTR and AL types. In the absence of monoclonal proteins in serum or urine, increased myocardial PYP

take has >99% specificity and positive predictive value for cardiac TTR amyloidosis.[4] Technetium (Tc) -99m PYP, Tc-99mhydroxymethylene diphosphonate (HMDP), and Tc-99 mdicarboxypropane diphosphonate (DPD) bone scans have been used for ATTR CA.[23] Visual grading system (grades 0–3) can be used to quantify Tc-99m uptake for ATTR CA (Figure 13). Uptake of grade 2/3 is considered positive for ATTR cardiac amyloidosis.

False positives may result from blood pool activity in LV and increased adjacent rib uptake. Single photon emission CT (SPECT) enables accurate discrimination of myocardial uptake from cardiac blood pool (Figure 14). Semi-quantitative analysis of myocardial uptake can also be performed using heart-to-whole body (H/WB) ratio or heart-to-contralateral lung (H/CL) ratio. Mean H/WB ratio of ATTR CA is reported to be 10%, while H/CL ratio with a cut-off value of 1.5 can differentiate ATTR from AL. Amyloid-targeting PET tracers 11c PIB, 18f florbetapir, 18f florbetaben, and 18f flutemetamol are currently being developed.[24] Early results with 18f florbetapir PET demonstrate higher myocardial uptake for AL than for ATTR.[25]

Conclusion

No diagnostic test is perfect; false-positives and false-negatives occur throughout diagnostic medicine. Nevertheless, awareness of how similar the conditions we seek to distinguish from CA can look like CA is important. Where the diagnosis can lead to substantial change in management, such as with CA, we advise more liberal pathological correlation.

References

1) Gilstrap LG, Dominici F, Wang Y, et al. Epidemiology of cardiac amyloidosis–associated heart failure hospitalizations among fee-for-service medicare beneficiaries in the United States. *Circ Hear Fail*. 2019;12(6):e005407. doi:10.1161/CIRCHEARTFAILURE.118.005407

2) Fontana M, Chung R, Hawkins PN, Moon JC. Cardiovascular magnetic resonance for amyloidosis. *Heart Fail Rev*. 2015;20(2):133-144. doi:10.1007/s10741-014-9470-7

3) Oda S, Kidoh M, Nagayama Y, et al. Trends in diagnostic imaging of cardiac amyloidosis: emerging knowledge and concepts. *RadioGraphics*. 2020;40(4):961-981. doi:10.1148/rg.2020190069

4) Brownrigg J, Lorenzini M, Lumley M, Elliott P. Diagnostic performance of imaging investigations in detecting and differentiating cardiac amyloidosis: a systematic review and meta-analysis. *ESC Hear Fail*. 2019;6(5):1041-1051. doi:10.1002/ehf2.12511

5) Maceira AM, Joshi J, Prasad SK, et al. Cardiovascular magnetic resonance in cardiac amyloidosis. *Circulation*. 2005;111(2):186-193. doi:10.1161/01.CIR.0000152819.97857.9D

6) Ana M-N, A. TT, Amna A-G, et al. Magnetic resonance in transthyretin cardiac amyloidosis. *J Am Coll Cardiol*. 2017;70(4):466-477. doi:10.1016/j.jacc.2017.05.053

7) Kyriakou P, Mouselimis D, Tsarouchas A, et al. Diagnosis of cardiac amyloidosis: a systematic review on the role of imaging and biomarkers. *BMC Cardiovasc Disord*. 2018;18(1):221. doi:10.1186/s12872-018-0952-8

8) Pan JA, Kerwin MJ, Salerno M. Native T1 mapping, extracellular volume mapping, and late gadolinium enhancement in cardiac amyloidosis: a meta-analysis. *JACC Cardiovasc Imaging*. 2020;13(6):1299-1310. doi:10.1016/j.jcmg.2020.03.010

9) Fontana M, Banypersad SM, Treibel TA, et al. Native T1 mapping in transthyretin amyloidosis. *JACC Cardiovasc Imaging*. 2014;7(2):157-165. doi.org/10.1016/j.jcmg.2013.10.008

10) Hinojar R, Varma N, Child N, et al. T1 mapping in discrimination of hypertrophic phenotypes: hypertensive heart disease and hypertrophic cardiomyopathy. *Circ Cardiovasc Imaging*. 2015;8(12):e003285. doi:10.1161/CIRCIMAGING.115.003285

11) Karamitsos TD, Piechnik SK, Banypersad SM, et al. Noncontrast T1 mapping for the diagnosis of cardiac amyloidosis. *JACC Cardiovasc Imaging*. 2013;6(4):488-497. doi: 10.1016/j.jcmg.2012.11.013

12) Haaf P, Garg P, Messroghli DR, Broadbent DA, Greenwood JP, Plein S. Cardiac T1 mapping and extracellular volume (ECV) in clinical practice: a comprehensive review. *J Cardiovasc Magn Reson*. 2016;18(1):89. doi:10.1186/s12968-016-0308-4

13) Rapezzi C, Lorenzini M, Longhi S, et al. Cardiac amyloidosis: the great pretender. *Heart Fail Rev*. 2015;20(2):117-124. doi:10.1007/s10741-015-9480-0

14) Georgiopoulos G, Figliozzi S, Sanguineti F, et al. Prognostic impact of late gadolinium enhancement by cardiovascular magnetic resonance in myocarditis. *Circ Cardiovasc Imaging*. 2021;14(1):e011492. doi:10.1161/CIRCIMAGING.120.011492

15) Pica S, Sado DM, Maestrini V, et al. Reproducibility of native myocardial T1 mapping in the assessment of Fabry disease and its role in early detection of cardiac involvement by cardiovascular magnetic resonance. *J Cardiovasc Magn Reson*. 2014;16(1):99. doi:10.1186/s12968-014-0099-4

16) Cavalcante JL, Rijal S, Abdelkarim I, et al. Cardiac amyloidosis is prevalent in older patients with aortic stenosis and carries worse prognosis. *J Cardiovasc Magn Reson*. 2017;19(1):98. doi:10.1186/s12968-017-0415-x

17) Christian N, R. SP, P. PK, et al. Prevalence and outcomes of concomitant aortic stenosis and cardiac amyloidosis. *J Am Coll Cardiol*. 2021;77(2):128-139. doi:10.1016/j.jacc.2020.11.006

18) Castaño A, Narotsky DL, Hamid N, et al. Unveiling transthyretin cardiac amyloidosis and its predictors among elderly patients with severe aortic stenosis undergoing transcatheter aortic valve replacement. *Eur Heart J*. 2017;38(38):2879-2887. doi:10.1093/eurheartj/ehx350

19) Treibel TA, Fontana M, Gilbertson JA, et al. Occult transthyretin cardiac amyloid in severe calcific aortic stenosis. *Circ Cardiovasc Imaging*. 2016;9(8):e005066. doi:10.1161/CIRCIMAGING.116.005066

20) Ternacle J, Krapf L, Mohty D, et al. Aortic stenosis and cardiac amyloidosis: JACC review topic of the week. *J Am Coll Cardiol*. 2019;74(21):2638-265. doi: 10.1016/j.jacc.2019.09.056

21) Hotta M, Minamimoto R, Awaya T, Hiroe M, Okazaki O, Hiroi Y. Radionuclide imaging of cardiac amyloidosis and sarcoidosis: roles and characteristics of various tracers. *RadioGraphics*. 2020;40(7):2029-204. doi:10.1148/rg.2020200068

22) Ruberg FL, Berk JL. Transthyretin (TTR) cardiac amyloidosis. *Circulation*. 2012;126(10):1286-1300. doi:10.1161/CIRCULATIONAHA.111.078915

23) Perugini E, Guidalotti PL, Salvi F, et al. Noninvasive etiologic diagnosis of cardiac amyloidosis using 99mTc-3,3-diphosphono-1,2-propanodicarboxylic acid scintigraphy. *J Am Coll Cardiol*. 2005;46(6):1076-1084. doi:10.1016/j.jacc.2005.05.073

24) Gallegos C, Miller EJ. Advances in PET-based cardiac amyloid radiotracers. *Curr Cardiol Rep*. 2020;22(6):40. doi:10.1007/s11886-020-01284-3

25) Dorbala S, Vangala D, Semer J, et al. Imaging cardiac amyloidosis: a pilot study using 18F-florbetapir positron emission tomography. *Eur J Nucl Med Mol Imaging*. 2014;41(9):1652-1662. doi:10.1007/s00259-014-2787-6

Imaging Testicular Torsion

Michael Louis Francavilla, MD

Testicular torsion, or more accurately, spermatic cord torsion, is an important cause of an acute scrotum. Clinically, patients may present with any of the following symptoms: acute scrotal pain not relieved by scrotal elevation; scrotal swelling; absent cremasteric reflex; nausea; and vomiting. Radiologists play a critical role in the evaluation of the acute scrotum and must be able to recognize complete and incomplete testicular torsion.

Two types of testicular torsion with different peaks have been described. Extravaginal testicular torsion occurs primarily in utero or in neonates. Intravaginal testicular torsion is most common around 12 years of age but can occur at any age.[1] The bell clapper anomaly is the primary risk factor for intravaginal torsion; the condition usually presents bilaterally and is estimated to occur in 12% of testes.[2]

The tunica vaginalis begins as the processus vaginalis, an outpouching of peritoneum. It surrounds the testis as it descends into the scrotum and then obliterates proximally. Normally, the tunica vaginalis attaches to the posterolateral aspect of the testis and covers only its anterior surface. In the bell clapper anomaly, the tunica vaginalis attaches to the spermatic cord abnormally high in the scrotum and completely encircles the epididymis, distal spermatic cord, and testis. Thus, these structures hang freely in the intravaginal space and can more easily twist and torse.

Testicular torsion can be complete (360° up to 1,080° [3 full turns]) or incomplete (less than 360°). The twist may be either clockwise or counterclockwise. The vascular twisting causes venous obstruction initially, followed by arterial obstruction and eventually testicular ischemia. Treatment consists of either manual or surgical detorsion. Salvage is more likely with earlier detorsion, decreasing from 90% salvage rate before 12 hours, to 54% between 13 and 24 hours, and to 18% beyond 24 hours.[3] Imaging plays a crucial role in the timely and accurate diagnosis of testicular torsion. Treatment delays resulting from repeat imaging have been associated with increased risk of orchiectomy.[4]

Imaging Protocol

Color Doppler ultrasound is the modality of choice for investigating the acute scrotum. The scan is performed with a high-frequency linear-array transducer.[5] The examination should begin with a side-by-side, short axis comparison (sometimes referred to as a buddy shot, sunglasses view, or saddle view) in grayscale and color Doppler. This view facilitates detection of subtle asymmetry in echotexture or color Doppler flow.

The examination should then proceed with imaging of the asymptomatic side first, permitting optimization of the focal zone, depth, grayscale gain, and Doppler parameters.[5] These images will establish a baseline for comparison. Images of the upper, middle, and lower testicle should be obtained in the medial, middle, and lateral portions of the testis. Evaluation of the upper, middle, and lower epididymis should occur next. The exam of the asymptomatic side concludes with following the spermatic cord from the inguinal canal to the testis and is repeated on the symptomatic side.

Imaging Findings

Color Doppler Flow

Absent or significantly reduced color Doppler flow in the symptomatic testis compared with the asymptomatic testis is highly predictive of acute testicular torsion (Figures 1, 2). Perfusion of only the periphery of the testis at color Doppler is also abnormal and concerning for torsion (Figure 3). A study in which

Affiliation: Department of Radiology, University of South Alabama, Mobile, Alabama.
Conflict of interest/author disclaimer: None.
Keywords: testicular, torsion, ultrasound, Doppler

Figure 1. Teenager with left testicular torsion. A side-by-side transverse color Doppler image of the testes demonstrates symmetric blood flow (A). Duplex Doppler images of each testis were also symmetric (not shown). Evaluation of the left spermatic cord with both longitudinal color Doppler (B) and grayscale transverse (C) views demonstrate the whirlpool sign (*).

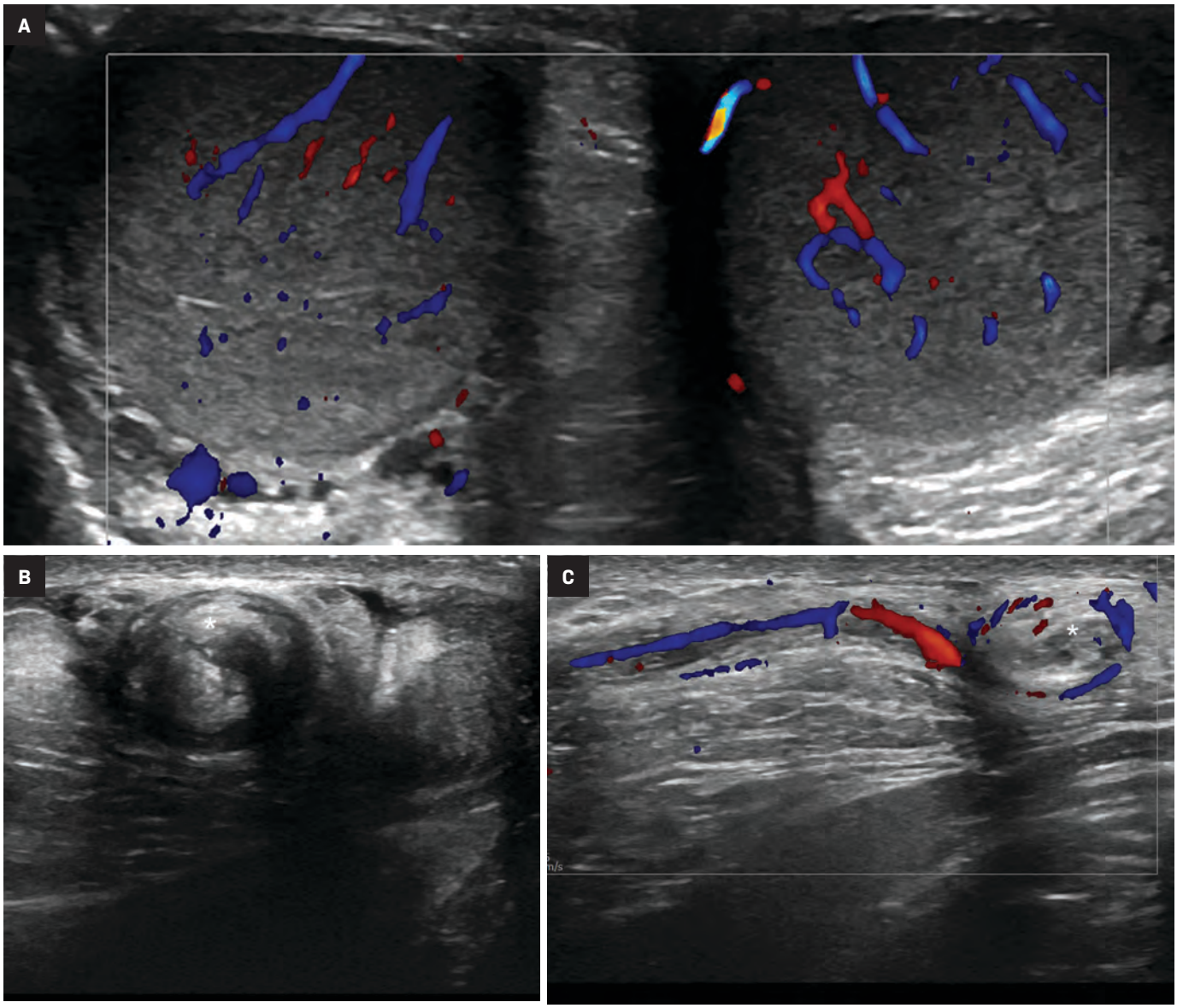

all patients with an acute scrotum were taken to surgery found these signs to have a sensitivity of 96.8% and specificity of 97.9%.[6] Altered testicular Doppler flow indirectly indicates the presence of spermatic cord torsion. Note that in cases of incomplete torsion with preserved flow, color Doppler flow may be decreased, symmetrical or, rarely, even increased.[7] For this reason, familiarity with additional signs of testicular torsion is helpful. Additionally, visualization of color Doppler flow has been a reported limitation in boys 2-4 years of age, particularly when the testis is in the inguinal canal.

Whirlpool sign

The most reliable sign of testicular torsion is the spermatic cord whirlpool sign, a direct indication of torsion. The whirlpool sign appears as an abrupt, spiral-like change in the course of the spermatic cordon either grayscale or color Doppler US (Figure 1). Sensitivity of 92% and specificity of 99% have been reported In older children.[8]

Redundant Spermatic Cord/ Torsion Knot

There should normally be no free piece of spermatic cord in the scrotum. The presence of a redundant, wavy piece of cord indicates an anomalous tunica vaginalis attachment (the bell clapper anomaly). In testicular torsion, the redundant, bunched-up cord may be seen lying

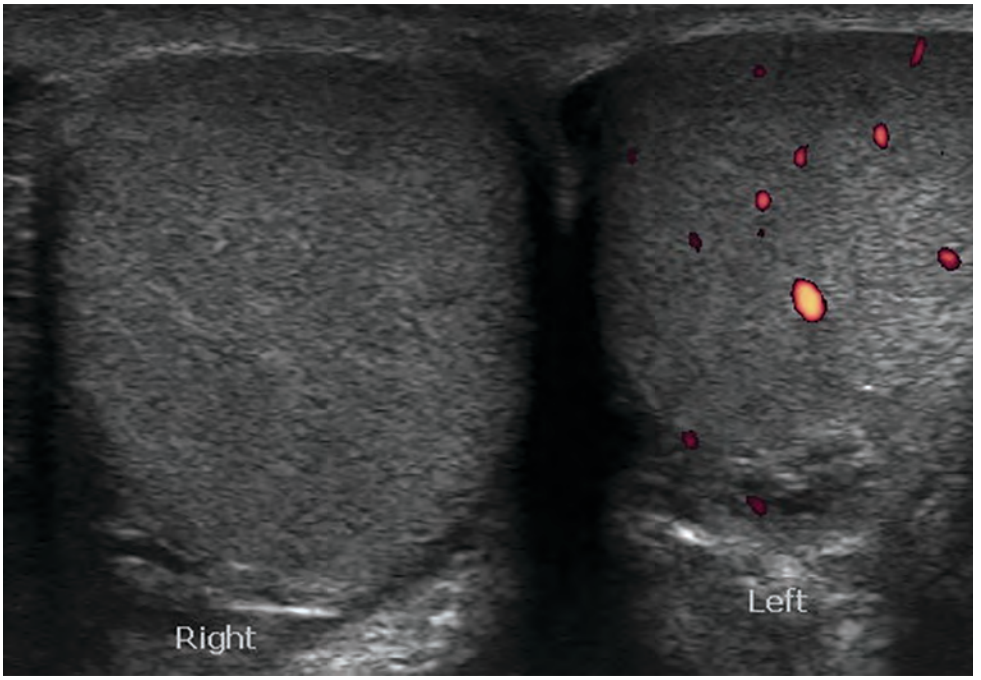

Figure 2. Teenager with complete right testicular torsion. Power Doppler image demonstrates asymmetric Doppler flow with absence of flow in the mildly enlarged right testicle.

Figure 3. Teenager presenting with abdominal pain and vomiting, found to have incomplete left (270°) testicular torsion. Duplex and color Doppler ultrasound scans of the left testicle show Doppler flow only in the periphery of the testis (A, B). There is a positive whirlpool sign (B, *) Hematocele (star) is also shown (A, B). Echogenicity of the testicle was decreased compared to the right testicle, and the left testicle was black and necrotic at surgery.

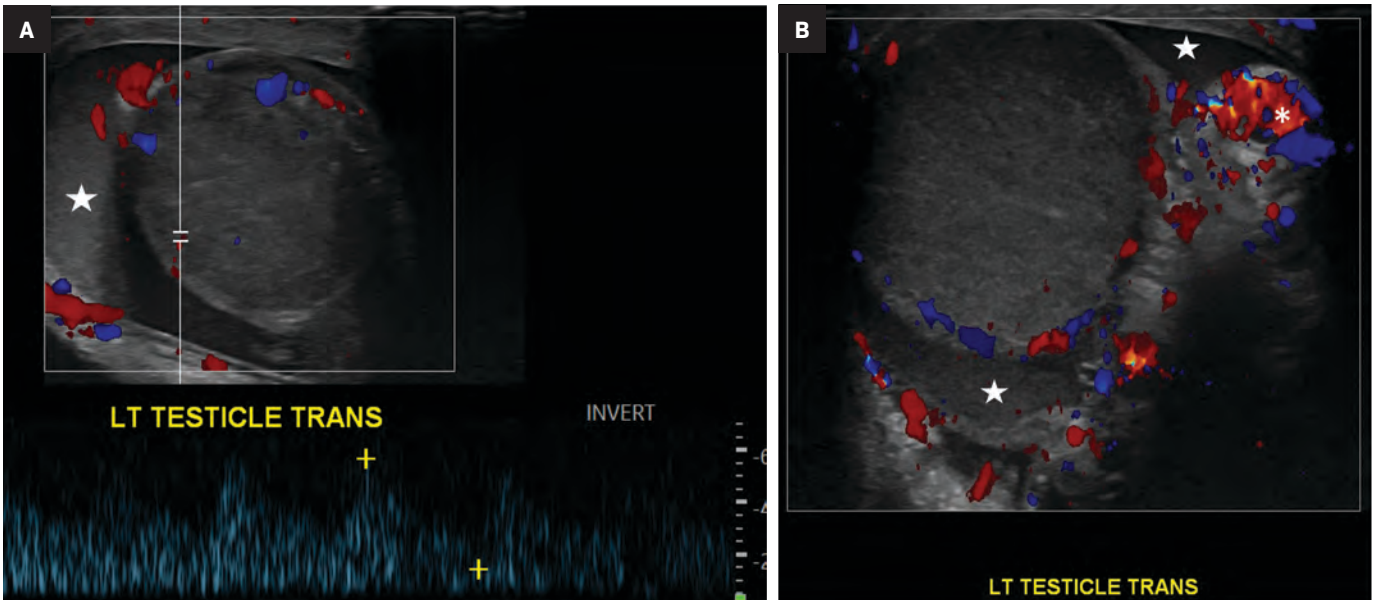

freely in the superior scrotum. It often looks like an ovoid, extra-testicular, heterogeneous mass and is known as a "boggy pseudo-mass" or "torsion knot" (Figure 4).[7] Flow may be present in some or all of the torsion knot, depending on the degree of torsion. The torsion knot is also a direct sign of testicular torsion.

Altered Lie

Normal testes are oriented vertically with the mediastinum testis located posterolaterally. An altered (horizontal or oblique) lie suggests anomalous tunica vaginalis attachment (the bell clapper anomaly) and also can be associated with intermittent testicular torsion (Figure 5).[9]

Concerning Nonspecific Findings

The following findings are abnormal but not specific to testicular torsion: globular testicular enlargement; heterogeneous echotexture; epididymal enlargement without hyperemia; and abnormal spectral Doppler flow (decreased or reversed diastolic flow). Hydroceles or

Figure 4. Teenager with right testicular torsion and preserved flow. Side-by-side color Doppler image shows subtly decreased flow in the right testicle (A). Transverse grayscale view at the superior aspect of the right testis shows an echogenic mass, a torsion knot (B,*).

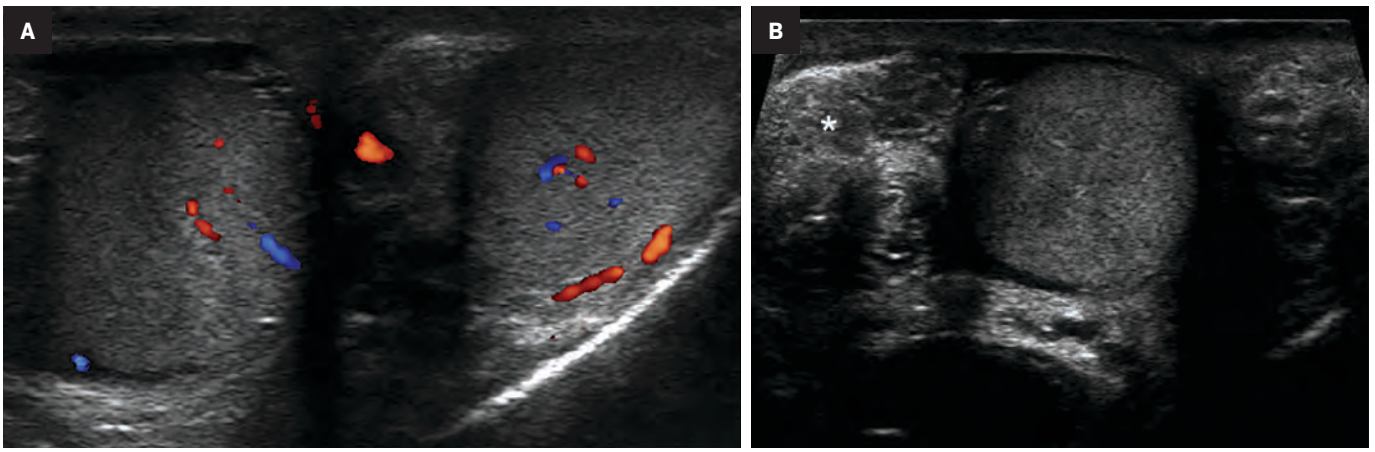

Figure 5. Adolescent with bell clapper deformity. Side-by-side grayscale image shows the left testis has an abnormal, oblique lie with a medially directed mediastinum testis, suggestive of a bell clapper anomaly.

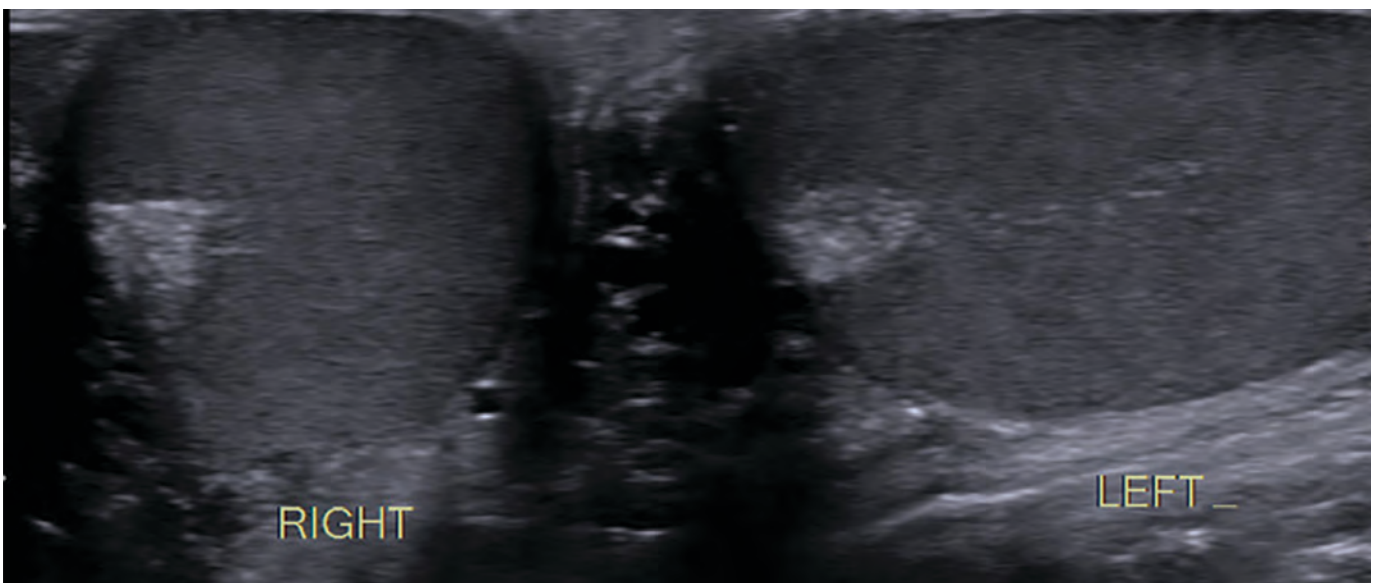

hematoceles are common. Normal testicular echogenicity (with or without mild testicular enlargement) is a good sign of viability. Marked enlargement, heterogeneous echotexture, and scrotal wall hypervascularity are signs of testicular infarction and necrosis.[10] Hemorrhagic infarction may occur with diffuse, focal, or multifocal testicular hyperechogenicity.[10]

Extravaginal Testicular Torsion Findings

The testis is usually necrotic at birth and the hemiscrotum is swollen and discolored. US findings vary, but complex hydrocele and calcification of the tunica albuginea are common (Figure 6).

Testicular Torsion Mimics

Epididymitis

Differentiating torsion from epididymitis, an infection of the epididymis and sometimes the testis, is important. In an analysis of malpractice claims related to testicular torsion, epididymitis was the most cited misdiagnosis (61%).[11] At grayscale imaging, the epididymis is enlarged with variable or heterogeneous echogenicity. The epididymal head is most often affected. Color Doppler flow is increased within the epididymis, testis, or both (Figure 7). Analysis of the epididymal waveform may reveal a low-resistance pattern as compared with the normal pattern.

While absent epididymal vascularity most often results from complete torsion, flow may be maintained and the epididymis enlarged and heterogeneous in cases of incomplete torsion, potentially leading to misdiagnosis. It is critical to pay careful attention to testicular Doppler flow

Figure 6. Newborn with swollen right scrotum at delivery due to testicular torsion. Side-by-side color Doppler image demonstrates absence of Doppler flow, heterogeneity, and enlargement of the right testis (*) and epididymis (star), as well as swelling of the right scrotum. The tunica albuginea (arrow) is echogenic, reflecting calcification. There are small right-sided and large left-sided hydroceles. Color Doppler flow to the left testis is normal for age.

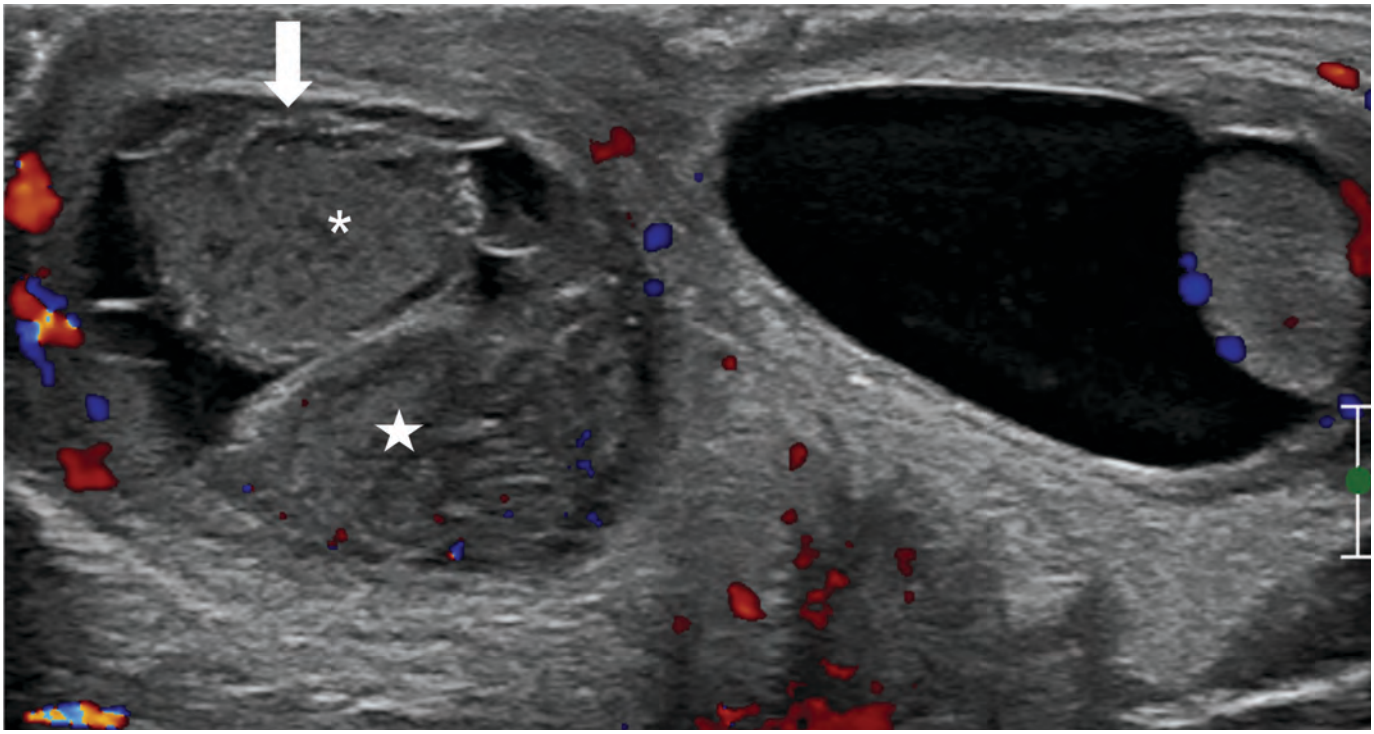

Figure 7. Teenager with left testicular pain due to epididymitis. Color Doppler images of the epididymis and testicle show that the left epididymal head is hyperemic (A, *) compared to the contralateral side (B), while the testicular Doppler flow is symmetric.

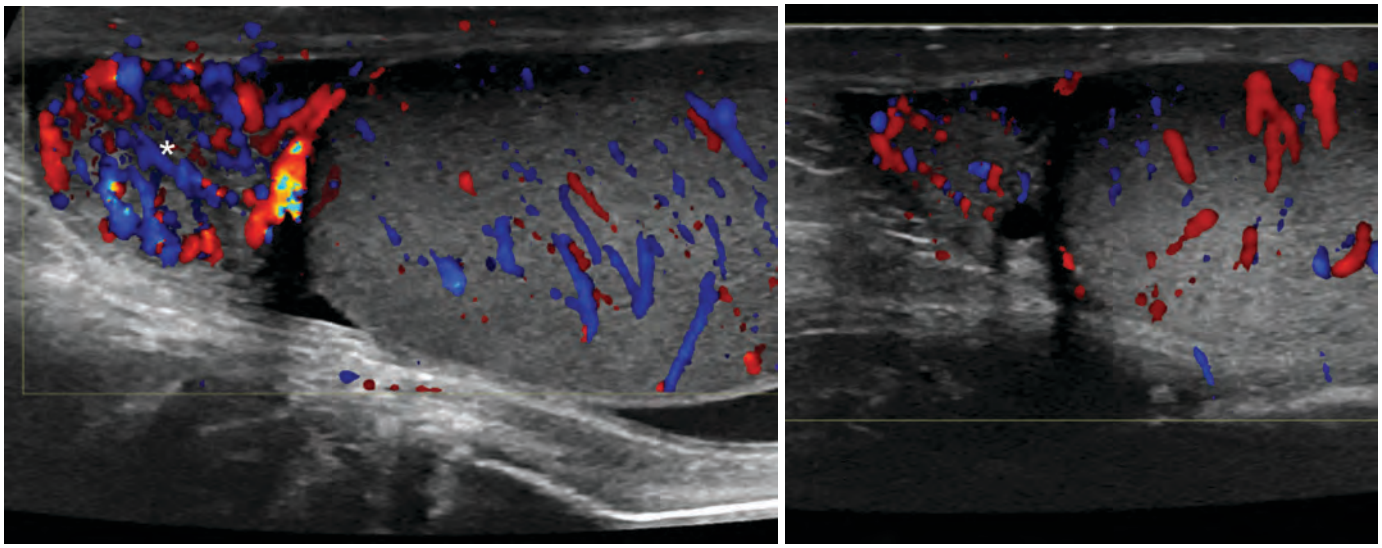

to detect subtle asymmetry, as well as to the spermatic cord to identify a whirlpool sign or a torsion knot. Spontaneous detorsion can manifest as hyperemia of the epididymis and testis. Importantly, detorsion will result in resolution of symptoms.

Appendage Torsion

Torsion of one of the appendages about the testis is a common cause of pediatric acute scrotum.[5] The appendages of the testis and epididymis are remnants of the mesonephric and paramesonephric ducts and, as sessile structures, are predisposed to torsion. The torsed appendage appears as a round, avascular extra-testicular structure with variable echogenicity. The epididymis and scrotum may be hypervascular and swollen. Unlike cases of testicular torsion, testicular vascularity is not decreased.

Correlation with the patient's symptoms is essential to correct diagnosis. Sudden onset of pain and severe nausea and vomiting both suggest testicular torsion. Swelling of the scrotal soft tissues, a finding that occurs only late in torsion, is more common in inflammatory conditions such as epididymitis and appendage torsion.

Conclusion

Radiologists play a critical role in the evaluation of the acute scrotum and must be able to recognize complete and incomplete testicular torsion. Ultrasound is the imaging modality of choice. Incomplete torsion can be difficult to recognize. Careful attention to grayscale spermatic cord findings and color Doppler testicular flow symmetry are keys to the diagnosis. Scrotal exploration should be considered in the presence of high clinical suspicion for testicular torsion, even if the ultrasound findings are nonspecific.

References

1) Zhao LC, Lautz TB, Meeks JJ, Maizels M. Pediatric testicular torsion epidemiology using a national database: incidence, risk of orchiectomy and possible measures toward improving the quality of care. *J Urol*. 2011;186(5):2009-2013. doi:10.1016/j.juro.2011.07.024

2) Caesar RE, Kaplan GW. Incidence of the bell-clapper deformity in an autopsy series. *Urology*. 1994;44(1):114-116. doi:10.1016/S0090-4295(94)80020-0

3) Mellick LB, Sinex JE, Gibson RW, Mears K. A systematic review of testicle survival time after a torsion event. *Pediatr Emerg Care*. September 25, 2017. doi:10.1097/PEC.0000000000001287

4) Huang A, Delozier S, Lauderdale CJ, et al. Do repeat ultrasounds affect orchiectomy rate in patients with testicular torsion treated at a pediatric institution? *J Pediatr Urol*. 2019;15(2):179.e1-179.e5. doi:10.1016/j.jpurol.2018.12.002

5) Aso C, Enríquez G, Fité M, et al. Grayscale and color Doppler sonography of scrotal disorders in children: an update. *Radiographics*. 2005;25(5):1197-1214. doi:10.1148/rg.255045109

6) Waldert M, Klatte T, Schmidbauer J, Remzi M, Lackner J, Marberger M. Color Doppler sonography reliably identifies testicular torsion in boys. *Urology*. 2010;75(5):1170-1174. doi:10.1016/j.urology.2009.07.1298

7) Bandarkar AN, Blask AR. Testicular torsion with preserved flow: key sonographic features and value-added approach to diagnosis. *Pediatr Radiol*. 2018;48(5):735-744. doi:10.1007/s00247-018-4093-0

8) McDowall J, Adam A, Gerber L, et al. The ultrasonographic "whirlpool sign" in testicular torsion: valuable tool or waste of valuable time? A systematic review and meta-analysis. *Emerg Radiol*. 2018;25(3):281-292. doi:10.1007/s10140-018-1579-x

9) Eaton SH, Cendron MA, Estrada CR, et al. Intermittent testicular torsion: diagnostic features and management outcomes. *J Urol*. 2005;174(4 Pt 2):1532-1535; discussion 1535. doi:10.1097/01.ju.0000177726.84913.cc

10) Tsili AC, Bougia CK, Pappa O, Argyropoulou MI. Ultrasonography of the scrotum: Revisiting a classic technique. *Eur J Radiol*. 2021;145:110000. doi:10.1016/j.ejrad.2021.110000

11) Matteson JR, Stock JA, Hanna MK, Arnold TV, Nagler HM. Medicolegal aspects of testicular torsion. *Urology*. 2001;57(4):783-786; discussion 786. doi:10.1016/s0090-4295(00)01049-9

MRI Safety: Prepare for New Guidance

Tobias Gilk, MRSO (MRSC™), MRSE (MRSC™)

For more than two decades, the American College of Radiology (ACR) has offered a collection of guidance documents outlining a number of best practices to maximize safety in hospital-based and freestanding MRI facilities.

These documents are poised to receive significant expansion under an effort to update the ACR's 2020 "Manual on MR Safety."[1] Public comment on the proposed changes is now closed, but if implemented in its entirety, the 135-page document will include a wide range of additions.[1] These include:

- An introduction to the risks of MRI;
- Expanded information on MRI safety management policies and procedures;
- Recommendations of minimum training criteria for Level 1 and Level 2 safety training;
- An initial safety framework particular to remote-scanning environments;
- Significantly expanded content on risk identification, assessment, and mitigation;
- Guidance for physiologic monitoring of patients;
- Guidance on emergency response practices;
- Discussion of "alternative MRI environments," including PET/MR, MR-guided Linac devices, and point-of-care systems; and,
- New appendices with checklists for site policies, spatial field gradient data, and conducting risk assessments of implanted devices.

Additionally, the draft document has been organized into chapters to allow for easier navigation, and a number of figures and illustrations have been added to provide examples of risks, harms, and best practices.

One of the most important improvements to the document lies in explaining the 'why' of MRI risks and not just enumerating the tasks that prevent them. This expansion of scope consists of a description of risks throughout the document, including the new appendix dedicated to conducting MRI risk assessments. These changes alone represent a shift in the ACR's intent to transform the document from an "instruction manual" to more of a "teaching tool."

Since implementing its original MRI safety guidance in 2002, the ACR has long advocated for two distinct levels of training but had not—prior to this draft publication—provided any specific guidance on what each of those levels should contain. Until now, the details of training content and implementation has been determined by the supervising radiologist.

The proposed draft also addresses remote scanning, which is perhaps the most contentious of MRI safety issues. Virtually all contemporary MRI safety guidance (including the ACR's) is predicated on the notion that the technologist performing the exam is physically present at the point-of-care. Increasingly, however, and similar to how radiologists have had the ability to read electronic studies remotely, new software options from many of the leading MRI manufacturers now allow the operating MRI technologist to be in an entirely different location from where the images are being acquired. With the MRI technologist located remotely (sometimes controlling two or more remote MRI scanners simultaneously), standards of point-of-care workflow and responsibilities have not yet been clearly defined.

The new section on remote scanning seeks to lay out an alternative path for remote scanning safety without entirely rewriting guidance for point-of-care scanning. One of the challenges, however, is the multiplicity of ways that remote scanning can be deployed (eg, technical, teaching, expert model, and full operation). At last year's RSNA meeting Siemens provided several presentations in their booth about how Advent Health, an integrated healthcare system headquartered in Florida, was deploying remote scanning.

Advent Health's use of remote scanning includes remote updating of scanner protocols and pulse sequences, "over-the-shoulder" training of remote technologists by senior MR technologists, remote expert scans (eg, a remote cardiac MR expert executing a specialty scan at a remote community hospital or imaging center), and full-shift coverage of remote MR facilities

Affiliation: Founder, Gilk Radiology Consultants, Overland Park, Kansas.

operation during unplanned technologist absences.

The sections of the proposed draft that cover remote scanning are largely dedicated to a discussion of staffing location, with comparatively little discussion devoted to how workflows, decision making, and communications would be required to change under remote scanning.

Owing to the shifting nature of MRI scanning hardware, the draft Manual also features a section on "alternative MR environments." From portable devices like the Hyperfine Swoop, to dedicated neonatal systems like the Aspect Embrace, to MR-Linacs designed to be retrofitted into existing radiation therapy bunkers, MRI scanners are now found throughout many areas of the hospital besides the radiology department. This necessitates alternative sets of standards as well as careful integration of MRI safety practices within the area(s) where the MRI scanner is operating.

As of this writing the ACR has not offered an anticipated release date for the final document; it is expected to take quite some time for the ACR to consider and decide what additions and/or deletions to make prior to publication. Ultimately, however, the next edition of the ACR Manual on MR Safety can likely be expected to continue defining the standard of care with respect to MR imaging performance and safety.

Reference

1) Watson R, Altman D, Dillman J, et al. Draft ACR Manual on MR Safety. American College of Radiology. 2023.

Commentary: Safety Guidance Requires Minimum Standards

Tobias Gilk, MRSO (MRSC™), MRSE (MRSC™)

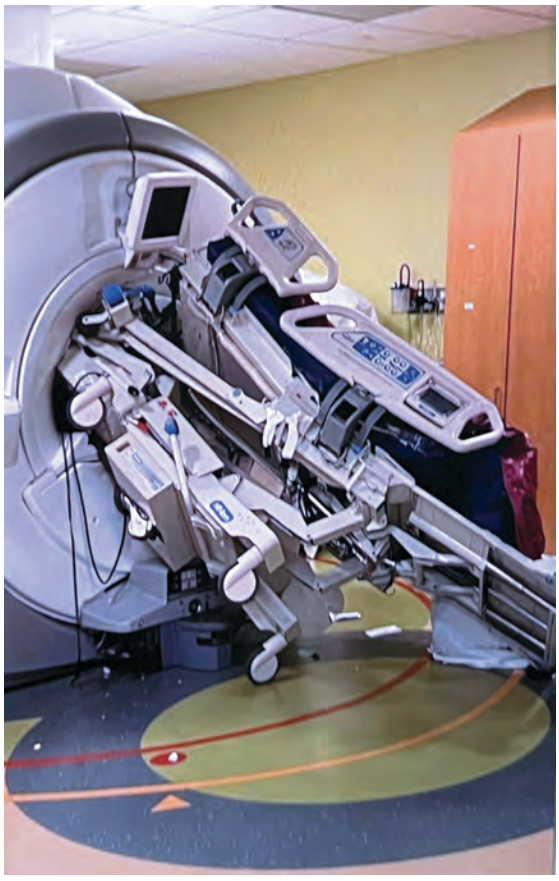

Figure. A nurse at Redwood City Hospital in Redwood City, California, became trapped and seriously injured when an ICU bed was accidentally wheeled into the facility's MRI suite. The ICU patient on the bed at the time was unharmed. *Photo appears in the State of California Department of Industrial Relations Citation and Notification of Penalty Inspection Report (#1654644).*

Earlier this year, a nurse at Redwood City Hospital in Redwood City, California, was seriously injured after becoming pinned between an MRI scanner and a hospital bed that had been wheeled into the MRI scanner room (Figure).

The CMS-2567 "Statement of Deficiencies/ Plan of Corrections"[1] and the Cal/OSHA inspection report have already uncovered a number of gaps between site practice and best practice guidance.[2] These include:

- Indications of an apparent misunderstanding of which radiologist(s) were serving as the site's medical director for MRI safety at the time;
- The designated MR Safety Officer was a radiologist and, given standard workload models for radiologists, that person may not have been capable of ensuring application of site policy at the point of care;
- The intensive care unit nurse was said to be Level 2 MRI safety trained (equivalent to the training level of an MRI technologist), despite having been to the MRI suite only once prior to the accident;
- The site used the same materials for Level 1 and Level 2 MRI safety training; ie, there was no difference in content between the two;
- The MRI suite layout did not comply with the ACR 4-zone criteria although it apparently did meet the criteria for the hospital's Joint Commission accreditation; and,
- The department's contracted medical physicist completed the ACR MRI Safety Program Assessment Checklist and gave the site "perfect marks" for safety, even though the hospital did not maintain ACR MRI accreditation.

Table. Percentage change in US MRI procedure volume (in blue) shown with percentage change in US FDA MRI-classified adverse events (in red). Statistical analysis shows MRI adverse events growing at nearly 3x the rate of MRI procedure volume growth.

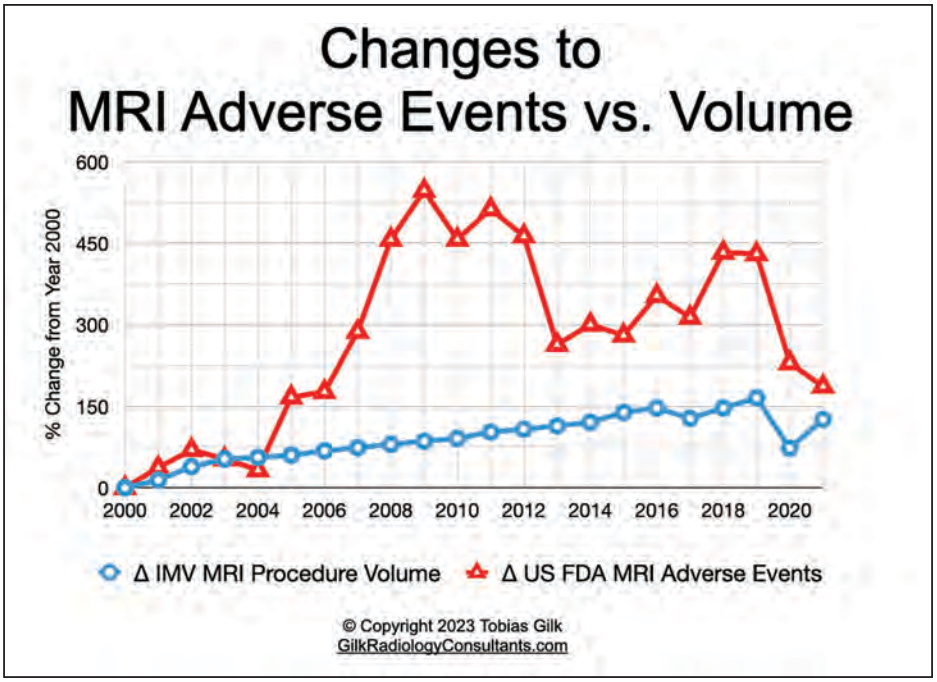

All of which raises the question: Why do serious but preventable MRI accidents continue to occur, even as our collective wisdom about MRI safety has grown over the past 20 years?

Institutional accreditation organizations are expected to assure the public of the quality and safety of healthcare delivery from any given accredited facility. It is that dual promise that is the central point of nearly all accreditation marketing to both healthcare organizations and the public that they serve. However, are accreditation organizations' promises of safety met with corresponding minimum standards to prevent MRI injuries?

In a word, no.

The number of MRI accidents reported to the US Food and Drug Administration over the past two decades has been growing nearly three times as fast as MRI procedure volume (Table). Paradoxically, the more safety guidance that becomes available, the less safe that MRI procedures seem to grow.

An analysis presented at the 2012 RSNA meeting[3] looked at injury prevention best practices for burns, projectiles, and hearing damage. Accident report narratives were tested against each best practice. The analysis indicated that three existing best practices for burn prevention could have prevented 97% of MRI-related burns; three measures for safety from projectiles could have prevented 94% of projectile-related injuries; and one best practice for hearing protection could have prevented 29% of the hearing-related injuries. In aggregate, the study found that these seven practices could likely have prevented 84% of the MRI injury incidents.

Today, more than a decade since that analysis, these best practices remain nearly entirely absent from licensure or accreditation standards for MRI providers. As a result, MRI providers are free to act as they see fit in ensuring the safety of their staff and patients. To be sure, many MRI providers do adhere to accepted best practices, such as those put forth by the ACR. However, there remains no "gold seal" to inform patients whether a given site is among them.

Given this current state of affairs, expecting meaningful reductions in the rates of adverse events in MRI suites may be unrealistic. If, as the saying goes, the "chain is only as strong as its weakest link," the proliferation of safety guidance will have minimal impact on the prevention of MRI-related accidents unless it is accompanied by the establishment, and enforcement, of minimum practice standards.

References

1) CMS-2567 Statement of Deficiencies Plan of Correction Survey Report. US Department of Health and Human Services Centers for Medicare & Medicaid Services. completion date: March 17, 2023.

2) Cal/OSHA Inspection Report #027-23. Aug.7, 2023.

3) Gilk T, Kanal E. MRI accidents and adverse events: empirical analysis of frequency, type, severity, trends and preventions. Presented at The Radiological Society of North America Scientific Exhibition and Annual Meeting, Chicago, Illinois. Nov. 27, 2012.

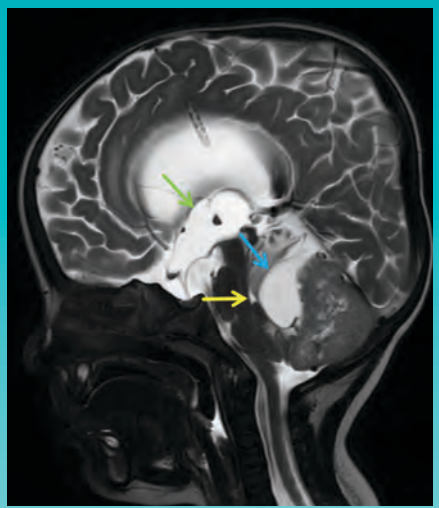

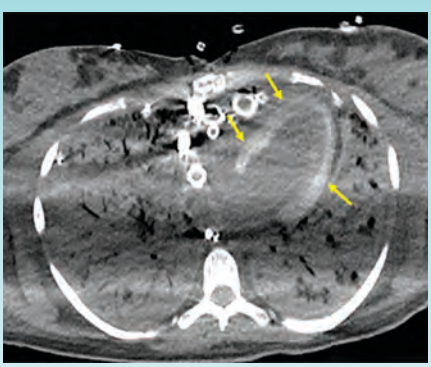

AppliedRadiology®

The Journal of Practical Medical Imaging and Management

Call for Cases

If you have an interesting case we want to know about it!

Sharing your case is a fantastic opportunity to gain recognition for your work and receive feedback from peers all over the world!

Author Guidelines* can be found at

https://appliedradiology.com/author-guidelines

- Abdominal
- Thoracic
- Genitourinary
- GI
- Emergency
- Interventional
- Vascular
- Peds
- Breast
- Neuro
- MSK
- Oncologic
- Cardiac
- Molecular Imaging
- Nuclear Medicine

* Cases undergo peer review before being accepted for publication.

PRINT / ONLINE

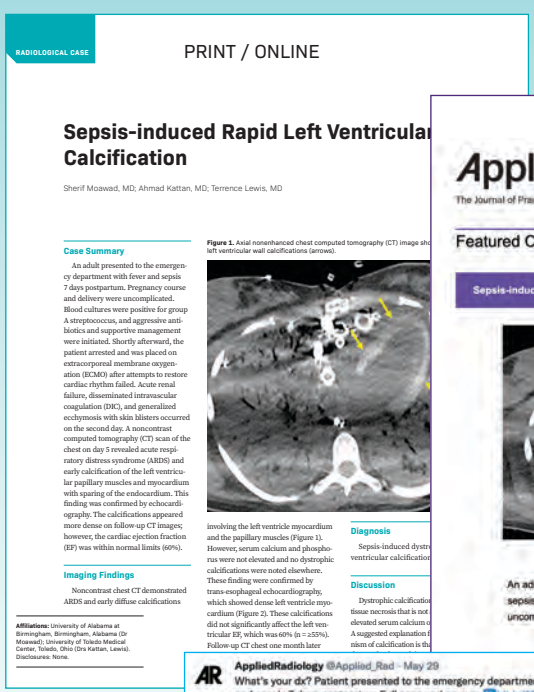
RADIOLOGICAL CASE

Sepsis-induced Rapid Left Ventricular Calcification

Sherif Moawad, MD; Ahmad Kattan, MD; Terrence Lewis, MD

Case Summary

An adult presented to the emergency department with fever and sepsis 7 days postpartum. Pregnancy course and delivery were uncomplicated. Blood cultures were positive for group A streptococcus, and aggressive antibiotics and supportive management were initiated. Shortly afterward, the patient arrested and was placed on extracorporeal membrane oxygenation (ECMO) after attempts to restore cardiac rhythm failed. Acute renal failure, disseminated intravascular coagulation (DIC), and generalized ecchymosis with skin blisters occurred on the second day. A noncontrast computed tomography (CT) scan of the chest on day 5 revealed acute respiratory distress syndrome (ARDS) and early calcification of the left ventricular papillary muscles and myocardium with sparing of the endocardium. This finding was confirmed by echocardiography. The calcifications appeared more dense on follow-up CT images; however, the cardiac ejection fraction (EF) was within normal limits (60%).

Imaging Findings

Noncontrast chest CT demonstrated ARDS and early diffuse calcifications involving the left ventricle myocardium and the papillary muscles (Figure 1). However, serum calcium and phosphorus were not elevated and no dystrophic calcifications were noted elsewhere. These finding were confirmed by trans-esophageal echocardiography, which showed dense left ventricle myocardium (Figure 2). These calcifications did not significantly affect the left ventricular EF, which was 60% (n = ≥55%). Follow-up CT chest one month later

Figure 1. Axial nonenhanced chest computed tomography (CT) image sho left ventricular wall calcifications (arrows).

Diagnosis

Discussion

Affiliations: University of Alabama at Birmingham, Birmingham, Alabama (Dr Moawad); University of Toledo Medical Center, Toledo, Ohio (Drs Kattan, Lewis).
Disclosures: None.

EMAIL ANNOUNCEMENT

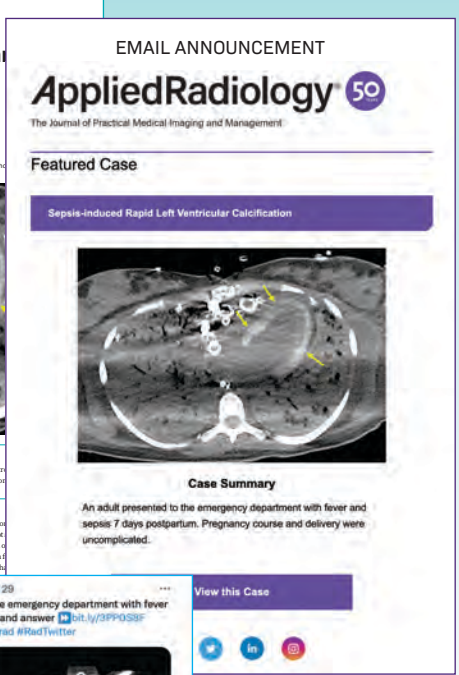
AppliedRadiology 50

The Journal of Practical Medical Imaging and Management

Featured Case

Sepsis-induced Rapid Left Ventricular Calcification

Case Summary

An adult presented to the emergency department with fever and sepsis 7 days postpartum. Pregnancy course and delivery were uncomplicated.

View this Case

SOCIAL MEDIA


AppliedRadiology @Applied_Rad · May 29

What's your dx? Patient presented to the emergency department with fever and sepsis 7 days postpartum Full case and answer bit.ly/3PP0S3F #radiology #RadRes #FOAMed #FOAMrad #RadTwitter

AI in Radiology: A Progress Report

Pierre-Marc Jodoin

AI has made great strides in recent years in demonstrating numerous benefits for researchers, medical administrators, physicians, and patients. So much so that machine learning (ML) is often seen as the bedrock of tomorrow's medicine.

As of today, the most commonly targeted applications for medical ML are image and signal processing, disease diagnosis and prognosis, drug discovery, large medical databases, electronic health record (EHR) management, innovative treatments, computer-assisted medical interventions, and gene manipulation. In addition, many medical generative models, all to some degree inspired by chatGPT, have given rise to surprisingly accurate medical chatbots.

However, these advances have been more the prerogative of academic researchers than of clinicians and their patients, as few AI-powered software solutions have made their way to the market. Last year, the FDA reported that fewer than 200 AI/ML medical devices have received premarket clearances, an arguably low number considering the market size and the capabilities of large neural networks.[1]

There are several reasons for this. First, getting AI/ML software approved by regulatory bodies such as the FDA is difficult. These agencies impose so-called Good Machine Learning Practices that go far beyond the standards commonly used by the research community.[2] The FDA also imposes principles of transparency and explainability, whereby the process by which an AI solution makes a decision must be understood by a physician, something often incompatible with the "black box" nature of deep neural networks.

In addition, despite their power, many intelligent algorithms are poorly integrated into the medical routines of clinicians; this makes it difficult for the medical community to adopt them. What's more, like any new technology, AI-powered software sometimes struggles to gain the trust and buy-in of physicians and patients.

As of today, 76% of all cleared AI/ML medical devices have an intended use in radiology.[1] This means that today's devices are used primarily for the processing and analysis of medical images, predominantly in MRI, CT, radiography, and ultrasound. In addition, they are applied mostly in the fields of oncology, neuroimaging, pulmonology, cardiology, urology, vascular medicine, and ophthalmology, where their central focus is on volumetry. For example, some devices localize, segment, and characterize tumors, while others segment the spatiotemporal dynamics of the ventricles, atria, and myocardium of the heart.

In neuroimaging, many AI/ML medical devices segment and measure regions of the brain like the ventricles, white matter, and gray matter, as well as subregions and deep nuclei such as the hippocampus. Some high-end devices are even used to process and organize white matter fibers extracted from diffusion MRI into meaningful bundles connecting various regions of the gray matter. Such tools (including diffusion tensor imaging, (DTI) have recently been cleared by the FDA.

Soon, the influence of AI will surpass mere volumetric analysis and embed itself within crucial areas of clinical practice. Two such areas are computational processes and diagnostic support. Taking the example of brain DTI analysis, the computational pipelines that support these results involve dozens of sometimes lengthy and error-prone steps. By replacing them with AI, medical devices will become faster and more accurate (Figure 1).[2,3]

Furthermore, AI is expected to play a central role in the harmonization of data acquired from disparate scanning locales—a notably salient

Affiliation: Mr Joidin is a professor of computer science at the University of Sherbrooke, Montreal, Quebec, Canada. He is also the co-founder of and scientific adviser for Imeka Solutions Inc., Sherbrooke, Montreal, Canada.

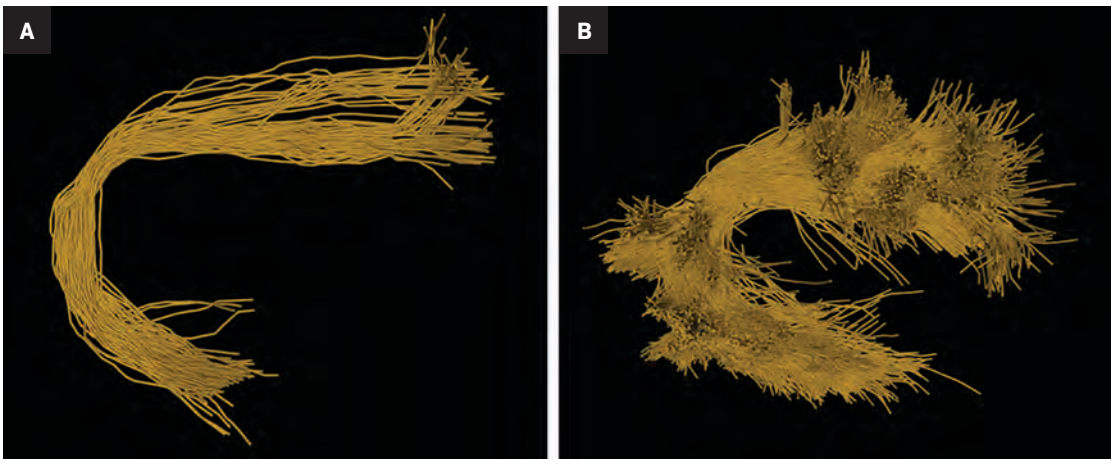

Figure 1. White matter brain fibers of the left arcuate fasciculus. (A) Incomplete results obtained with a deterministic tractometry pipeline. (B) better result obtained with the same pipeline enhanced with AI.

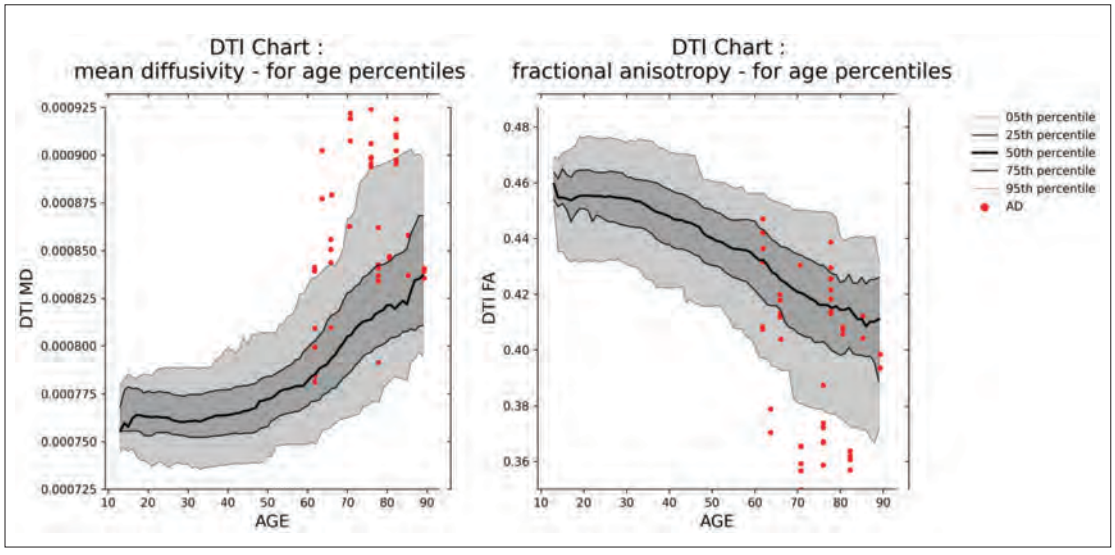

Figure 2. Two normative DTI charts (gray) derived from thousands of harmonized white matter skeletons. The mean diffusivity and fractional anisotropy (red) of subjects suffering from Alzheimer disease, most of it showcased as outliers.

issue with MRI. It will assist in the construction of normative datasets, amalgamating substantial cohorts of normative controls, and highlight the degree of deviation of a patient from this collective. This will permit the evaluation of a patient's white matter integrity via juxtaposition of DTI metrics pertinent to cerebral microstructure with a reference model.

This will also come with great benefits, since metrics such as fractional anisotropy and mean diffusivity, as well as advanced intra- and extracellular information such as apparent fiber density and free water metrics, have been shown for decades to correlate with assorted neurodegenerative diseases, including Alzheimer, multiple sclerosis, and Parkinson, as well as traumatic brain injury. Figure 2 provides an example of two harmonized DTI normative charts.

While AI is poised to profoundly impact medical practice, many experts suggest it will not supplant human practitioners.[4] Instead, AI is envisioned to enhance the daily operations of medical professionals by furnishing them with expeditious, reproducible, and interpretable data analysis software, integrally embedded within the core of their practice.

References

1) Artificial Intelligence and Machine Learning (AI/ML)-Enabled Medical Devices. U.S. Food and Drug Administration. www.fda.gov/medical-devices/software-medical-device-samd/artificial-intelligence-and-machine-learning-aiml-enabled-medical-devices. Accessed Oct. 5, 2023.

2) Yoon S, Amadiegwu A. Emerging tech, like AI, is poised to make healthcare more accurate, accessible and sustainable. World Economic Forum. www.weforum.org/agenda/2023/06/emerging-tech-like-ai-are-poised-to-make-healthcare-more-accurate-accessible-and-sustainable/. June 21, 2023.

3) Use of AI in healthcare & medicine is booming – here's how the medical field is benefiting from AI in 2023 and beyond. *Insider Intelligence*. www.insiderintelligence.com/insights/artificial-intelligence-healthcare/. January 11, 2023.

4) Komaroff AL. Will artificial intelligence replace doctors? Harvard Health Online. https://www.health.harvard.edu/staying-healthy/will-artificial-intelligence-replace-doctors. June 1, 2023.

Playing with Fire: Burnout Among Radiologists a Growing Concern

Kerri Reeves

Kerri Reeves is a contributing editor based in Ambler, PA.

Earlier this year, Medscape's Physician Burnout and Depression Report[1] revealed what radiologists already know: they are among the most burned-out specialists in medicine. Some 54% report experiencing "long-term, unresolved, job-related stress leading to exhaustion, cynicism, detachment from job responsibilities, and lacking a sense of personal accomplishment."

Implications of burnout and poor work-life balance across the specialty include the risk of depression, perpetuation of a negative professional culture, and performance difficulties.

"Burnout is an extraordinarily important topic across medicine … and in radiology, there has been a significant increase in reported burnout compared to the rest of medicine and, of course, the general population," says Clifford Weiss, MD, professor of radiologic science and biomedical engineering at Johns Hopkins University in Baltimore.

"Studies report increasing disengagement across many, if not all medical specialties," observes Dr Weiss, also director of the Johns Hopkins Hereditary Hemorrhagic Telangiectasia Center of Excellence.

In addition to disengagement, burnout sufferers can experience irritability, anger, emotional instability, distractedness, and a general lack of interest or excitement in performing work.

"Mentally checking out" often prevents physicians from doing their share, which can impact entire departments, says Christopher Bailey, MD, assistant professor of vascular and interventional radiology in the Russell H. Morgan department of radiology and radiological science at Johns Hopkins.

"Physicians have a team mentality and radiology is certainly a team sport both on the diagnostic and interventional side. Burnout affects overall team morale and the day to day. You have a group of people who aren't excited to come to work and get the work done together," Dr Bailey says.

Academic, diagnostic, interventional—burnout is prevalent across radiology, both pre- and post-pandemic. One survey of breast radiologists[2] found that 78.4% of respondents were highly burned out in at least one dimension of burnout. In a survey of academic radiologists,[3] 29% of respondents met all three criteria for high burnout, including high emotional exhaustion, high depersonalization, and low personal accomplishment, while 79% had at least one symptom. Of neuroradiologists, at least one burnout measure was reported by 85.2% of respondents.[4]

"[The prevalence] of signs and symptoms of burnout in our surveys is growing," reports Frank Lexa, MD, MBA, professor and vice chair of radiology at the University of Pittsburgh. "This wasn't true 20 years ago … it's getting worse. People are being asked to work much harder while work structures are changing, so they are feeling burned out."

While early signs may present as behavioral changes like aggression, rudeness, hiding from work responsibilities, or working excessively, prolonged or severe burnout can lead to relationship problems, self-medicating, neglect of personal hygiene, or self-harm.

"On a psychological level, burnout is on the depression spectrum and can contribute to physician suicide," says Dr Weiss, co-author of an article on

burnout, "Understanding and appreciating burnout in radiologists."[5] "In our article,we try not to dichotomize depression and burnout. There is evidence that burnout is at least partially a depressive syndrome."

As more radiologists experience chronic job-related stress, it's important to identify specialty-specific causes of burnout and consider mitigation strategies for achieving healthy work-life balance.

Growing Workload, Shrinking Staff Add Fuel to the Fire

It's no revelation that physicians are trained to push their limits to care for patients under stress, a physically and mentally draining responsibility. While it was initially thought that working long hours was the primary catalyst for burnout, the experience of radiologists today reveals varied and complex contributing factors.

Regardless of environment or subspecialty, radiologists experience unique work conditions. Scans are often read in isolation, which became more prevalent during the pandemic. For radiologists energized by social interaction, the shift to remote workstations along with the proliferation of IT systems that reduce personal communication with others is a contributing factor to burnout, Dr Lexa says. Further, an aging population demands more studies and follow-ups, with a growing complexity in interpretation, he adds.

"A head CT has changed radically in my own lifetime, from 37 images to 10 times as many per study," says Dr Lexa, who is also the chief medical officer of the Radiology Leadership Institute of the American College of Radiology. "So we're getting half as many dollars to read ten times as many images. That's one big issue."

Requirements of various classification systems and detailed reporting criteria are also growing, further weighing down radiologists.

The surging volume and accompanying expectation of referring physicians simply do not honor the value of the interpretation by board-certified diagnostic radiologists, Dr Bailey says. "The radiologist is being treated almost like a blood test: 'I ordered this CT and I just need it read.' There's so much imaging availability, which contributes significantly to burnout," he says.

An aging, sicker population, fear of litigation, and a trend toward preventive medicine all contribute to imaging overutilization, explains Rama Ayyala, MD, associate professor of radiology at Cincinnati Children's Hospital Medical Center and division director of thoracoabdominal imaging. "We have to support radiologists and also ensure clinicians are aware of the repercussions of ordering these exams, hopefully decreasing waste," Dr Ayyala argues.

Dr Bailey notes that interventional radiologists have become overwhelmed with procedures like central line placements and paracenteses, which were previously performed by other physicians. He says many hospitals have transitioned to centralizing procedures to one service, leading to a much larger workload for interventionalists. "It ends up creating a huge backlog," he says.

Across settings, radiologists are finding it nearly impossible to get their work done during shifts, crowding out other professional interests and causing laborious workarounds.

"They do a couple hours of work at home in the morning, drive to work, work hard, come home

Fighting the Fire: This Radiologist is Using Her Experience to Help Others

At one of her first jobs in radiology, Rama Ayyala, MD, experienced a strange contradiction: while she loved her job and her colleagues, she dreaded going to work.

"I started withdrawing from friends and family and spent most of my time working and very little time doing anything for myself," recalls Dr Ayyala. "I was slowly becoming depressed."

"It came down to being asked to do more than what I could do—more than I should have been expected to do," she says. "I was losing my joy of why I went into pediatric radiology because I felt like I was just doing work too quickly without being able to enjoy it."

After hearing others' experiences, Dr Ayyala realized she was burnt out. She took steps to assess both her job and herself by talking to trusted colleagues and a mental health therapist about her struggles. She has switched jobs—a few times—to find the right professional fit. Today, she prioritizes her family, friends, staying healthy, and taking care of herself.

Dr Ayyala has also published a number of wellness-related studies to advocate for and support radiologists who are feeling burnt out.

"Radiologists are at higher risk for burnout than other subspecialities … there's a lot that's asked of us," Dr Ayyala says, citing challenges related to imaging overutilization and the high cognitive load required by interpretations.

Dr Ayyala also notes that, with their responsibilities at work and home, women are more prone to burnout than are men. "There's also this idea in healthcare that we need to do more to prove ourselves compared to men," she adds, noting that burnout is a systemic issue that cannot necessarily be cured at the individual level.

However, she is grateful to have found relief through guidance, mentorship, and meaningful change. "Addressing my burnout was a combination of getting support at work and being able to have the time to invest in myself," she says.

—Kerri Reeves

late, maybe eat dinner with their spouse, then do more at night. That's the only way to get it done," Dr Lexa says. "That burns people out. That's cognitive dissonance."

Mounting radiologist workloads result in large part from physician and staff shortages, says Dr Weiss, calling attention to the "gap" between the number of new radiologists entering the field and the growing workload.

"The national shortage of radiologists will be extremely hard to address," agrees Dr Lexa, adding that insufficient radiologic technologist and nurse staffing contribute to the strain on radiologists. While locum tenens can help, he says, they cannot replace the experience and expertise of tenured technologists.

Amid such conditions, radiologists are often forced to perform tasks that are far below their level of training, such as managing insurance issues or transporting patients, further compounding frustration and burnout.

Tangled up in Red Tape

Backlogged tasks and insurance company headaches can also be a significant source of stress, says Dr Weiss, citing growing bureaucracy, documentation, regulations, and focus on financial performance.

Dr Lexa notes that the corporatization of medicine means more radiologists are working for large, third-party groups—and losing autonomy over daily workflow decisions and technology implementation.

"People who work for themselves are less likely to feel burned out, because they're passionate about practicing and feel in control," Dr Lexa says, noting the inverse is true. "When you're just working for someone else and they don't appreciate you or care about your opinion, you may feel that it's 'just a job,' and possibly not a very good one," he says.

"In 2023, there's a lot of administrative oversight by individuals who may not be medical professionals and don't have the same perspective. If there's something that causes burnout and destroys demeanor, it's that loss of autonomy," agrees Dr Bailey. "It can get taken away or muzzled. It's so important to protect."

Mitigating Burnout is a Team Effort

While the experience of burnout varies with individuals, it isn't typically confined to one person in a given group or department. Solutions must be implemented institution-, practice-, hospital-, or even system-wide, says Dr Lexa.

"If I were in charge … I'd stop reducing how much we get paid per study because it's insulting. It means that every year we have to work harder to get paid less," he says. "Using work RVU reimbursement as the metric of how we pay radiologists needs to be reframed because we bring value that's above and beyond this metric that keeps getting discounted."

Dr Weiss suggests that implementing artificial intelligence and new protocols to reduce workloads is one way to make things easier on radiologists.

"Take away what's [not essential] to provide patient care. Remove obstacles between me and my patients," he says, arguing that reigniting a commitment to and passion for patient care is key to combatting radiologist burnout.

"I'd love to see physicians wide eyed and excited again, like they were when they entered medical school. Ask yourself, 'how can I find that again?' As an institution, how can you help move people toward this?" he says.

Dr Lexa, who mentors other radiologists, takes such an approach when he works with those who are experiencing burnout.

"I begin with helping them frame their attitude toward the job—how it fits with the career they wanted and the career they'd like to have in five or 10 years," he says, noting that this often requires identifying a passion project like research and asking for the resources to carry it out. "People will be happier and work harder if they get time to work on things close to their heart."

It also requires setting boundaries around oneself with respect to what is and isn't acceptable to maintain well-being.

"Being active in one's self-care and being conscious of stress is vital. You have to set limits," says Dr Weiss. He suggests that radiologists constrain extraneous work activities by, for example, limiting the length and number of meetings or after-hours paperwork. "It's really about taking care of yourself, building your resilience, taking back some of your autonomy, and deciding what's important in life," Dr Weiss says.

"It's easy to get lost in medicine as it becomes part of your identity because you've dedicated so much thought and energy to it," agrees Dr Bailey. "But it's just one part. You have to remember to focus on other priorities."

If measures like these don't seem to help, it's time to take advantage of wellness and other programs that include therapy or peer-to-peer support. Something as simple as a sympathetic ear can help bring relief.

"If you look hard in your institution and understand that perhaps up to half [of your colleagues] may be at risk of burnout, you can see the symptoms occurring—whether it be someone checking out, acting out, or no longer taking care of themselves," Dr Lexa says. "Talk to your fellow radiologist. If you see someone getting into trouble, take care of each other."

References

1) Kane L. "I cry but no one cares": Physician burnout and depression report 2023. Medcape, https://www.medscape.com/slideshow/2023-lifestyle-burnout-6016058?faf-1#1. Accessed Oct. 25 2023.

2) Parikh JR, Sun J, Mainiero MB. Prevalence of burnout in breast imaging radiologists. *JBI*. 2020; 2(2): 112–118. doi: https://doi.org/10.1093/jbi/wbz091

3) Ganeshan D, Rosenkrantz AB, Bassett RL Jr, Williams L, Lenchik L, Yang W. Burnout in academic radiologists in the United States. *Acad Radiol.* 2020 Sep;27(9):1274-81. doi: 10.1016/j.acra.2019.12.029. Epub 2020 Feb 7. PMID: 32037261.

4) Chen JY, Vedantham S, Lexa FJ. Burnout and work-work imbalance in radiology- wicked problems on a global scale. A baseline pre-COVID-19 survey of US neuroradiologists compared to international radiologists and adjacent staff. *Eur J Radiol.* 2022 Oct;155:110153. doi: 10.1016/j.ejrad.2022.110153. Epub 2022 Jan 7. PMID: 35058099

5) Bailey C, Bailey A, McKenney AS, Weiss C. Understanding and appreciating burnout in radiologists. *Radiographics* online; Jul 15 2022. doi: https://doi.org/10.1148/rg.220037

Interview Day: How to Stand Out from the Crowd

Yasha Parikh Gupta, MD

One look at the calendar will tell you that it's not just autumn. It's ERAS® season and time to prepare for your all-important *Interview Day*.

Most Interview Days are still virtual, at least for the time being. This makes them a slightly different beast than traditional, in-person Interview Days. Not only that, but the number of applications per program has skyrocketed. All of which makes the need to stand out from the crowd of other applicants more important than ever.

So how do you do that? How can you be sure to ace Interview Day? It starts with acing the basics, from beginning to end. This means responding to the program director's emails in a timely manner, making sure your internet service is fast and reliable enough to handle Zoom calls without glitches (and having a backup plan just in case), double-checking the interview schedule, verifying the links 24-48 hours in advance, being polite to your interviewer(s), and studying the program in advance.

These truly are the basics and following them will go a long way toward ensuring you have a successful day. Unfortunately, although the first few interviews might feel exciting, "interview fatigue" sets in more quickly than you might expect. The following "best practices," if you will, can help you make the best of the season.

Get the 4-1-1

One of the most important things you can do on Interview Day is to attend the information sessions and social events for the residency programs you are most interested in entering. You may come to realize that residency programs are more similar to each other than they are different; nevertheless, I cannot overstate how important it is to attend these sessions.

They will give you insights that you may not find on the program's website. This may include details such as call schedule or daily work hours, as well as insights into the personality of the program director or other speakers. You may find yourself thinking, "I'd love to work with this person!" Your attendance also signals that your interest in the program goes above and beyond the act of perfunctorily completing and sending in your application.

Finally, these sessions can provide you with valuable insight into the culture of the program, especially during the question-and-answer period. Indeed, it is often the program's culture, and not necessarily its "brand," that can make or break your experience.

But don't stop there. I also recommend that you look for additional information about the program on its social media pages and by talking to current

Dr Gupta is a breast and oncologic imaging fellow/PGY-6 at Memorial Sloan Kettering Cancer Center in New York, New York. She is also a member of the editorial advisory board of *Applied Radiology*.

residents from the program. Gathering as much information as possible will demonstrate your genuine interest in the program to your interviewer.

Rehearse, Rehearse, Rehearse

Another exercise I recommend is rehearsing your answers to help you communicate clear, concise, and goal-oriented responses to common interview questions. These include, "Why did you decide to specialize in radiology?" and "Why are you interested in joining this program?" The purpose of the interview is to give your interviewer insight into you and why you would be a good fit for the program. It goes without saying—but I'll say it, anyway—that you should come to your interview well prepared for anything your interviewer might ask about your ERAS application—so be sure to review it thoroughly prior to interviewing.

Spend time reviewing what attracts you to the program and why. For example, if the program has a strong culture of research, draw attention to your publications. Also, call out any past leadership positions to help demonstrate your goal of achieving greater leadership opportunities. Be as specific as possible rather than quoting general information anyone can get from the website; this will help you stand out from the crowd.

Attitude Is Everything

Finally, demonstrate an enthusiastic attitude throughout the day. Interview fatigue is a very real risk to guard against; staying "on" as much as possible is crucial to making a good impression. I have found that talking with my hands, even on a Zoom call, helps me feel as though I am speaking with the person in the same room. It's also a good idea to keep your camera on during group sessions to demonstrate your full engagement with the activities.

Remember: every minute of Interview Day is important. Look and speak the part from the very beginning to the very end. Good luck!

Reference

1. Radiology-Diagnostic – AAMC. www.aamc.org/media/39801/download. Accessed October 1, 2023.

Acute Acalculous Cholecystitis

Paul C. Chroneos, MD; Richard B. Towbin, MD; Carrie M. Schaefer, MD; Alexander J. Towbin, MD

Case Summary

A child with acute myelogenous leukemia underwent a bone marrow transplantation that was complicated by graft versus host disease and progressively worsening abdominal pain and distention.

Imaging Findings

An ultrasound of the gallbladder (GB) demonstrated a sludge-filled and distended GB with marked wall thickness, but no significant pericholecystic fluid (Figure 1). The child was too unstable for surgical cholecystectomy so a percutaneous cholecystostomy (PC) was performed (Figure 2).

Diagnosis

Acute acalculous cholecystitis. The differential diagnosis includes acute calculous cholecystitis, acute pancreatitis, hepatic abscess, or right sided pyelonephritis.[1]

Discussion

Acute acalculous cholecystitis (AAC) may be suspected in pediatric patients presenting with abdominal pain, signs of sepsis without a clear source, or with jaundice. The condition is the most common form of acute cholecystitis in children, representing approximately 50-70% of all cases. Pediatric patients most commonly present with right upper quadrant or diffuse abdominal pain. Other symptoms and signs such as nausea, vomiting, fever, jaundice, anorexia, and weight loss may be present. Laboratory findings include leukocytosis as well as elevated bilirubin, alkaline phosphatase, aspartate aminotransferase, alanine aminotransferase, and γ-glutamyl transferase levels.[2]

Pediatric AAC is typically caused by bile stasis and/or GB ischemia. It most often occurs after a viral infection such as Epstein-Barr and hepatitis A.[3] Other associations include burns, sepsis, immune compromise, immune-mediated disorders (eg, systemic lupus erythematosus), vasculitis (eg, Kawasaki disease or Henoch-Schoenlein purpura), malignancy, and genetic disorders (eg, cystic fibrosis or type 1 diabetes mellitus).[4]

Ultrasound is the preferred imaging modality for initial assessment owing to its greater availability, short examination time, and lack of ionizing radiation. Prior studies have shown that ultrasound has equal sensitivity and superior specificity compared to CT, MRI, and hepatobiliary iminodiacetic acid (HIDA) scanning.[5] In the absence of gallstones, at least two of the following findings are required to diagnose cholecystitis: GB wall edema, increased wall thickness (>3.5-4 mm), pericholecystic fluid, intraluminal sludge, or GB distention.[6] A sonographic Murphy sign, defined as maximal abdominal tenderness from pressure of the ultrasound probe over the GB, may also be present.

Contrast-enhanced CT of the abdomen and pelvis, MRI, MR cholangiopancreatography (MRCP), or HIDA scan are alternative diagnostic

Affiliations: University of Arizona College of Medicine-Phoenix Campus (Dr Chroneos); Department of Radiology, Phoenix Children's Hospital (Drs Schaefer, R. Towbin); Department of Radiology, Cincinnati Children's Hospital; Department of Radiology, University of Cincinnati College of Medicine (Dr A. Towbin)

Figure 1. Short (A) and long (B) axis ultrasound of the GB demonstrates distention, diffuse wall thickening (measuring 11 mm), and sludge. Additionally, there was a sonographic Murphy sign.

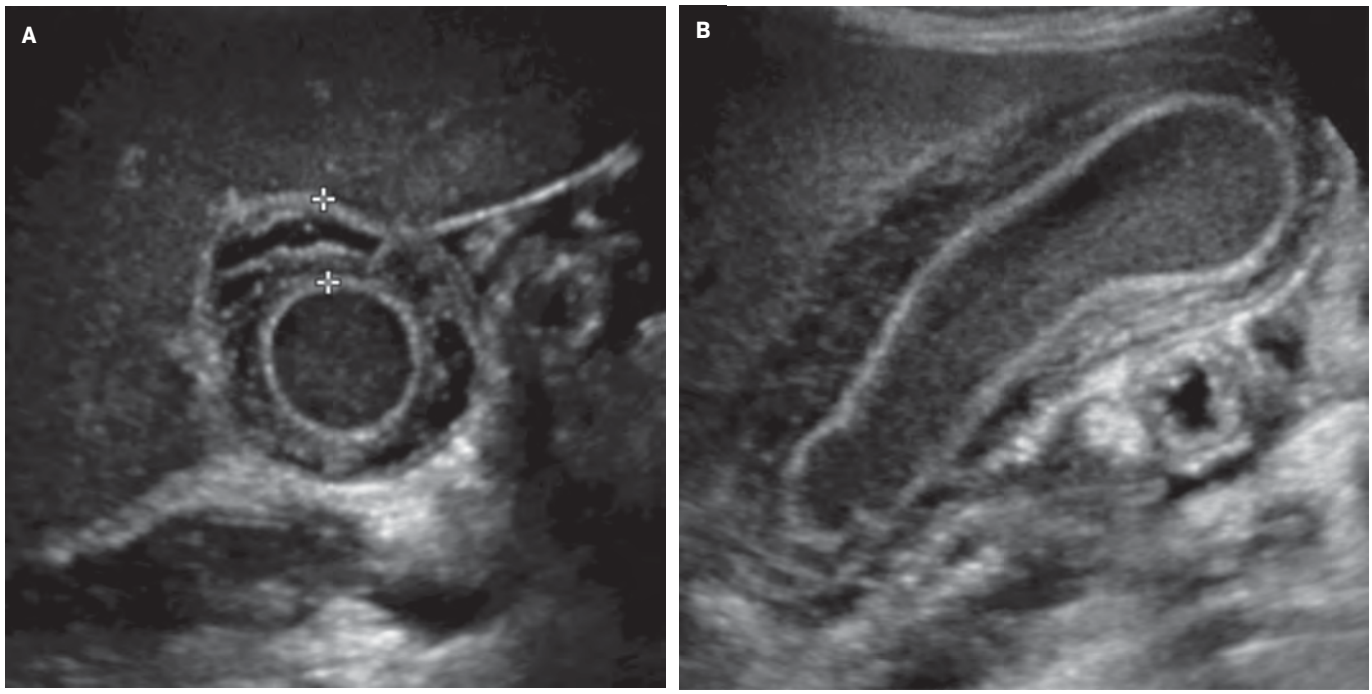

Figure 2. (A) Short axis image of GB during cholecystotomy with sheathed needle in the GB lumen (blue arrow) and tenting of the GB wall (yellow arrow). (B) Placement of percutaneous GB drain (cholecystostomy). Image demonstrates 8.5F drain in the gallbladder lumen and instillation of contrast in the GB after aspirating 25 mL of black-colored bile.

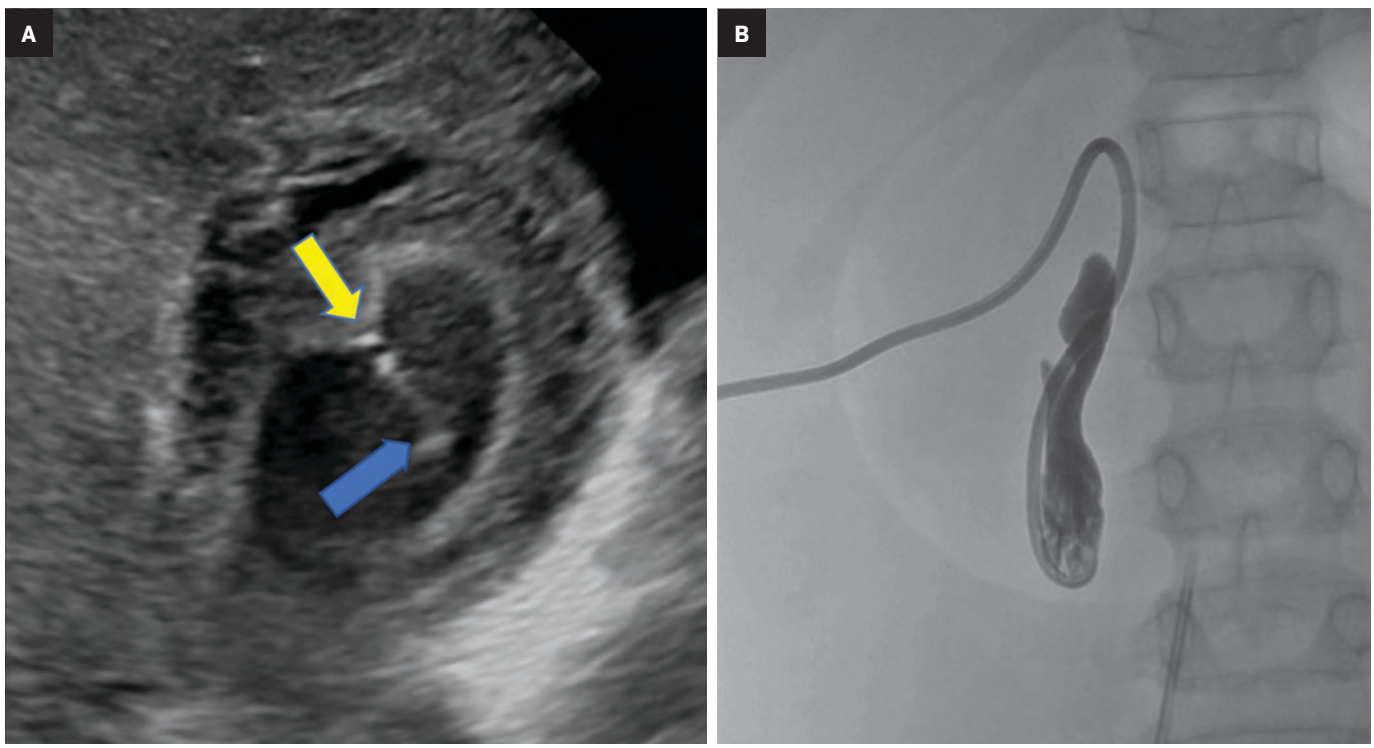

options. On computed tomography, AAC appears with increased GB wall thickness >3-4 mm, pericholecystic fluid, subserosal edema, intramural gas, GB sludge, and hydrops.[7] Unfortunately, CT is not always sensitive to gallstones. Thus, excluding AAC from the differential diagnosis is difficult. MRI and MRCP findings are similar to those of CT. MRI is more sensitive than CT for cholelithiasis or choledocholithiasis; however, MRI takes longer and often requires sedation. This often precludes its use in critically ill, unstable patients.

AAC is diagnosed on HIDA when the GB is not visualized 1 hour postinjection with radiolabeled technetium. Imaging can be augmented with intravenous morphine. Morphine causes the sphincter of Oddi to contract and helps the GB to fill; AAC is diagnosed if the GB is not visualized after 30 minutes.

AAC is often initially treated with nasogastric suctioning, intravenous fluids, and parenteral antibiotics. Although a cholecystectomy may be performed, PC is preferred in critically ill patients who are unlikely to tolerate surgery. In addition, the GB may be salvaged. A PC is less invasive and effectively drains the GB, leading to improvement in clinical status and symptoms. If necessary, open cholecystectomy can be performed electively in patients who are not critically ill.[8]

Conclusion

AAC most commonly presents in the setting of viral infection but may also be seen in immunocompromised children and those with vasculitis and autoimmune and genetic diseases. The most common presenting symptom is abdominal pain, with other signs and symptoms including nausea, vomiting, jaundice, fever, and anorexia. Laboratory results supporting a diagnosis of AAC include leukocytosis and elevation of markers suggestive of cholestasis and hepatic dysfunction. Ultrasound is the preferred initial imaging modality and often reveals GB wall edema, increased wall thickness (>3.5-4 mm), pericholecystic fluid, mucosal membrane sludge, and GB distention. Percutaneous cholecystostomy is the preferred treatment for critically ill patients who are unlikely to tolerate a cholecystectomy.

References:

1) Poddighe D, Sazonov V. Acute acalculous cholecystitis in children. *World J Gastroenterology.* 2018 Nov 21; 24(43): 4870–4879.

2) Poddighe D, Tresoldi M, Licari A, Marseglia GL. Acalculous Acute Cholecystitis in Previously Healthy Children: General Overview and Analysis of Pediatric Infectious Cases. *Int J Hepatol.* 2015;2015:459608. doi: 10.1155/2015/459608. Epub 2015 Nov 11. PMID: 26640715; PMCID: PMC4658411.

3) Tsakayannis DE, Kozakewich HP, Lillehei CW. Acalculous cholecystitis in children. *Journal of Pediatric Surgery.* 1996 Jan;31(1):127-30.

4) Yi DY, Chang EJ, et al. Age, Predisposing Diseases, and Ultrasonographic Findings in Determining Clinical Outcome of Acute Acalculous Inflammatory Gallbladder Diseases in Children. *J Korean Med Sci.* 2016 Oct;31(10):1617-23.

5) Mirvis SE, Vainwright JR, Nelson AW, et al. The Diagnosis of Acute Acalculous Cholecystitis: A Comparison of Sonography, Scintigraphy, and CT. *American Journal of Roentgenology.* 1986;147: 1171-1175.

6) Barie P, Eachempati S. Acute acalculous cholecystitis. *Gastroenterology Clinics of North America Journal.* 2010;39(2):343-57.

7) Imamoglu M, Sarihan H, Sari A, Ahmetoglu A. *Journal of Pediatric Surgery.* 2002 Jan;37(1):36-9.

8) Schaefer C, Towbin R, Aria D, Kaye R. Safety and effectiveness of percutaneous cholecystostomy in critically ill children who are immune compromised. *Pediatric Radiology* (2016) 46: 1040-1045. Published online: 2016 Feb 17.

STATEMENT OF OWNERSHIP MANAGEMENT AND CIRCULATION (REQUIRED BY 39 U.S.C. 3685)

Title of Publication: APPLIED RADIOLOGY

Publication Number: 943180

Filing Date: 09/30/22

Frequency: Bi-Monthly

Number of Issues Published Annually: 6

Annual Subscription Price: $115 (1 year),

Known office of publication and the mailing address:

APPLIED RADIOLOGY
Anderson Publishing, Ltd.
180 Glenside Avenue
Scotch Plains, NJ 07076

Publisher: Kieran N. Anderson

Editor: Erin Simon Schwartz, MD, FACR

Managing Editor: Joseph Jalkewicz

Owners: O. Oliver Anderson
Brenda M. Anderson

	Average # copies for 12-month period	*Actual # copies for July/August 2023 issue*
Total # copies (Net Press Run)	14,947	14,678
Outside County Paid/Requested Mail Subscriptions	9,261	9,193
Total Paid and/or Requested	9,261	9,193
Outside County Nonrequested Copies	5,476	5,276
Nonrequested Copies Distributed Outside the Mail	113	150
Total Nonrequested Distribution	5,589	5,426
Total Distribution	14,850	14,619
Copies Not Distributed	97	59
TOTAL	14,947	14,947
Percent Paid and/or Requested Circulation	62.4%	62.9%
Electronic Copy Circulation	1,485	1,462
Total Requested and Paid Printed Copies	10,746	10,655
Total Requested Copy Distribution	16,335	14,678
Percent Paid and/or Requested Circulation	65.8%	66.3%

I certify these statements are correct and complete.
Kieran N. Anderson, Publisher
September 30, 2023
PS Form 3526-R

AppliedRadiology®

The Journal of Practical Medical Imaging and Management

RSNA 2023

LEADING THROUGH CHANGE

November 26–30, 2023

Booth 2700 | South Hall

Hope to see you in Chicago!

Embryonal Rhabdomyosarcoma of the Bladder

Ruoyan Zhu;, Richard B. Towbin, MD; Carrie M. Schaefer, MD; Alexander J. Towbin, MD

Case Summary

A male toddler presented with recent onset of straining during voiding and bowel movements. Ultrasound detected a large mass in the bladder lumen. Ultrasound-guided biopsy revealed an embryonal rhabdomyosarcoma (RMS) of the bladder and prostate. There was no evidence of metastases. The tumor was classified as stage III, group II. Subsequent mass excision was performed, followed by cystoscopically guided bilateral ureter reimplantation and bladder neck reconstruction.

Imaging Findings

Ultrasound (Figure 1) detected a large, lobulated mass in the bladder lumen. Contrast-enhanced CT of the abdomen and pelvis (Figure 2) identified a lobulated mass at the base of the bladder extending into the proximal urethra.

Diagnosis

Embryonal rhabdomyosarcoma of the bladder. The differential diagnosis includes other subtypes of RMS, papillary urothelial neoplasm of low malignant potential, and fibroepithelial polyp.

Discussion

Rhabdomyosarcomas are the most common malignant, soft-tissue sarcomas in children and are divided into 4 subtypes: embryonal, alveolar, pleomorphic, and spindle cell/sclerosing.[1] Embryonal is the most common, accounting for approximately 60% of all cases. It predominantly occurs in children under 5 years of age, although a smaller peak has also been noted in adolescence.[2] This subtype usually occurs in the head, neck, and genitourinary regions and has a male-to-female ratio of 1.5:1.[2]

While the etiology of RMS is still unknown, an increased prevalence is associated with genetic syndromes such as Li-Fraumeni, Gardner, Beckwith-Wiedemann, and neurofibromatosis type 1.[3] Embryonal RMS is characterized by a loss of heterozygosity at *11p15.5* and whole or partial gains of chromosomes 2, 8, 12, 13, and/or 20.[2] Mutations in the FGFR4/RAS/AKT pathway and increased PTEN hypermethylation has also been detected in this subtype.[2]

Patients often present with signs and symptoms resulting from mass effect, such as urinary retention for tumors in the genitourinary region.[2] Ultrasound should be used initially to confirm the presence of a tumor. Computed tomography or MRI can be performed to further assess the tumor, as well as to identify potential complications and potential sites of metastasis.[4]

Biopsy is necessary for diagnosis. On histology, embryonal RMS is characterized by rhabdomyoblasts at variable stages of differentiation in sheets and nests within a myxoid matrix.[3] Tumors are commonly classified by pre-treatment tumor, nodes, metastasis (TNM) staging and the postoperative Intergroup Rhabdomyosarcoma Study grouping system.[5] It is estimated that 15% of pediatric RMS patients present with metastasis. The outcome for these patients is poor.[5]

Tumors of the bladder and prostate region must be classified at least stage II owing to their unfavorable location.[7] The tumor group is based on histology results. Group I tumors constitute completely resected localized disease.[7] Group II tumors make up completely resected masses with evidence of regional spread. Group III comprises incompletely resected tumors, and group IV masses are accompanied by distant metastases. Clinical risk is determined by tumor stage, group, and histology.

There are 3 risk categories: low, intermediate, and high.[7] Low risk

Affiliations: University of Arizona College of Medicine-Phoenix Campus (Mr Zhu), Department of Radiology, Phoenix Children's Hospital (Drs Schaefer, R Towbin), Department of Radiology, Cincinnati Children's Hospital, University of Cincinnati College of Medicine (Dr A Towbin).

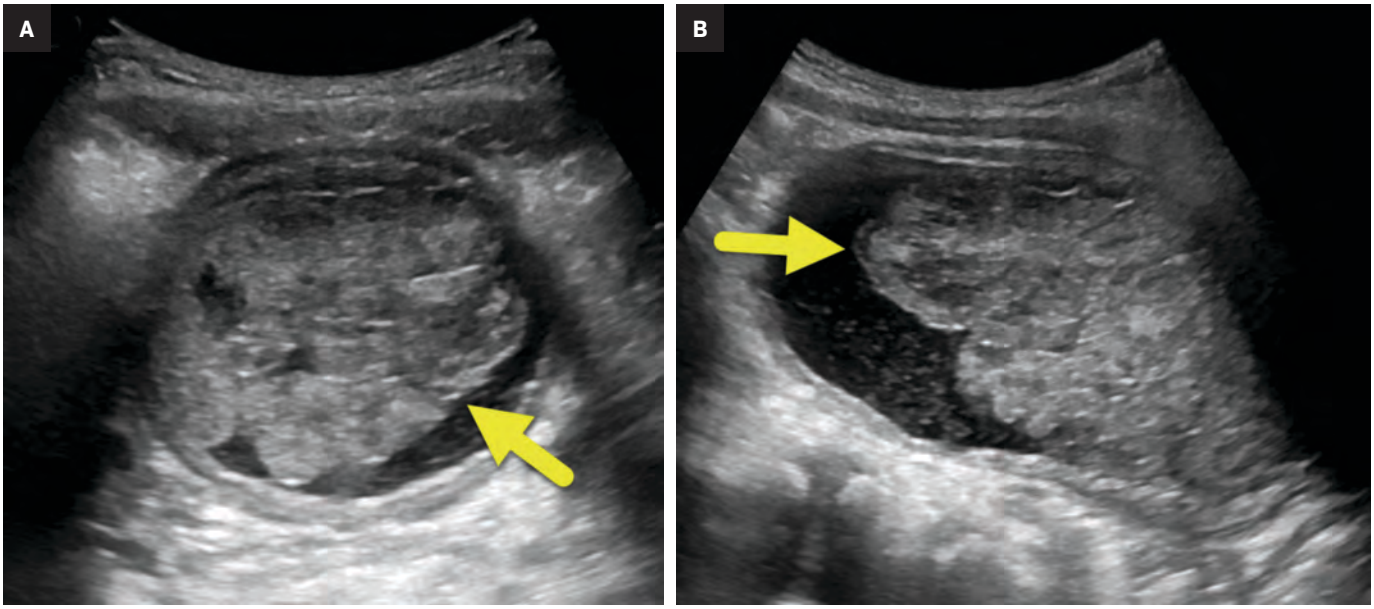

Figure 1. (A) Transverse and (B) longitudinal ultrasound of the bladder shows a lobulated mass (arrow) filling the bladder lumen. The urine has internal debris.

Figure 2. Sagittal reformation contrast-enhanced CT of the pelvis shows the lobulated embryonal rhabdomyosarcoma (arrow) filling the bladder lumen and extending into the proximal urethra.

consists of stage II and III, groups I and II embryonal tumors; these have an 88% 3-year, failure-free survival rate. Intermediate-risk tumors (stages II and III, group III) have a 55-76% 3-year, failure-free survival rate, and high-risk tumors (stage IV, group IV) have < 30% 3-year, failure-free survival rate.[7]

Treatment of RMS takes a multimodal approach involving surgery, chemotherapy, and radiotherapy.[5] Two main treatment protocols exist for pediatric bladder and prostate RMS: the North American approach, developed by the Children's Oncology Group, and the European approach, developed by the International

Society of Pediatric Urology. While both protocols involve chemotherapy following histological diagnosis, the North American approach recommends radiotherapy to better establish local control for organ preservation.[6] In most cases, surgery consists of partial resection with the goal of bladder preservation.[6]

Multimodal therapy offers good outcomes, with estimated 5-year overall survival for bladder/prostate RMS as high as 86% and 5-year, event-free survival as high as 79%.[7] However, treatment may result in abnormal lower urinary tract function (ie, incontinence, infection, decreased renal function, and chronic hematuria) in up to 60% of patients and sexual dysfunction, with the proportion of each increasing with longer follow-up time.[6] The true frequency of sexual dysfunction is uncertain in survivors but is noted in older patients.

Conclusion

Embryonal rhabdomyosarcomas are the most common subtype of RMS. They usually present in the head, neck, and genitourinary regions of males under age 5 years. Their etiology is not yet known, but RMSs have been associated with genetic syndromes. Pelvic RMS can present with urinary retention and other signs of mass effect. Multimodal treatment involving chemotherapy, surgery, and radiotherapy can be effective.

References

1) Choi JH, Ro JY. The 2020 WHO Classification of Tumors of Soft Tissue: Selected Changes and New Entities. *Adv Anat Pathol*. 2021;28(1):44-58. doi:10.1097/PAP.0000000000000284

2) Kohashi K, Kinoshita I, Oda Y. Skeletal muscle tumors: a clinicopathological review. *Head Neck Pathol*. 2020;14(1):12-20. doi:10.1007/s12105-019-01113-2

3) Dziuba I, Kurzawa P, Dopierała M, Larque AB, Januszkiewicz-Lewandowska D. Rhabdomyosarcoma in children – current pathologic and molecular classification. *Pol J Pathol*. 2018;69(1):20-32. doi:10.5114/pjp.2018.75333

4) Shelmerdine SC, Lorenzo AJ, Gupta AA, Chavhan GB. Pearls and pitfalls in diagnosing pediatric urinary bladder masses. *RadioGraphics*. 2017;37(6):1872-1891. doi:10.1148/rg.2017170031

5) Melcón SG, Codina JS de T. Rhabdomyosarcoma: present and future perspectives in diagnosis and treatment. *Clin Transl Oncol*. 2005;7(1):35-41. doi:10.1007/BF02710026

6) Castagnetti M, Herbst KW, Esposito C. Current treatment of pediatric bladder and prostate rhabdomyosarcoma (bladder preserving vs. radical cystectomy). *Curr Opin Urol*. 2019;29(5):487-492. doi:10.1097/MOU.0000000000000651

7) Saltzman AF, Cost NG. Current treatment of pediatric bladder and prostate rhabdomyosarcoma. *Curr Urol Rep*. 2018;19(1):11. doi:10.1007/s11934-018-0761-8

Ureteral Obturator Hernia

Bryan H. Louie, BS; Simon Lemieux, MD; Preya Shah, MD, PhD; Lindsey Negrete, MD

Case Summary

An elderly patient with a remote history of renal transplantation presented with several days of dysuria, malaise, and nausea. The patient was also tachycardic with suprapubic tenderness and laboratory evaluation revealed creatinine elevation.

Imaging Findings

Abdominal contrast-enhanced CT (Figures 1,2) demonstrated hydroureteronephrosis of the transplant kidney in the right iliac fossa and distal herniation of the ureter into the right obturator canal. Follow-up radiography demonstrated contrast opacifying the bladder (Figure 3), indicating delayed passage of urine into the bladder. The patient's renal function returned to baseline with fluid resuscitation, and they did not require immediate intervention for obstructive uropathy.

Diagnosis

Ureteral obturator hernia

Affiliations: University of California San Diego, School of Medicine, La Jolla, California (Mr Louie); Department of Radiology, Stanford University, Stanford, California (Drs Lemieux, Shah, Negrete).

Figure 1. Oblique view of abdominal CT demonstrates hydroureteronephrosis of the transplant kidney with the ureter herniating into the right obturator canal (arrow).

Discussion

Ureteral hernia is a rare condition most commonly found incidentally on imaging or during surgical procedures.[1] Ureteral herniation can occur in a number of anatomic locations, including the inguinal canal, femoral ring, sciatic foramen, obturator foramen, and diaphragm.[2] Among these, obturator herniation is exceptionally rare, with only three cases having been reported in the literature.[3–5]

There are several important characteristics of ureteral obturator hernias (UOHs). First, they are a rare type of abdominal wall hernia that is nine times more common in women than in men.[6] This may be due in part to their wider pelvis, more triangular obturator canal opening, and larger transverse diameter. Other factors that increase the risk of UOH are related to progressive relaxation of the pelvic floor, which is associated with advanced age, emaciation, increased intrabdominal pressure, and multiparity.[7] Loss of preperitoneal fat and lymphatic tissue over the obturator canal with aging and/or

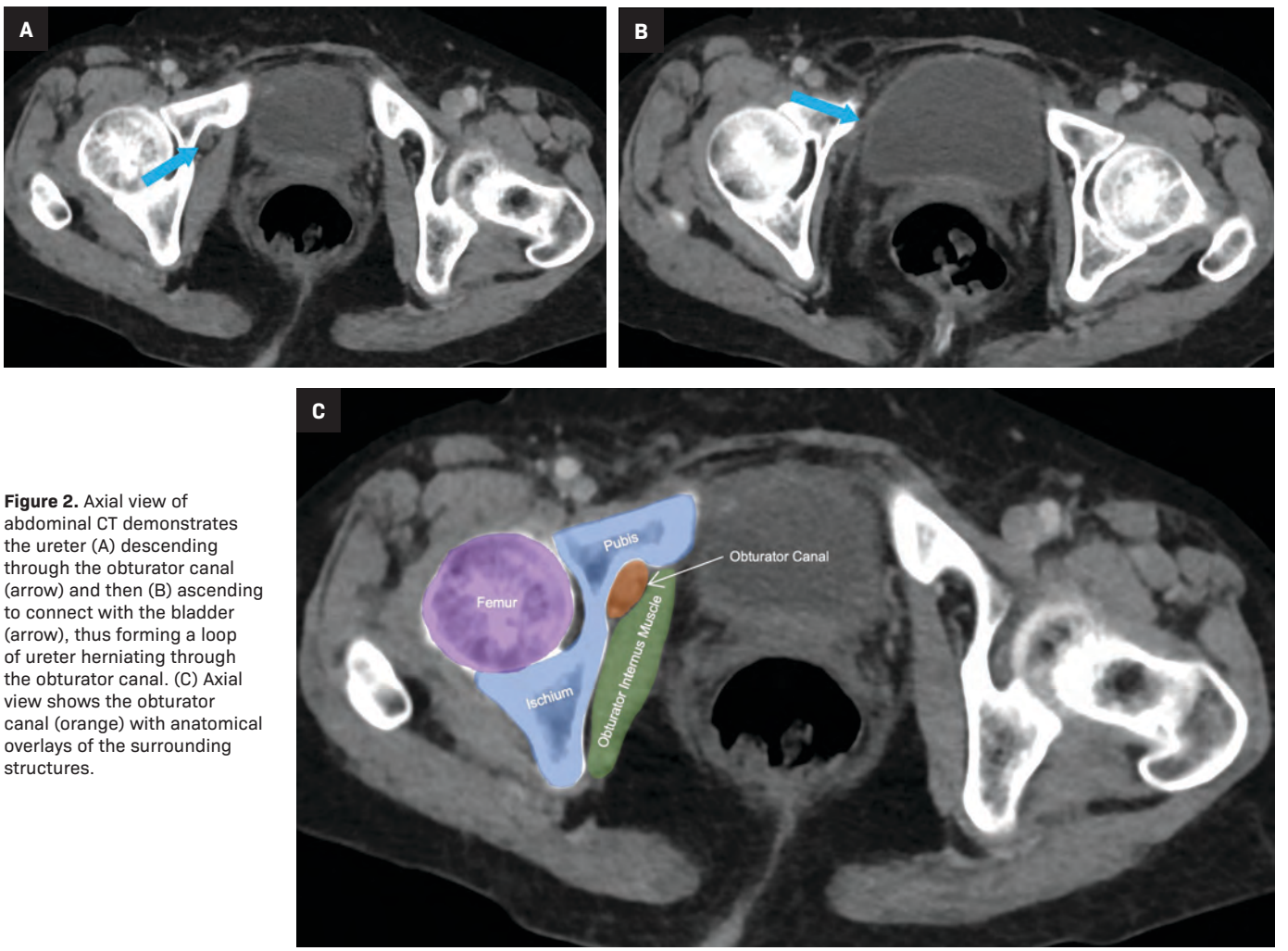

Figure 2. Axial view of abdominal CT demonstrates the ureter (A) descending through the obturator canal (arrow) and then (B) ascending to connect with the bladder (arrow), thus forming a loop of ureter herniating through the obturator canal. (C) Axial view shows the obturator canal (orange) with anatomical overlays of the surrounding structures.

malnutrition also increases the space around the vessels and nerves, thus predisposing to herniation. Diagnosis is difficult as symptoms are often nonspecific, and palpable masses or associated pain are often not present at physical exam.[4] Therefore, UOHs are often found incidentally on imaging or during surgery for intestinal obstruction or peritonitis.[7]

There are several additional factors to consider. First, UOHs are considerably more rare than are hernias involving the bowel. They often present with nonspecific urinary symptoms such as dysuria, abdominal pain, nausea, and vomiting.[3] As in our case, renal transplant is associated with increased risk of ureteral herniation, particularly as time from transplant increases.[5,8] This may be due to redundancy of the transplant ureter or the anterior and inferior location of many transplanted kidneys.[9]

The main complication of UOH is ureteral obstruction, which can lead to hydronephrosis and, potentially, kidney damage and/or infection. Previous cases of UOH with ureteral obstruction and worsening kidney function have required urgent nephrostomy and/or surgical hernia repair.[3–5] However, in our case, follow-up imaging demonstrated contrast passage into the bladder, indicating urine excretion. Along with the patient's decreasing creatinine, this reduced the concern for major obstruction and renal damage. Therefore, urgent intervention was not required. However, the patient was scheduled for a nonurgent surgical evaluation for potential ureteral obturator hernia repair.

Because its symptoms overlap with other conditions, UOH often is not diagnosed until surgery. However, imaging can visualize the hernia and sequelae such as hydroureteronephrosis from obstruction. In cases where imaging is indeterminate, delayed-phase CT with contrast excretion from the renal transplant

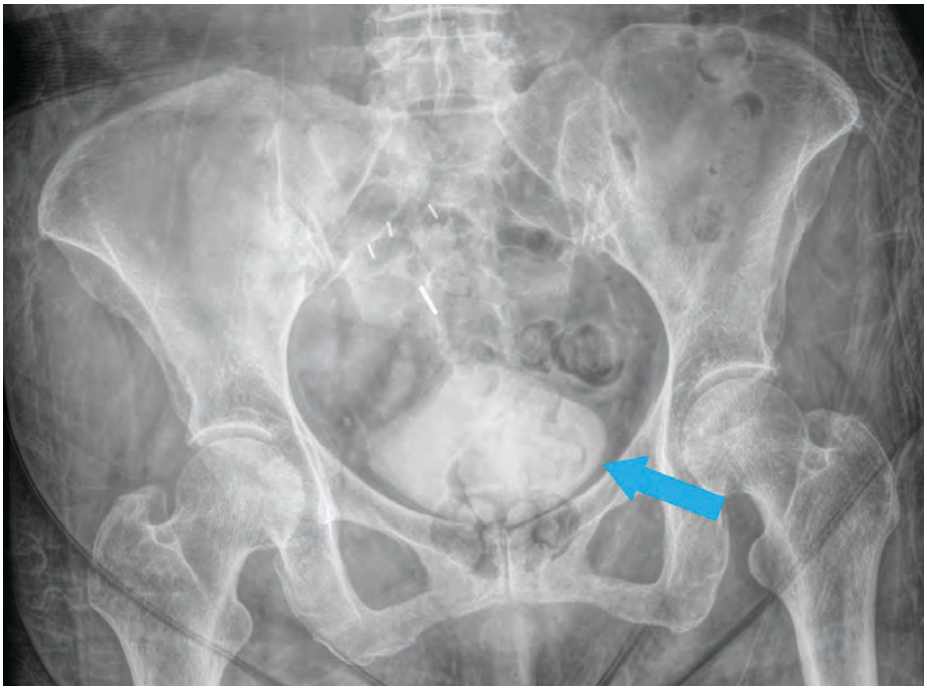

Figure 3. Follow-up plain film X-ray several hours after the CT shows contrast opacifying the bladder (arrow), indicating delayed but intact passage of urine into the bladder.

may help to better delineate the course of the ureter.

Conclusion

We present a rare case of a ureteral obturator hernia. This entity occurs almost exclusively in elderly women and is often accompanied by nonspecific urinary and/or abdominal symptoms. Ureteral obturator hernias may be associated with prior renal transplants. Owing to the ambiguity of symptoms, imaging plays an important role in diagnosing the condition and evaluating for ureteral obstruction, which may necessitate urgent diversion with nephrostomy and/or surgical hernia repair.

References

1) Pollack HM, Popky GL, Blumberg ML. Hernias of the ureter—an anatomic-roentgenographic study. *Radiology*. 1975;117(2):275-281. doi:10.1148/117.2.275

2) Lin FC, Lin JS, Kim S, Walker JR. A rare diaphragmatic ureteral herniation case report: endoscopic and open reconstructive management. *BMC Urol*. 2017;17:26. doi:10.1186/s12894-017-0207-5

3) Hong Y, Zhang S, Kong X, Zhang Y, Hong S, Chen Y. Case report of ureter obturator hernia and literature review analysis. *BMC Urol*. 2021;21:86. doi:10.1186/s12894-021-00851-2

4) Izzo M, Regusci L, Fasolini F. Obturator hernia with ureteral entrapment. *Case Rep Gastroenterol*. 2014;8(2):156-161. doi:10.1159/000363176

5) Weingarten KE, D'Agostino HB, Dunn J, Steiner RW. Obturator herniation of the ureter in a renal transplant recipient causing hydronephrosis: perioperative percutaneous management. *J Vasc Interv Radiol*. 1996;7(6):939-941. doi:10.1016/s1051-0443(96)70874-6

6) Kulkarni SR, Punamiya AR, Naniwadekar RG, et al. Obturator hernia: A diagnostic challenge. *Int J Surg Case Rep*. 2013;4(7):606-608. doi:10.1016/j.ijscr.2013.02.023

7) Park J. Obturator hernia: Clinical analysis of 11 patients and review of the literature. *Medicine*. 2020;99(34):e21701. doi:10.1097/MD.0000000000021701

8) Lmc M, Sf X, Wf A, H TS, J MP. Ureteral herniation in kidney transplant - case report. *Trends in Transplant*. 2020;13(2). doi:10.15761/TiT.1000275

9) Merani S, Aufhauser DD, Maskin AT, Mezrich J, Al-Adra D. Not as rare as initially described: transplant ureter incarceration within inguinal hernia. Two cases, literature review, and management algorithm. *Transplantation Proceedings*. 2021;53(7):2285-2290. doi:10.1016/j.transproceed.2021.07.012

Extrauterine Adenomyoma

Laurence J. Spitzer, MD

Case Summary

An adult presented with a history of refractory morbid obesity, despite previous gastric banding. The patient's surgical history also included cholecystectomy, endometrial ablation, and subsequent hysterectomy.

Despite the previous surgery for weight loss, the patient continued to struggle with morbid obesity (BMI: 44-49 range) and ultimately underwent vertical sleeve gastrectomy.

Approximately two weeks post-surgery, the patient complained of abdominal pain and a "pelvic mass" sensation. Evaluation included an abdominopelvic MRI, which demonstrated a right lower quadrant soft-tissue mass protruding through the muscular layers of the anterior abdominal wall. They underwent exploratory laparotomy and tumor resection.

Imaging Findings

Magnetic resonance imaging (MRI) of the abdomen and pelvis revealed a T1 and T2-isointense mass with small foci of intrinsic T1 shortening suggesting areas of blood products (Figures 1-3). Overall, the mass avidly enhanced following gadolinium administration, with some peripheral nonenhancing areas. Chest CT was negative for pulmonary nodules and metastatic disease.

Diagnosis

Extrauterine adenomyoma.

The differential diagnosis of a solid, abdominal wall mass includes sarcoma, abdominal wall desmoid tumor, and endometrioma. Much less likely diagnoses would include solitary lymphoma, metastatic disease, and neurofibroma.

Discussion

Adenomyosis, a common condition, is the presence of endometrial glands and stroma within the myometrium. The condition has an incidence ranging from 20%-60%. Adenomyomas, the localized form, are benign tumors containing smooth muscle cells, and endometrial glands and stroma. They differ from adenomyosis by their distinct borders and being well-circumscribed masses separate from surrounding tissues. The most common locations to find adenomyomas are within the pararectal space, ovary, and broad ligament.[1] Infrequently, adenomyomas can occur outside the uterus and, even more infrequently, outside the pelvis. It is often difficult to diagnose adenomyomas preoperatively based on imaging alone, as other benign and malignant entities can have similar imaging appearance.

Currently, there are five proposed theories for the pathophysiology of extrauterine adenomyomas. The first, by Cozzuto et al,[2] the first to report extrauterine adenomyoma, suggests they form when a focus of endometriosis undergoes metaplasia to become smooth muscle. The second theory, from Rosai et al in 1982,[3] suggests that extra-uterine adenomyomas form from uterine fusion defects, such as a unicornuate uterus, whereby the single horn can detach and implant elsewhere. In 2005, Redman et al[4] postulated a sub-coelomic mesenchymal metaplasia theory in which a pleuripotent cell layer beneath the mesothelial layer could differentiate under various hormonal stimuli. The most recent theory, proposed by Batt,[5] argues that heterotopic Mullerian-like tissue of embryonic origin could develop within other normal organs. However, a theory proposed by Belmarez et al[6] in 2019 fits this patient best. This theory suggests that pelvic seeding can occur during previous surgery, especially when involving morcellation.

Affiliation: Division of Community Radiology, Hospital of the University of Pennsylvania, Philadelphia, Pennsylvania

Figure 1. Single shot fast spin echo (SSFSE) axial image of the abdomen at the level of the umbilicus demonstrates a large, macrolobulated soft-tissue mass within the right lower quadrant of the abdomen. The mass is T2 isointense. There is mass effect on the right psoas muscle.

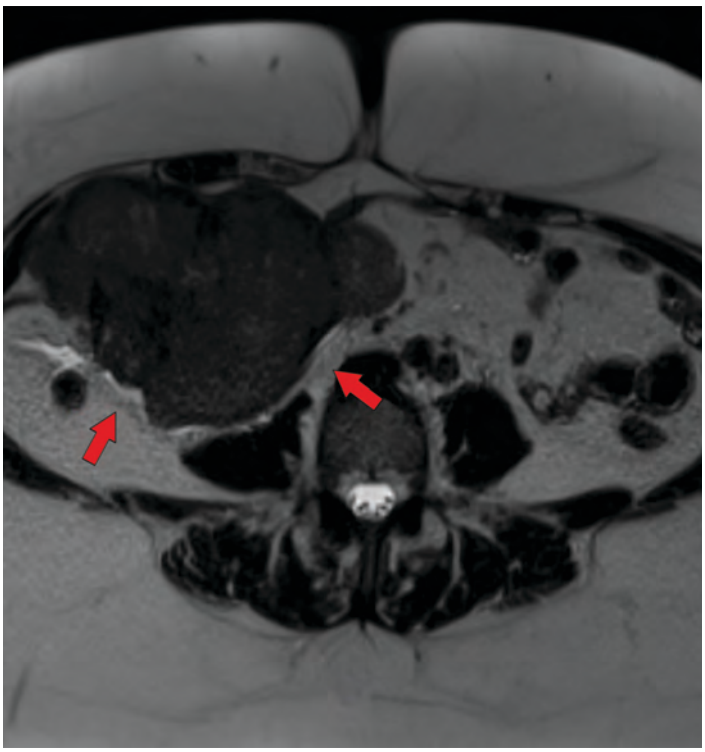

Figure 2. SSFSE sagittal image of the abdomen demonstrates the separation of the mass from the right kidney. The image also demonstrates the mass pushing on the anterior abdominal wall.

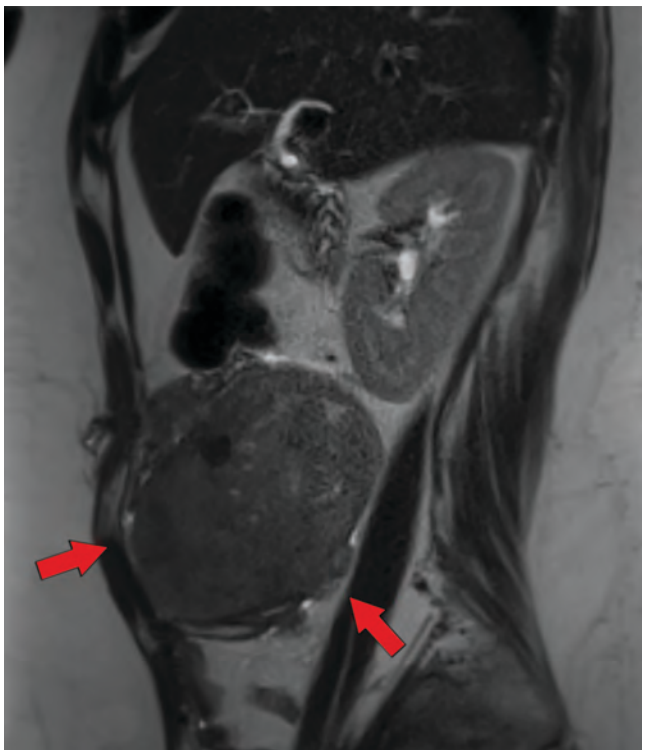

Figure 3. (A) Precontrast T1 axial image with fat suppression demonstrates mass isointensity with small foci of hyperintense T1 signal, suggesting areas of blood products. The image also demonstrates protrusion of the mass through the muscular layers of the abdominal wall (arrow). (B) Postcontrast (early venous phase) T1 axial image with fat suppression demonstrates avid enhancement with some peripheral nonenhancing areas.

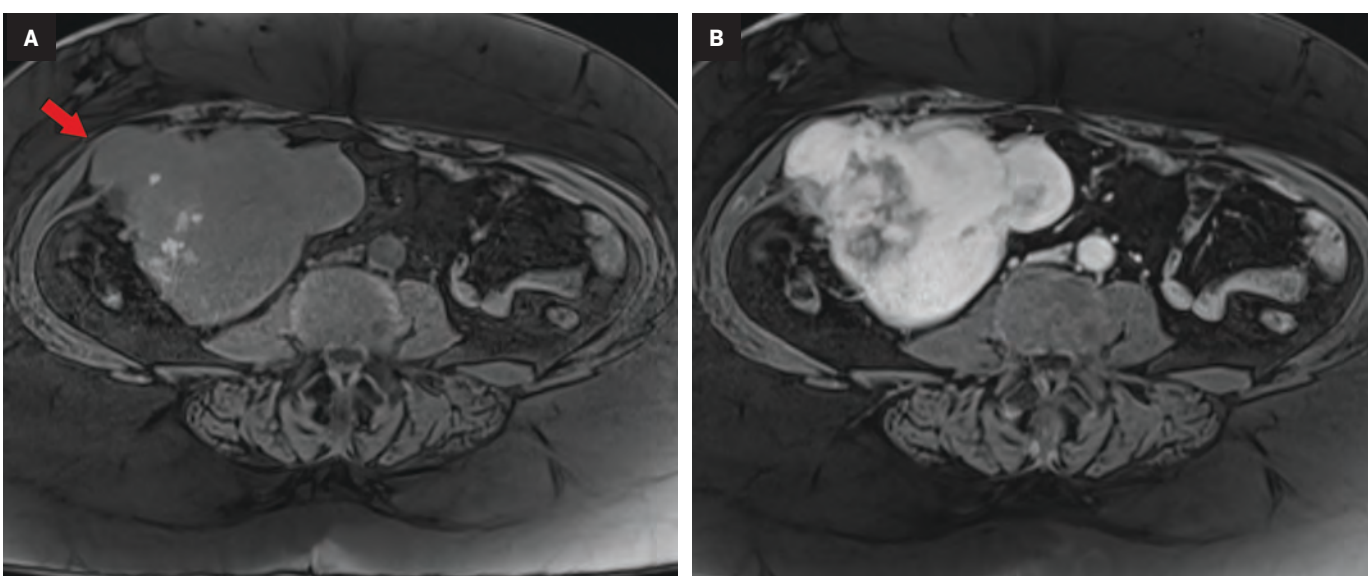

The most common complaint in patients with extrauterine adenomyoma is abdominal pain. Occasionally, patients will have abnormal vaginal bleeding or infertility. Of the 34 or so reported cases of extrauterine adenomyomas in the literature, only eight have been extrapelvic,[1] and only one is reported to have occurred in the abdominal wall.[7] There is scant literature on the radiological appearance, and preoperative diagnosis can be challenging.

Ultrasound, CT, and MRI are the most common modalities used for evaluation; in almost all reported cases, definitive diagnosis was only obtained through histopathologic analysis. On ultrasound these lesions appear as hypoechoic, solid masses with internal vascular flow utilizing color Doppler. On CT and MRI they demonstrate well-defined borders, often lobulated in contour. They are hypointense on T1 and usually isointense to smooth muscle on T2, much like uterine leiomyoma. This signal pattern contrasts with the more common adnexal mass, endometrioma, which is usually bright on T1, owing to the presence of blood products, and dark on T2.

Adenomyomas generally do not demonstrate restricted diffusion. They almost never demonstrate calcifications, and they enhance robustly after administration of IV contrast. MRI is the only modality that demonstrates somewhat reliable findings in differentiating adenomyomas from other adnexal or pelvic masses. The more common form is adenomyosis, seen as diffuse or focal thickening of the T2 hypointense junctional zone. It is common to find punctate foci of high T2 signal scattered throughout the myometrium, indicating islands of ectopic endometrial tissue. When it is a focal mass (ie, an adenomyoma) it may appear as intramyometrial, most often in the body of the uterus. Adenomyomas do not demonstrate the "T2 shading" resulting from the presence of blood degradation products typical of endometriomas.

Surgical resection is almost always curative, although recurrence, and rarely, malignant transformation, have been reported. Clear cell and focal endometriod adenocarcinomas have been reported in extrauterine adenomyomas.[8,9]

Conclusion

Extrauterine adenomyoma is a benign tumor containing endometrial tissue and smooth muscle cells. It is extremely rare outside of the pelvis. Preoperative diagnosis is often a challenge, as other tumors can have similar appearance. The pathogenesis of these tumors is unclear; however, some evidence implicates hormonal influences, embryologic development errors, and/or mechanical or iatrogenic mechanisms. Definitive diagnosis can only be made by histopathologic analysis.

References

1) Paul PG, Gulati G, Shintre H, Mannur S, Paul G, Mehta S. Extrauterine adenomyoma: a review of the literature. *Eur. J. Obstet. Gynecol. Reprod. Biol.* 2018; 228:130–136.

2) Cozzutto C. Uterus-like mass replacing ovary: report of a new entity. *Arch. Pathol. Lab. Med.* 1981;105(10):508–511.

3) Rosai J. Uteruslike mass replacing ovary. *Arch Pathol Lab Med*. 1982 Jul;106(7):364-365. PMID: 6896452.

4) Redman R, Wilkinson E J, Massoll N A. Uterine-like mass with features of an extrauterine adenomyoma presenting 22 years after total abdominal hysterectomy-bilateral salpingo-oophorectomy: a case report and review of the literature. *Arch. Pathol. Lab. Med.* 2005;129(8):1041–1043.

5) Batt R E. Pathogenesis of a parauterine uterus-like mass: developmentally misplaced mullerian tissue–mullerianosis. *Fertil. Steril.* 2010;94(2):e45.

6) Belmarez J A, Latifi H R, Zhang W, Matthews C M. Simultaneously occurring disseminated peritoneal leiomyomatosis and multiple extrauterine adenomyomas following hysterectomy. *Proc. (Bayl. Univ. Med. Cent).* 2019;32(1):126–128.

7) Sampaio R, Garcia J P, Macedo C S, Vizcaíno J R. A 22nd case report of extrauterine adenomyoma of the abdominal wall. *Case Rep Clin Pathol.* 2017; 4(2) :11.

8) Torres D, Parker L, Moghadamfalahi M, Sanders M A, Metzinger D S. Clear cell adenocarcinoma arising in an adenomyoma of the broad ligament. *Int J Surg Pathol. 2015;*23(2): 140-143.

9) Ulm, M A, Robins D B, Thorpe Jr. E M, Reed M E. Endometrioid adenocarcinoma in an extrauterine adenomyoma. *Obstet Gynecol.*2014; 124:445-448.

Postpartum Retroperitoneal Hemorrhage Secondary to Ovarian Artery Pseudoaneurysm

Christopher C. Zarour, MD, MHA, RPVI; Kaitlin M. Zaki-Metias, MD; Tima F. Tawil, MBBS; Huijuan Wang, MD; Stephen M. Seedial, MD, RPVI

Case Summary

A G8P4 patient with sickle cell trait presented to the emergency department with diffuse, cramping abdominal pain ten days after an uncomplicated vaginal delivery. The patient also reported worsening shortness of breath and two syncopal episodes since the delivery. They had light vaginal bleeding and malodorous discharge for one day. Initial vital signs demonstrated tachycardia and tachypnea. They were normotensive, afebrile, and saturating well on room air. Physical examination demonstrated mild abdominal distension with tenderness to palpation of the left upper quadrant with guarding. Speculum examination revealed a moderate amount of blood in the vaginal vault without abnormal discharge. There was no vulvar hematoma evident.

Imaging Findings

Transabdominal ultrasound (Figure 1) demonstrated a heterogeneous collection extending from the inferior aspect of the left kidney to the left adnexa. CT angiography of the abdomen and pelvis (Figure 2) demonstrated a mixed-attenuation collection in the left retroperitoneal space extending inferiorly into the pelvis, surrounding the left ovarian vessels. The tortuous left ovarian artery was faintly visualized coursing through the hematoma with a small outpouching of contrast at the mid-segment.

Catheter angiography (Figure 3) demonstrated multiple stenoses with a beaded appearance of the proximal left ovarian artery. Within the mid-segment, there was a 1 cm focal outpouching with active extravasation. The artery and pseudoaneurysm were successfully embolized.

Figure 1. Ultrasound of the pelvis with color Doppler demonstrates a large heterogeneous structure with scattered internal vascularity in the left adnexa extending from the level of the left kidney inferiorly into the pelvis.

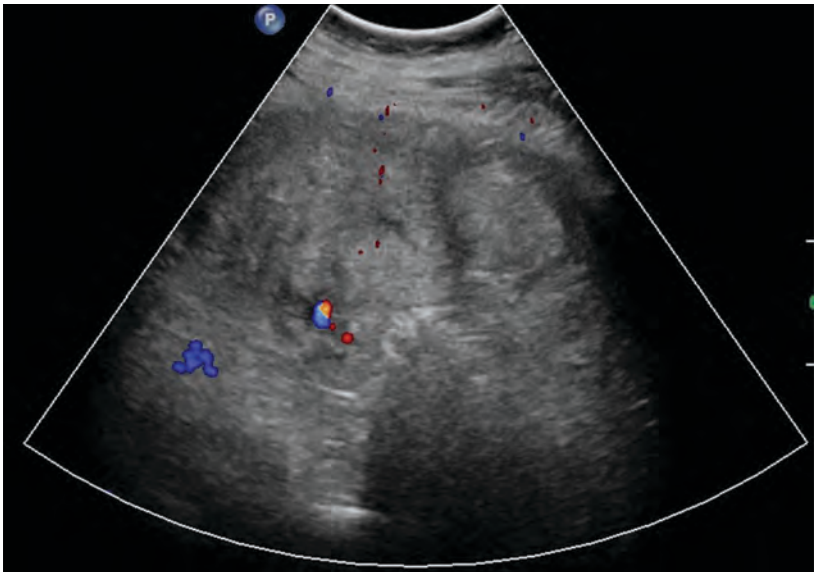

Diagnosis

Postpartum retroperitoneal hemorrhage secondary to ovarian artery pseudoaneurysm.

Discussion

Retroperitoneal postpartum hemorrhage is a rare complication of childbirth that most commonly occurs following assisted delivery or

Affiliations: Trinity Health Oakland Hospital/Wayne State University School of Medicine, Pontiac, Michigan (Drs Zarour, Zaki-Metias, Tawil, Wang, Seedial); Huron Valley Radiology, Ypsilanti, Michigan (Dr Seedial).

Figure 2. Axial (A) and coronal (B) CT angiograms of the abdomen and pelvis demonstrate a large left retroperitoneal hematoma. Within the central portion of the hematoma along the course of the left ovarian vessels there is a small outpouching of contrast (arrowhead) suspicious for left ovarian artery pseudoaneurysm.

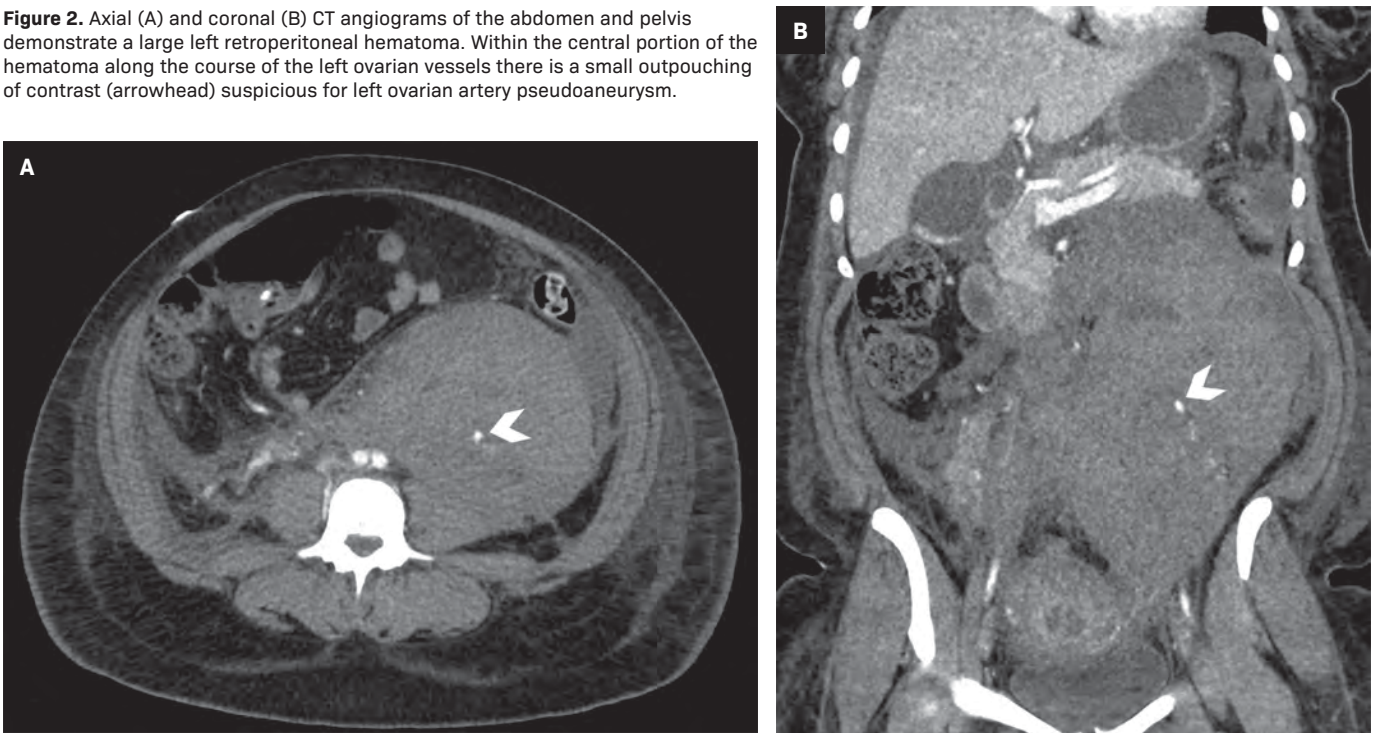

Figure 3. (A,B) Selective catheter angiogram shows a pseudoaneurysm of the mid left ovarian artery (arrowhead) with active contrast extravasation (curved arrow). The left ovarian artery is tortuous and demonstrates beading (arrows). (B,C) During and following coil embolization (block arrows) of the proximal and mid left ovarian artery, angiogram demonstrates resolution of the pseudoaneurysm and absence of contrast blush.

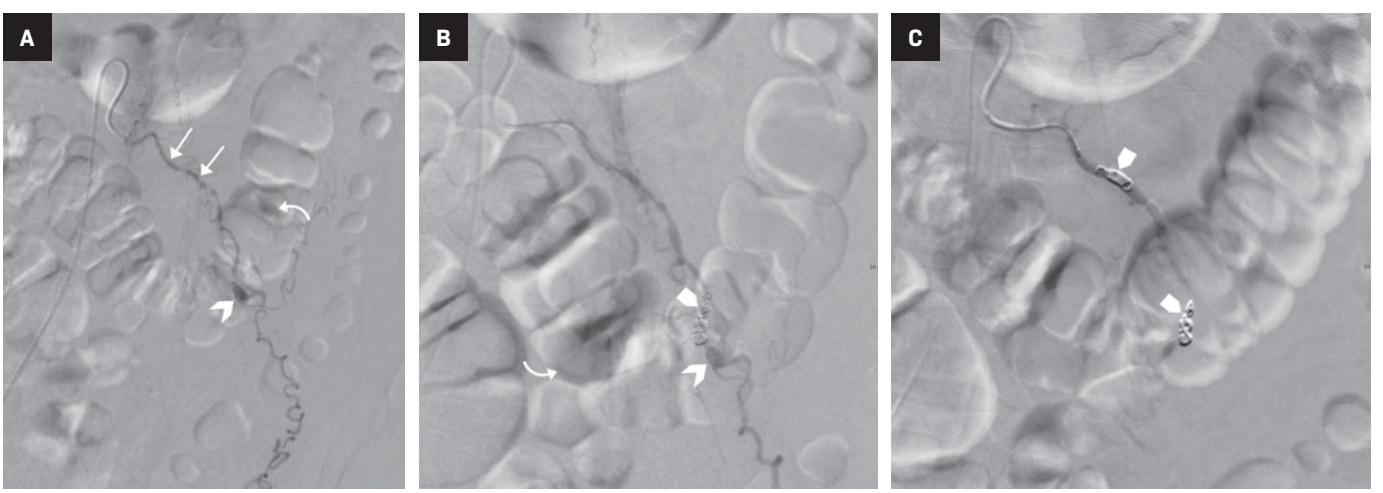

Caesarean section.[1] Anticoagulation therapy, prolonged labor, and manual placental removal have also been associated with the development of postpartum retroperitoneal hemorrhage.[2] The incidence of puerperal hematoma formation is approximately between 1 in 309 and 1 in 1500 deliveries.[1]

Although there is little published information regarding retroperitoneal hemorrhage in the pregnant and postpartum population, data suggest a correlation between parity and ovarian artery aneurysm and pseudoaneurysm formation.[2] Twenty-five cases of spontaneous ovarian artery aneurysm (OAA) rupture have been reported in the literature, of which 72% were associated with pregnancy.[3,4] Pregnant patients were all multigravida, suggesting that multiparity is a risk factor.[5,6] No ruptured OAA have been reported in nulliparous patients, reinforcing the correlation between OAA formation and pregnancy, leading to an increased risk of retroperitoneal hemorrhage.[5]

However, the mechanism of OAA formation is not well understood. Hemodynamic changes known to be related to pregnancy include increased cardiac output and blood

volume as well as systemic hypertension. Additionally, as the uterus expands, dilatation of the pelvic arteries directly increases uterine blood flow.[3] During normal uterine involution in the postpartum period, one or multiple segments of the ovarian artery may not involute; it is thought to be by this mechanism that the artery may become more susceptible to aneurysm formation in subsequent pregnancies.[3]

Hormonal alterations during pregnancy are also responsible for microscopic vascular wall changes, including intimal hyperplasia, smooth muscle hyperplasia of the media, fragmentation of reticular fibers, and loss of the normal corrugation of elastic fibers, rendering the wall of the ovarian artery susceptible to aneurysm formation.[3] Repeated pregnancies bring about further hemodynamic and endocrine changes which can exacerbate or rupture a pre-existing aneurysm. Another possible risk factor for OAA rupture is hypertension, found in four of nine ruptured OAA patients in one report.[7]

Patients with retroperitoneal hemorrhage from OAA rupture may present with severe or worsening flank pain, hemodynamic instability, syncope, and anemia.[8] Continuously declining hemoglobin in a postpartum patient should raise suspicion for occult hematoma formation in the absence of vaginal bleeding. Patients may also present with nausea, vomiting, malaise, and vague truncal pain.[8,9]

Retroperitoneal hematomas appear on ultrasound as heterogeneous structures along the pararenal space extending into the pelvis.[9] Triple-phase CT angiography can often determine the etiology of the hemorrhage.[9] CT angiography will show a heterogeneous retroperitoneal fluid collection with higher than simple fluid attenuation. Active hemorrhage appears as evolving high-density material within the collection on arterial and venous phase images. Pseudoaneurysms may be identified on CT angiography by their characteristic outpouching along the course of an artery that does not evolve on delayed images. Catheter angiography remains the gold standard for diagnosing and treating the cause of retroperitoneal hematomas with an identifiable etiology.[9]

Treatment options consist of conservative management, endovascular intervention, and surgical evacuation and vascular repair.[9] Conservative management is typically pursued in hemodynamically stable patients without significantly decreasing serum hemoglobin.[9] Transarterial embolization is typically performed in patients with continuously decreasing serum hemoglobin, with or without hemodynamic instability, where the etiology of hemorrhage is identified on cross-sectional imaging.[3,4] Catheter angiography may be pursued in unstable patients with active hemorrhage without an identified etiology.[3,4] Surgical evacuation is reserved for hemodynamically unstable patients in whom endovascular intervention is unsuccessful or the cause of hemorrhage cannot be identified.[8]

Conclusion

Nontraumatic obstetric retroperitoneal hematomas are an exceedingly rare complication of spontaneous vaginal delivery, with literature demonstrating a correlation between parity and ovarian artery aneurysms. Diagnostic and interventional radiologists should be aware of this complication and its associations to achieve timely diagnosis and management. Ovarian artery pseudoaneuryms, similar to pseudoaneurysms of other visceral arteries, may be treated with embolization.

References

1) Rafi J, Khalil H. Maternal morbidity and mortality associated with retroperitoneal haematomas in pregnancy. *JRSM Open*. 2018;9(1):2054270417746059. doi:10.1177/2054270417746059

2) Alturki F, Ponette V, Boucher LM. Spontaneous retroperitoneal hematomas following uncomplicated vaginal deliveries: a case report and literature review. *J Obstet Gynaecol Can.* 2018;40(6):712-715. doi:10.1016/j.jogc.2017.08.045

3) Kwon JH. Percutaneous transarterial embolization of spontaneously ruptured ovarian artery aneurysm using N-butyl cyanoacrylate. *Iran J Radiol.* 2014;11(3):e13371. doi: 10.5812/iranjradiol.13371

4) Distefano M, Casarella L, Amoroso S, Di Stasi C, Scambia G, Tropeano G. Selective arterial embolization as a first-line treatment for postpartum hematomas. *Obstet Gynecol.* 2013;121(2 Pt 2 Suppl 1):443-447. doi:10.1097/aog.0b013e31827d90e1

5) Tsai MT, Lien WC. Spontaneous rupture of an ovarian artery aneurysm. *Am J Obstet Gynecol*, 2009;200(3):e7-e9. doi: 10.1016/j.ajog.2008.09.875

6) Toyoshima M, Kudo T, Igeta, S, *et al.* Spontaneous retroperitoneal hemorrhage caused by rupture of an ovarian artery aneurysm: a case report and review of the literature. *J Med Case Reports* 9, 84 (2015). doi: 10.1186/s13256-015-0553-4.

7) Enakpene CA, Stern T, Barzallo Salazar MJ, Mukherjee P. Spontaneous rupture of an ovarian artery aneurysm: a rare postpartum complication. *Case Rep Obstet Gynecol*, 2016;2016:1029561. doi: 10.1155/2016/1029561

8) Garg D, McLaren RA, Silverman M. Postpartum retroperitoneal hematoma due to spontaneous rupture of ovarian artery pseudo-aneurysm. *Obstet Gynecol Int J,* 2016;5(6):00181. doi: 10.15406/ogij.2016.05.00181

9) Chan YC, Morales JP, Reidy JF, Taylor PR. Management of spontaneous and iatrogenic retroperitoneal haemorrhage: conservative management, endovascular intervention or open surgery? *IntJ Clin Practice.* 2008;62:1604-1613. doi: 10.1111/j.1742-1241.2007.01494.x

Shoulder Effusion as Ultrasound Mimic of Axillary Lymphadenopathy

Katie Shpanskaya, MD, and Eun L. Langman, MD

Case Summary

A woman with biopsy-proven invasive ductal carcinoma in the left breast and a metastatic left axillary lymph node presented following presurgical neoadjuvant chemotherapy for placement of an axillary localization device. During pre-procedural ultrasound (US) imaging, the axillary mass, initially queried as the metastatic lymph node, was characterized as a benign shoulder effusion. In this case, we discuss common axillary ultrasound findings and distinguishing characteristics.

Imaging Findings

Initial US evaluation (Figure 1) obtained 6 months prior to surgery demonstrated an enlarged left axillary lymph node with abnormal cortical thickening and internal vascularity. This was subsequently biopsied, with pathology demonstrating metastatic breast cancer. A post-biopsy mammogram (Figure 1) demonstrated an appropriately placed biopsy clip within the lymph node.

The patient underwent neoadjuvant chemotherapy for breast cancer prior to surgery. Pre-procedural US-guided localization of the metastatic node on the day of surgery (Figure 2) demonstrated a nearly anechoic, avascular oval mass in the left axilla with increased through transmission. Further imaging demonstrated its location adjacent to the humeral head with a tear-drop appearance and lack of internal vascularity. These findings are characteristic of a joint effusion. The prior biopsy site was later identified inferiorly in the axillary space as a normalized lymph node with central hyperechoic fatty hilum and cortical thickness measuring less than 3 millimeters. The echogenic biopsy clip was also visible in the node. This node was successfully localized and excised at surgery.

Diagnosis

Shoulder effusion as a mimic of axillary lymphadenopathy. The differential diagnosis includes benign and malignant causes of axillary lymphadenopathy, soft-tissue masses, synovial hypertrophy, and post-procedural seroma.

Discussion

Axillary ultrasound is often performed during breast imaging workup for suspected axillary pathology such as lymphadenopathy or for a palpable mass. Commonly described etiologies of pathology in the axilla include benign and malignant causes of lymphadenopathy, soft-tissue masses, and postsurgical or posttraumatic fluid collections.[1,2] Given the proximity of the axillary space to the shoulder, musculoskeletal pathology should be considered within this broad differential. Here, we present an uncommon mimic of axillary lymphadenopathy caused by a shoulder effusion.

Ultrasound imaging of the axilla may play an integral role in management of newly diagnosed breast cancer during initial staging assessment, image-guided biopsy of a suspicious abnormality, assessment of treatment response, and image-guided localization for surgery.[2-4] Malignant lymph node involvement may be characterized by eccentric or diffuse cortical thickening, effacement of the normal central fatty hilum, and loss of the normal nodal contour with a uniformly hypoechoic echotexture. Considering morphologic criteria alone, US has a sensitivity of 26-76% and a specificity of 88-89% for the detection of nodal malignancy.[4]

In breast cancer, ipsilateral axillary lymphadenopathy is concerning for nodal metastasis. However, a broad differential diagnosis should

Affiliation: Duke University Medical Center, Department of Radiology, Durham, North Carolina.

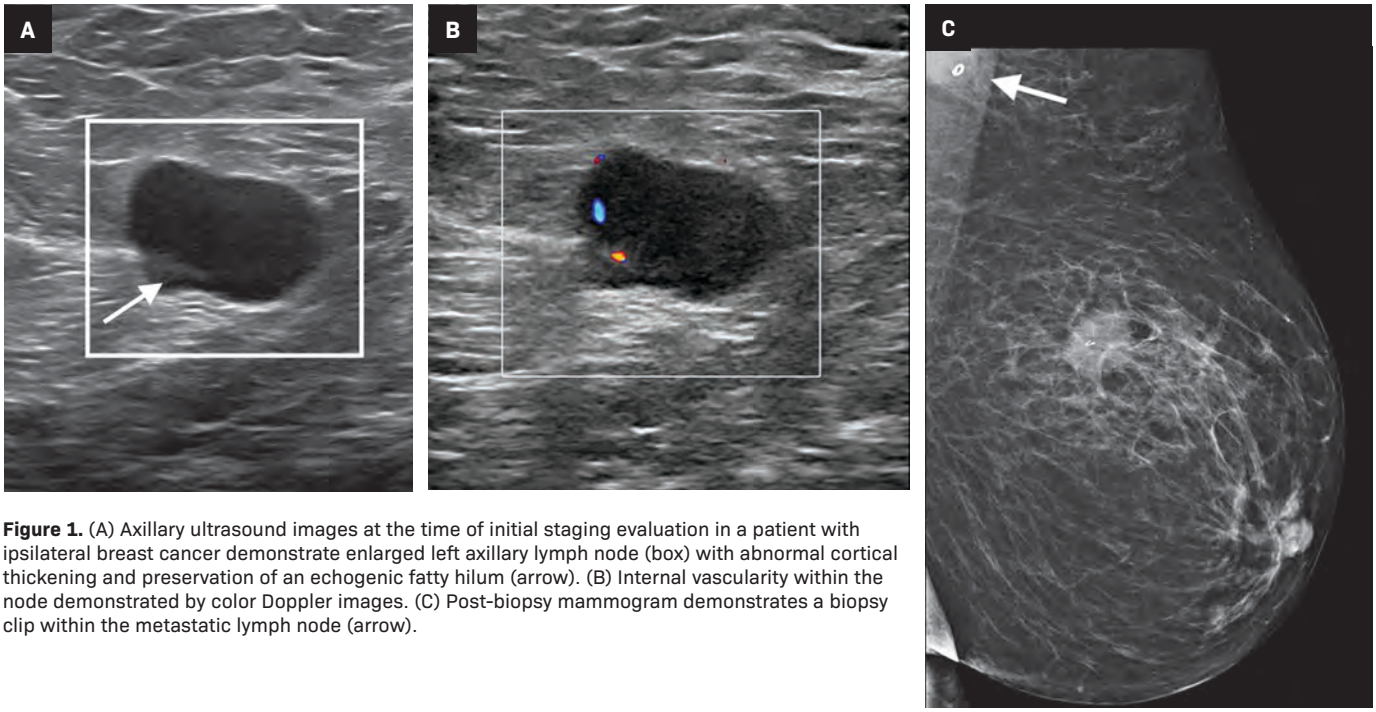

Figure 1. (A) Axillary ultrasound images at the time of initial staging evaluation in a patient with ipsilateral breast cancer demonstrate enlarged left axillary lymph node (box) with abnormal cortical thickening and preservation of an echogenic fatty hilum (arrow). (B) Internal vascularity within the node demonstrated by color Doppler images. (C) Post-biopsy mammogram demonstrates a biopsy clip within the metastatic lymph node (arrow).

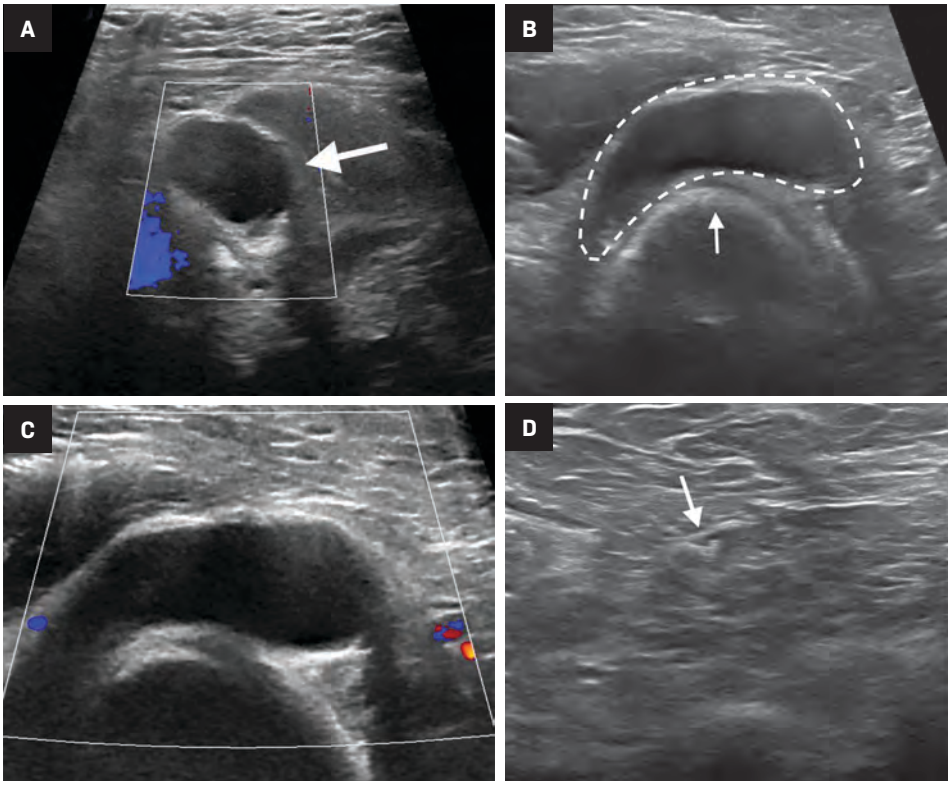

Figure 2. (A) Axillary ultrasound 6 months later, following neoadjuvant chemotherapy, demonstrates a nearly anechoic, avascular oval mass in the left axilla (arrow) with increased through transmission. (B) Image demonstrates the mass's location adjacent to the humeral head (arrow). The teardrop shape (dotted line) is characteristic of a joint effusion. (C) Doppler US demonstrates absence of Internal vascularity. (D) Ultrasound imaging performed more inferiorly in the axilla demonstrates the previously biopsied lymph node, which has normal in size and contains a linear echogenic biopsy clip (arrow). This was successfully localized and excised at surgery.

be considered when approaching axillary space pathology. These include alternative etiologies for lymphadenopathy such as benign reactive hyperplasia from infection or vaccines, underlying connective tissue disease, granulomatous disease, or other malignancies such as lymphoma.

The appearance of other axillary masses may also be difficult to differentiate from lymphadenopathy. These include mesenchymal soft-tissue masses such as peripheral nerve sheath tumors, postsurgical or posttraumatic fluid collections such as seromas and hematomas, or breast masses like fibroadenomas arising from axillary breast tissue.

Joint pathology associated with the shoulder may not readily be considered in the differential diagnosis of axillary findings identified during breast imaging.

The axillary space relevant to breast pathology begins below the glenohumeral joint to include the axillary lymph node stations defined in relation to the pectoralis minor muscle.[5] In musculoskeletal imaging, an axillary sonographic approach is uncommon but can be used as an adjunct in assessing the shoulder.[6] An axillary approach may be helpful in characterizing inferior shoulder pathology, including joint effusions, synovial hypertrophy, and adhesive capsulitis. Axillary ultrasound has been shown to have a sensitivity of 89% and a specificity of 76% in the detection of joint effusions.[7]

A shoulder joint effusion imaged with US characteristically appears as an anechoic, avascular structure adjacent to the humeral head, with posterior acoustic enhancement. These features can overlap with the appearance of a malignant lymph node, particularly if the shoulder effusion contains complicated fluid resulting in hypoechoic echogenicity which can be mistaken for solid tissue.

The key distinguishing feature of a joint effusion from lymphadenopathy or other axillary mass is its location adjacent to the humeral head. Care should be taken during patient and probe positioning to avoid imaging at or above the level of the glenohumeral joint, where musculoskeletal lesions may be more apparent. Joint effusions may also decrease in size when pressure is applied to the transducer, which can displace the joint fluid. These diagnostic characteristics can easily be demonstrated on US without requiring further imaging workup.

Conclusion

Accurate detection and diagnosis of axillary lymphadenopathy is important, particularly in the context of breast cancer. During breast imaging the proximity of the axillary space to the shoulder raises the possibility of detecting musculoskeletal pathology. This is illustrated in our case of a shoulder joint effusion as an uncommon mimic of malignant axillary lymphadenopathy. Key distinguishing features that can aid in correctly identifying a shoulder joint effusion include its characteristic location adjacent to the humeral head, lack of internal vascularity, and potential for displacement with application of transducer pressure.

References

1) Park Y M, Park J S, Yoon H K. Yang W T Imaging-pathologic correlation of diseases in the axilla. *AJR. Am J Roentgenol.* 2013(2): W130–W142. https://doi.org/10.2214/AJR.12.9259

2) Teichgraeber D, Perez F, Guirguis M, Kapoor M, Whitman, G. Ultrasound evaluation of the axilla in the breast imaging setting. *Ultrasound Quarterly.* 2021; 37(1): 43-51. doi: 10.1097/RUQ.0000000000000546

3) Chang J M, Leung J, Moy L, Ha S M, Moon W K. Axillary nodal evaluation in breast cancer: state of the art. *Radiology.* 2020; *295*(3): 500–515. https://doi.org/10.1148/radiol.2020192534

4) Ecanow J S, Abe H, Newstead G M, Ecanow D B, Jeske J M .Axillary staging of breast cancer: what the radiologist should know. *Radiographics.* 2023 (6), 1589–1612. https://doi.org/10.1148/rg.336125060

5) Alvarez S, Añorbe E, Alcorta P, López F, Alonso I, Cortés J. Role of sonography in the diagnosis of axillary lymph node metastases in breast cancer: a systematic review. *AJR. Am J Roentgenol.* 2006; *186*(5): 1342–1348. https://doi.org/10.2214/AJR.05.0936

6) Michelin P, Legrand J, Lee K S, et al. Axillary sonography of the shoulder: an adjunctive approach. *J Ultrasound Med. 2018; 37*(11), 2707–2715. https://doi.org/10.1002/jum.14601

7) Koski J M. Validity of axillary ultrasound scanning in detecting effusion of the glenohumeral joint. *Scand J Rheumatol. 1991; 20: 49-51.*

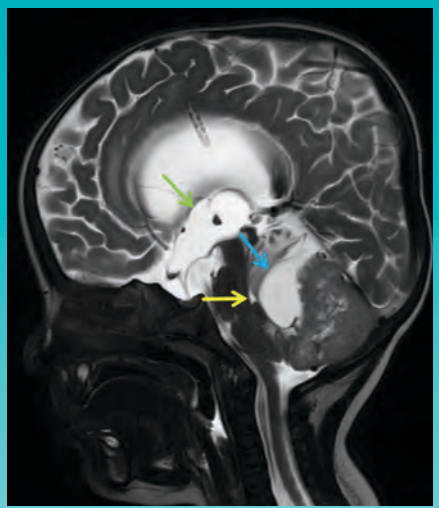

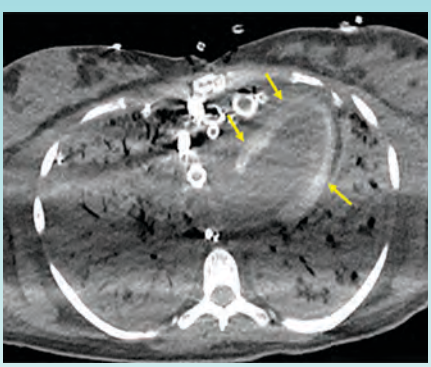

AppliedRadiology®

The Journal of Practical Medical Imaging and Management

Call for Cases

If you have an interesting case we want to know about it!

Sharing your case is a fantastic opportunity to gain recognition for your work and receive feedback from peers all over the world!

Author Guidelines* can be found at

https://appliedradiology.com/author-guidelines

- Abdominal
- Thoracic
- Genitourinary
- GI
- Emergency
- Interventional
- Vascular
- Peds
- Breast
- Neuro
- MSK
- Oncologic
- Cardiac
- Molecular Imaging
- Nuclear Medicine

* Cases undergo peer review before being accepted for publication.

PRINT / ONLINE

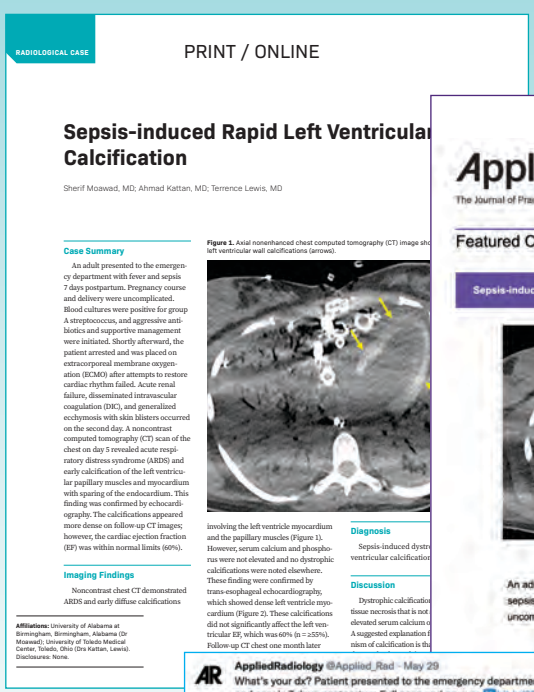
RADIOLOGICAL CASE

Sepsis-induced Rapid Left Ventricular Calcification

Sherif Moawad, MD; Ahmad Kattan, MD; Terrence Lewis, MD

Case Summary

An adult presented to the emergency department with fever and sepsis 7 days postpartum. Pregnancy course and delivery were uncomplicated. Blood cultures were positive for group A streptococcus, and aggressive antibiotics and supportive management were initiated. Shortly afterward, the patient arrested and was placed on extracorporeal membrane oxygenation (ECMO) after attempts to restore cardiac rhythm failed. Acute renal failure, disseminated intravascular coagulation (DIC), and generalized ecchymosis with skin blisters occurred on the second day. A noncontrast computed tomography (CT) scan of the chest on day 5 revealed acute respiratory distress syndrome (ARDS) and early calcification of the left ventricular papillary muscles and myocardium with sparing of the endocardium. This finding was confirmed by echocardiography. The calcifications appeared more dense on follow-up CT images; however, the cardiac ejection fraction (EF) was within normal limits (60%).

Imaging Findings

Noncontrast chest CT demonstrated ARDS and early diffuse calcifications involving the left ventricle myocardium and the papillary muscles (Figure 1). However, serum calcium and phosphorus were not elevated and no dystrophic calcifications were noted elsewhere. These finding were confirmed by trans-esophageal echocardiography, which showed dense left ventricle myocardium (Figure 2). These calcifications did not significantly affect the left ventricular EF, which was 60% (n = ≥55%). Follow-up CT chest one month later

Figure 1. Axial nonenhanced chest computed tomography (CT) image sho left ventricular wall calcifications (arrows).

Diagnosis

Discussion

Affiliations: University of Alabama at Birmingham, Birmingham, Alabama (Dr Moawad); University of Toledo Medical Center, Toledo, Ohio (Drs Kattan, Lewis).
Disclosures: None.

EMAIL ANNOUNCEMENT

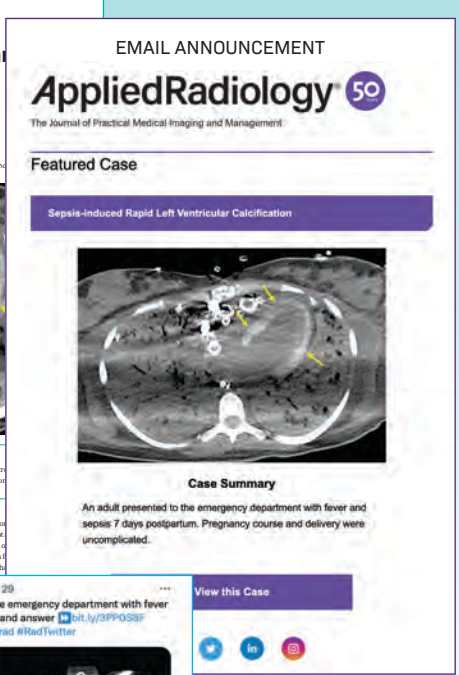
AppliedRadiology 50

The Journal of Practical Medical Imaging and Management

Featured Case

Sepsis-induced Rapid Left Ventricular Calcification

Case Summary

An adult presented to the emergency department with fever and sepsis 7 days postpartum. Pregnancy course and delivery were uncomplicated.

View this Case

SOCIAL MEDIA


AppliedRadiology @Applied_Rad · May 29

What's your dx? Patient presented to the emergency department with fever and sepsis 7 days postpartum Full case and answer bit.ly/3PP0S3F #radiology #RadRes #FOAMed #FOAMrad #RadTwitter

"The more I learn color, the more I love black and white."
—Sajal Sazzad

Are You Reading the Yellows, or Am I?

C. Douglas Phillips, MD, FACR

Worklists.

When did that word become a derogatory term? That is, for sure, a recent construct. I read from a worklist and I'll bet you do, too. Stat exams get a special feature of some form on the worklist I view. For me, fortunately, it is just colored red. Look here, radiologist. Read me. Again, my age gives me away, but I remember when stat exams got hung on a viewbox immediately by the film room staff. In front of me. While I watched. And they handed me the request and a tape to dictate it so they could immediately get it to the transcriptionist, who immediately transcribed it and returned it to me to sign. And, they stood patiently and watched me until I did it.

Easy peasy.

Today, we read from worklists. I guess, somehow, it was thought too easy to tell people to read from the top down (or maybe we all have that rebel in our soul, and everyone dives randomly for some exam in the mid-point) so the "stat" exams could just be placed at the top of the list. So, we exploit the color monitor, and the important studies came up in red. Very conspicuous.

The peacock of exams, calling attention to itself by its brilliant plumage.

But, what about the "super-stat" exam? Or the "urgent" exam? Or the "patient waiting in the clinic" exam? Or the "I've got a flight to catch, so you need to get me this report" exam? Oh, don't worry. I've got hundreds. What color do they get? Do they need another color? You know the answer to that one: damned straight they do, how else will you recalcitrant radiologists know the difference? So, the worklist got a few more colors. Red, yellow, purple, gold, green, etc, etc.

Clearly, this led to a moment of Zen for the radiologists, who then immediately understood the complexities not only of the exams but of the worklist and were able to quickly and efficiently move throughout, plucking the most important of studies first, and then moving down the queue to end their shift on time, having been super-efficient and getting the opportunity to break for lunch while not missing a beat. Do you believe that? Nope? You've been reading this column for too long.

I've seen colleagues with over six color-coded exam priorities. Let me tell you something, that's at least five too many. I've heard from one that has a FLASHING priority tag. Whoa. Put that thing back in the holster. Please, IT person, disable that function and step back. Too much information. Would a flashing yellow have priority over a solid red? Does the flash occur as Morse code? A green that is flashing S.O.S in Morse code. would be the penultimate. The top priority might be a Pac-Man-yellow priority tag that, just like Pac-Man, eats the other items on the worklist. It stands alone at the end, and you MUST read it.

Our lives have gotten so complicated. A worklist that requires a college education and an ergonomics professor to explain seems a bit much. Ooooh. What if you're color blind?

Come on, attend to that flashing yellow chest film on the worklist. Get that thing out of here. Keep doing that good work. Mahalo.

Dr Phillips is a Professor of Radiology, Director of Head and Neck Imaging, at Weill Cornell Medical College, NewYork-Presbyterian Hospital, New York, NY. He is a member of the *Applied Radiology* Editorial Advisory Board.

AppliedRadiology®

The Journal of Practical Medical Imaging and Management

UPDATE YOUR SUBSCRIPTION

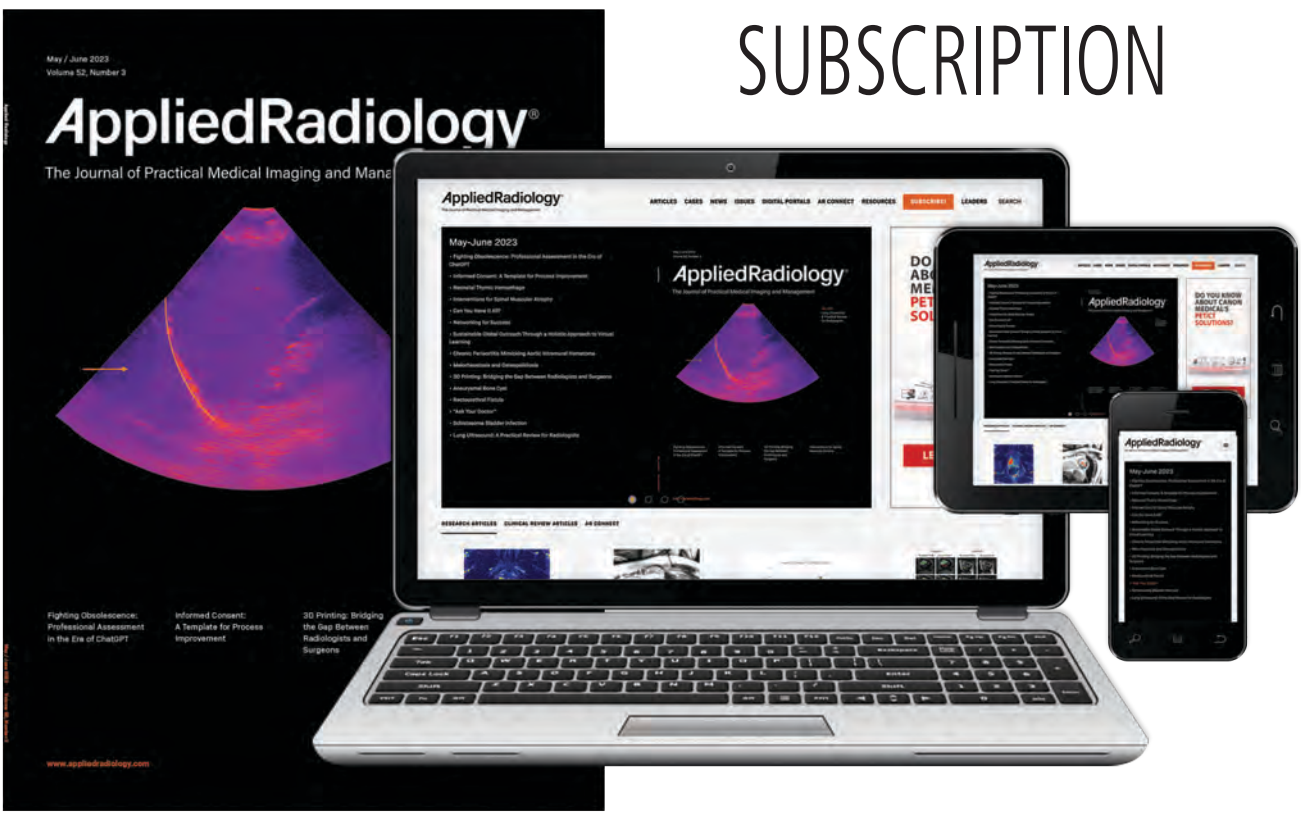

Since 1972, *Applied Radiology* has brought physician-authored clinical review articles to the radiology community.

Applied Radiology content includes clinical review articles, radiological cases, and specialty columns such as Eye on AI and the ever-popular Wet Read by C. Douglas Phillips, MD, FACR.

Now you can have it all your way (FREE) without missing a single issue.

Please take a moment to update your subscription preferences.

appliedradiology.com/#subscribe

CT Suite | MR Suite | Injectors and Digital Solutions

SmartInject
SOLUTIONS FROM BRACCO

Point-of-care imaging solutions that help promote patient safety and streamline workflow

NEXO®
Contrast management system

Advance patient care with smart injectors and digital solutions from Bracco.

Learn more at **SmartInject.com**

Bracco Diagnostics Inc.
259 Prospect Plains Road, Building H
Monroe Township, NJ 08831 USA

Phone: 609-514-2200
Toll Free: 1-877-272-2269 (U.S. only)
Fax: 609-514-2446

BRACCO
LIFE FROM INSIDE

Committed to Science,
Committed **to You.**™